SUPPORTING INFORMATION FOR

Sequential Insertion of Alkynes, Alkenes and CO into the Pd–C Bond of *ortho*-Palladated Primary Phenethylamines: from η^3-Allyl Complexes and Enlarged Palladacycles to Functionalized Arylalkylamines

José-Antonio García-López,*[a] María-José Oliva-Madrid,[a] Delia Bautista,[b] José Vicente,[a] and Isabel Saura-Llamas*[a]

[a]Grupo de Química Organometálica, Departamento de Química Inorgánica, Facultad de Química, Universidad de Murcia, E–30100 Murcia, Spain. [b]ACTI, Universidad de Murcia, E–30100 Murcia, Spain

^{1}H and ^{13}C{^{1}H} APT NMR spectra of compounds

Table S1. Crystal Data and Structure Refinement Details for Complexes *anti*-**1a**, *anti*-**1b**, *syn*-**1b**, and *anti*-**2a**·CH_2Cl_2.

	anti-**1a**	*anti*-**1b**	*syn*-**1b**	*anti*-**2a**·CH_2Cl_2
formula	$C_{32}H_{32}BrNO_2Pd$	$C_{32}H_{32}ClNPd$	$C_{32}H_{32}ClNPd$	$C_{30}H_{34}BrCl_2NO_4Pd$
fw	648.90	572.43	572.43	729.79
temp (K)	100(2)	100(2)	100(2)	100(2)
cryst habit	yellow block	colorless block	colorless prism	colorless prism
cryst size (mm)	0.20 x 0.18 x 0.10	0.38 x 0.26 x 0.17	0.26 x 0.19 x 0.07	0.230 x 0.080 x 0.030
cryst syst	triclinic	monoclinic	triclinic	monoclinic
space group	$P\bar{1}$	$P2_1/c$	$P\bar{1}$	$P2_1/n$
a (Å)	8.9631(8)	10.2233(9)	10.6754(9)	16.9537(8)
b (Å)	11.7417(11)	17.5358(16)	11.0500(11)	8.8151(4)
c (Å)	14.2801(12)	15.6984(14)	14.3048(11)	20.9006(9)
α (deg)	110.003(2)	90	70.041(2)	90
β (deg)	104.351(2)	106.430(2)	68.606(3)	107.9949(16)
γ (deg)	92.262(2)	90	61.474(2)	90
V (Å^3)	1355.3(2)	2699.4(4)	1351.3(2)	2970.8(2)
Z	2	4	2	4
ρ_{calcd} (Mg m^{-3})	1.590	1.409	1.407	1.632
μ(Mo, Kα) (mm^{-1})	2.189	0.807	0.806	2.186
F(000)	656	1176	588	1472
θ range (deg)	1.86–28.73	1.78–28.72	1.56–28.72	2.05–28.80
no. rflns collected	16 682	32 642	16 608	96 802
no. indep rflns	6365	6573	6351	7710
R_{int}	0.0173	0.0305	0.0170	0.0705
max, min transmsn	0.811, 0.674	0.875, 0.764	0.946, 0.786	0.937, 0.633
no. of restraints/params	2/347	1/326	5/375	1/355
goodness of fit on F^2	1.045	1.101	1.100	1.054
R1 ($I > 2\sigma(I)$)	0.0207	0.0346	0.0234	0.0370
wR2 (all rflns)	0.0536	0.0758	0.0578	0.0800
largest diff peak, hole (e·Å^{-3})	0.481, –0.579	0.665, –0.435	0.511, –0.611	1.315, –1.403

Table S2. Crystal Data and Structure Refinement Details for Complexes *syn*-**2a**, *anti*-**2b**·$CHCl_3$, *syn*-**2b**, and *syn*-**3b**·CH_2Cl_2.

	syn-**2a**	*anti*-**2b**·$CHCl_3$	*syn*-**2b**	*syn*-**3b**·CH_2Cl_2
formula	$C_{29}H_{32}BrNO_4Pd$	$C_{30}H_{33}Cl_4NO_2Pd$	$C_{29}H_{32}ClNO_2Pd$	$C_{41}H_{43}Cl_2F_3N_2O_3PdS$
fw	644.86	687.77	568.40	878.13
temp (K)	100(2)	100(2)	100(2)	100(2)
cryst habit	yellow lath	colorless prism	yellow prism	colorless block
cryst size (mm)	0.21 x 0.16 x 0.016	0.13 x 0.09 x 0.08	0.20 x 0.09 x 0.08	0.37 x 0.12 x 0.09
cryst syst	orthorhombic	triclinic	triclinic	triclinic
space group	$P2_12_12_1$	$P\ \bar{1}$	$P\ \bar{1}$	$P\ \bar{1}$
a (Å)	8.9693(5)	10.6530(8)	9.0931(6)	11.4056(8)
b (Å)	9.1468(5)	12.4688(9)	11.9585(8)	18.0651(13)
c (Å)	32.5761(18)	13.3325(11)	12.0592(8)	20.4085(15)
α (deg)	90	116.035(2)	80.987(2)	76.531(2)
β (deg)	90	93.499(3)	83.351(3)	83.006(3)
γ (deg)	90	103.312(2)	85.948(2)	80.422(2)
V (Å^3)	2672.6(3)	1521.7(2)	1284.57(15)	4017.2(5)
Z	4	2	2	4
ρ_{calcd} (Mg m^{-3})	1.603	1.501	1.470	1.452
μ(Mo, Kα) (mm^{-1})	2.225	0.989	0.853	0.701
F(000)	1304	700	584	1800
θ range (deg)	2.31–28.37	1.73–28.68	1.72–28.59	1.72–28.74
no. rflns collected	65 022	18 867	15 851	49 595
no. indep rflns	6654	7173	6030	18 882
R_{int}	0.0729	0.0266	0.0211	0.0260
max, min transmsn	0.862, 0.738	0.925, 0.815	0.935, 0.786	0.940, 0.850
no. of restraints/params	9/359	103/383	1/318	0/993
goodness of fit on F^2	1.032	0.937	1.091	1.204
R1 ($I > 2\sigma(I)$)	0.0309	0.0387	0.0286	0.0418
wR2 (all rflns)	0.0531	0.0883	0.0666	0.0880
largest diff peak, hole (e·Å^{-3})	0.496, –0.616	0.803, –0.785	1.061, –0.525	0.755, –0.628

Table S3. Crystal Data and Structure Refinement Details for Compounds **6b**·H_2O, **7c**·$CHCl_3$, **7d**·1/2$CHCl_3$, and **7f**.

	6b·H_2O	**7c**·$CHCl_3$	**7d**·1/2$CHCl_3$	**7f**
formula	$C_{33}H_{34}F_3NO_4S$	$C_{27}H_{33}Cl_4NPd$	$C_{27.5}H_{32.5}Cl_{2.5}NO_2Pd$	$C_{23}H_{30}ClNO_4Pd$
fw	597.67	619.74	604.07	526.33
temp (K)	100(2)	100(2)	100(2)	100(2)
cryst habit	pale yellow prism	colorless prism	colorless prism	yellow prism
cryst size (mm)	0.24 x 0.16 x 0.06	0.25 x 0.11 x 0.05	0.16 x 0.10 x 0.02	0.25 x 0.07 x 0.07
cryst syst	monoclinic	monoclinic	monoclinic	monoclinic
space group	$P2_1/c$	$P2_1/n$	$C2/c$	$P2_1/n$
a (Å)	22.3424(17)	11.4685(9)	23.7231(19)	12.0005(11)
b (Å)	10.7595(8)	10.8204(9)	14.2275(12)	13.1557(13)
c (Å)	12.6718(11)	21.5690(17)	17.3927(14)	14.2244(14)
α (deg)	90	90	90	90
β (deg)	91.435(2)	99.6340(10)	118.388(2)	105.146(2)
γ (deg)	90	90	90	90
V (Å^3)	3045.3(4)	2638.8(4)	5164.5(7)	2167.7(4)
Z	4	4	8	4
ρ_{calcd} (Mg m^{-3})	1.304	1.560	1.554	1.613
μ(Mo, Kα) (mm^{-1})	0.162	1.125	1.003	1.010
F(000)	1256	1264	2472	1080
θ range (deg)	1.82–28.76	1.89–28.70	1.73–27.88	1.98–28.67
no. rflns collected	36 514	31 637	30 962	26 555
no. indep rflns	7451	6410	6116	5278
R_{int}	0.0347	0.0293	0.0478	0.0306
max, min transmsn	0.990, 0.904	0.946, 0.837	0.980, 0.847	0.933, 0.831
no. of restraints/params	2/401	0/309	316/333	1/283
goodness of fit on F^2	1.187	1.135	1.107	1.061
R1 ($I > 2\sigma(I)$)	0.0627	0.0319	0.0435	0.0263
wR2 (all rflns)	0.1380	0.0692	0.0939	0.0614
largest diff peak, hole (e·Å^{-3})	0.627, –0.321	0.750, –0.507	1.144, –0.860	0.659, –0.322

Table S4. Crystal Data and Structure Refinement Details for Compounds **8f**, **9d**, **9f**·Et_2O, and **10c**·H_2O.

	8f	**9d**	**9f**·Et_2O	**10c**·H_2O
formula	$C_{24}H_{30}F_3NO_7S$	$C_{29}H_{34}F_3NO_7S$	$C_{29}H_{42}F_3NO_{10}S$	$C_{28}H_{36}F_3NO_6S$
fw	533.55	597.63	653.69	571.64
temp (K)	100(2)	100(2)	100(2)	100(2)
cryst habit	colorless prism	colorless needle	colorless lath	colorless prism
cryst size (mm)	0.23 x 0.14 x 0.11	0.13 x 0.03 x 0.03	0.20 x 0.15 x 0.03	0.09 x 0.07 x 0.014
cryst syst	triclinic	orthorhombic	monoclinic	triclinic
space group	$P\ \bar{1}$	*Pbca*	$P2_1/n$	$P\ \bar{1}$
a (Å)	9.4903(7)	18.0389(9)	8.7895(6)	8.9366(8)
b (Å)	9.9546(7)	15.3736(6)	25.4271(17)	12.0889(11)
c (Å)	13.3238(13)	19.6769(9)	13.8814(9)	13.8916(12)
α (deg)	105.493(2)	90	90	83.450(3)°
β (deg)	92.836(3)	90	96.550(2)	88.543(3)°
γ (deg)	96.262(2)	90	90	68.801(3)°
V (Å^3)	1201.68(17)	5456.9(4)	3082.1(4)	1389.9(2)
Z	2	8	4	2
ρ_{calcd} (Mg m^{-3})	1.475	1.455	1.409	1.366
μ(Mo, Kα) (mm^{-1})	0.204	0.189	0.181	0.179
F(000)	560	2512	1384	604
θ range (deg)	2.14–28.67	2.02–26.41	2.18–28.79	2.21–26.44
no. rflns collected	14 821	58 213	63 048	36 550
no. indep rflns	5647	5590	7999	5717
R_{int}	0.0184	0.1128	0.0584	0.0546
max, min transmsn	0.978, 0.849	0.862, 0.806	0.862, 0.799	0.862, 0.821
no. of restraints/params	1/337	3/385	0/415	6/376
goodness of fit on F^2	1.078	1.068	1.058	1.025
R1 ($I > 2\sigma(I)$)	0.0404	0.0496	0.0456	0.0437
wR2 (all rflns)	0.1012	0.1115	0.1034	0.1073
largest diff peak, hole (e·Å^{-3})	0.422, –0.430	0.745, –0.505	0.431, –0.399	0.517, –0.418

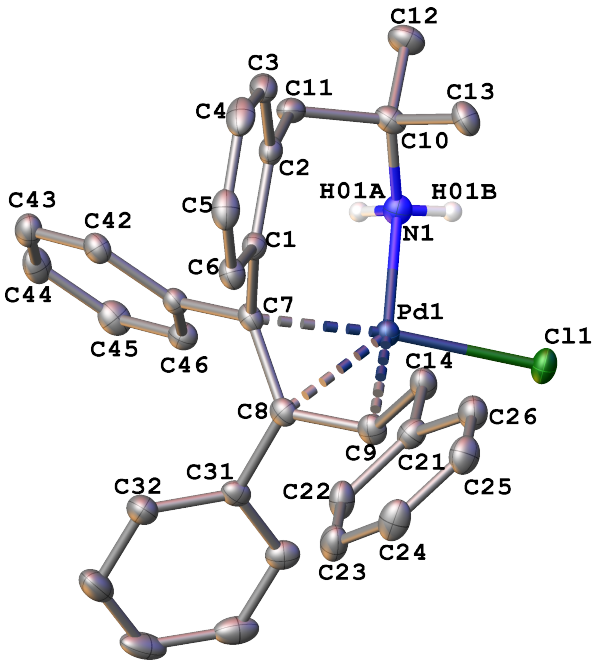

Figure S1. Thermal ellipsoid plot (50 % probability) of *anti*-**1b** along with the labeling scheme. The hydrogen atoms bonded to carbon have been omitted for clarity. Selected bond lengths (Å) and angles (deg): Pd(1)–Cl(1) = 2.3644(6), Pd(1)–N(1) = 2.1086(19), Pd(1)–C(7) = 2.118(2), Pd(1)–C(8) = 2.119(2), Pd(1)–C(9) = 2.114(2), C(7)–C(8) = 1.452(3), C(8)–C(9) = 1.430(3); Cl(1)–Pd(1)–N(1) = 88.46(6), C(7)–C(8)–C(9) = 121.24(19), C(8)–C(9)–C(14) = 132.3(2).

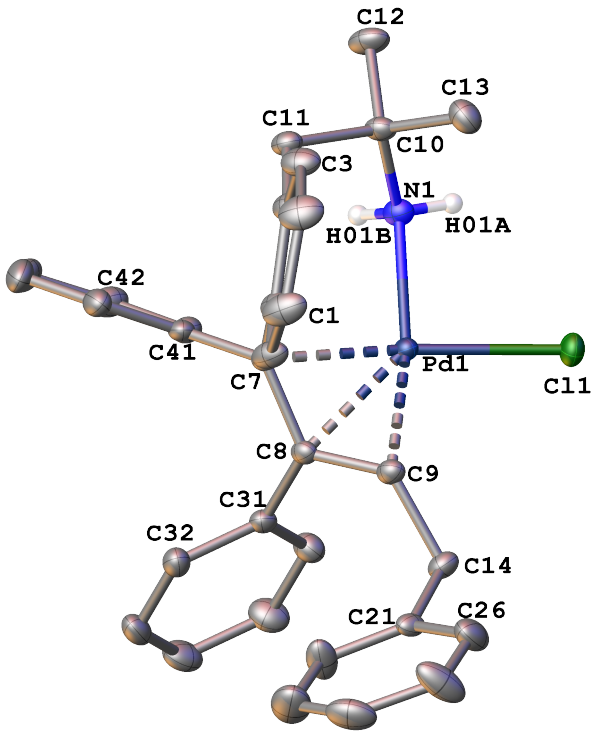

Figure S2. Thermal ellipsoid plot (50 % probability) of *syn*-**1b** along with the labeling scheme. The hydrogen atoms bonded to carbon have been omitted for clarity. Selected bond lengths (Å) and angles (deg): Pd(1)–Cl(1) = 2.3670(5), Pd(1)–N(1) = 2.1231(14), Pd(1)–C(7) = 2.1306(15), Pd(1)–C(8) = 2.1232(15), Pd(1)–C(9) = 2.1290(15), C(7)–C(8) = 1.445(2), C(8)–C(9) = 1.419(2); Cl(1)–Pd(1)–N(1) = 89.70(4), C(7)–C(8)–C(9) = 117.90(14), C(8)–C(9)–C(14) = 124.64(14).

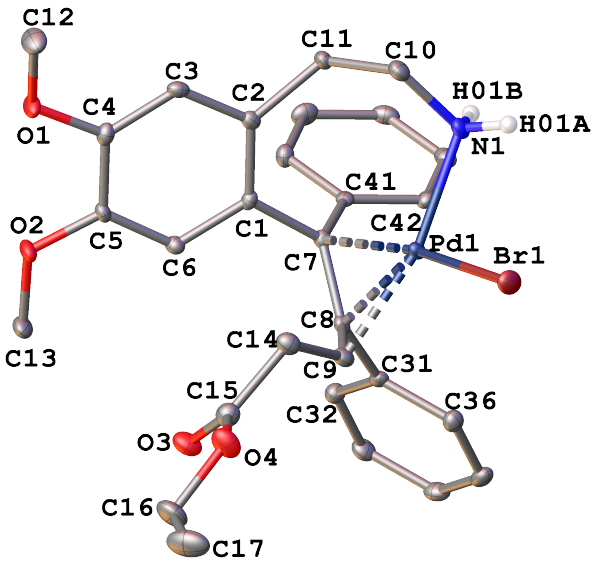

Figure S3. Thermal ellipsoid plot (50 % probability) of *anti*-**2a**·CH_2Cl_2 along with the labeling scheme. The solvent molecule and the hydrogen atoms bonded to carbon have been omitted for clarity. Selected bond lengths (Å) and angles (deg): Pd(1)–Br(1) = 2.4850(3), Pd(1)–N(1) = 2.105(2), Pd(1)–C(7) = 2.132(2), Pd(1)–C(8) = 2.108(3), Pd(1)–C(9) = 2.101(3), C(7)–C(8) = 1.447(4), C(8)–C(9) = 1.430(4); Br(1)–Pd(1)–N(1) = 91.03(6), C(7)–C(8)–C(9) = 120.4(2), C(8)–C(9)–C(14) = 132.1(3).

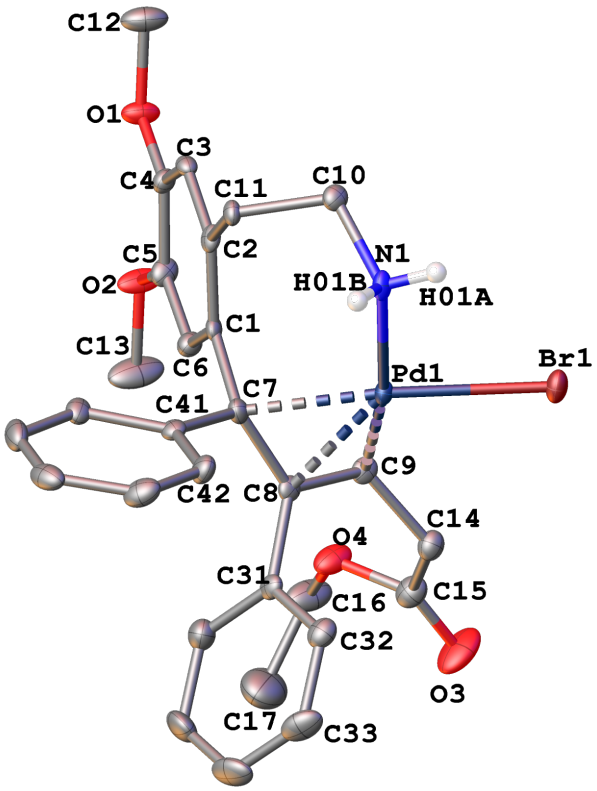

Figure S4. Thermal ellipsoid plot (50 % probability) of *syn*-**2a** along with the labeling scheme. The hydrogen atoms bonded to carbon have been omitted for clarity. Selected bond lengths (Å) and angles (deg): Pd(1)–Br(1) = 2.4878(5), Pd(1)–N(1) = 2.126(3), Pd(1)–C(7) = 2.132(4), Pd(1)–C(8) = 2.125(4), Pd(1)–C(9) = 2.115(3), C(7)–C(8) = 1.435(5), C(8)–C(9) = 1.418(5); Br(1)–Pd(1)–N(1) = 90.86(9), C(7)–C(8)–C(9) = 118.5(3), C(8)–C(9)–C(14) = 122.5(4).

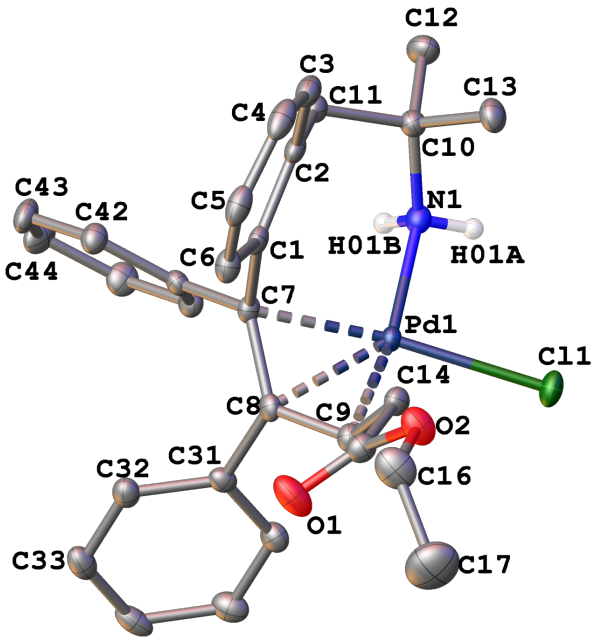

Figure S5. Thermal ellipsoid plot (50 % probability) of *anti*-**2b**·$CHCl_3$ along with the labeling scheme. The solvent molecule and the hydrogen atoms bonded to carbon have been omitted for clarity. Selected bond lengths (Å) and angles (deg): Pd(1)–Cl(1) = 2.3861(7), Pd(1)–N(1) = 2.119(2), Pd(1)–C(7) = 2.138(3), Pd(1)–C(8) = 2.114(3), Pd(1)–C(9) = 2.123(3), C(7)–C(8) = 1.439(4), C(8)–C(9) = 1.425(4); Cl(1)–Pd(1)–N(1) = 91.82(7), C(7)–C(8)–C(9) = 122.1(2), C(8)–C(9)–C(14) = 132.5(2).

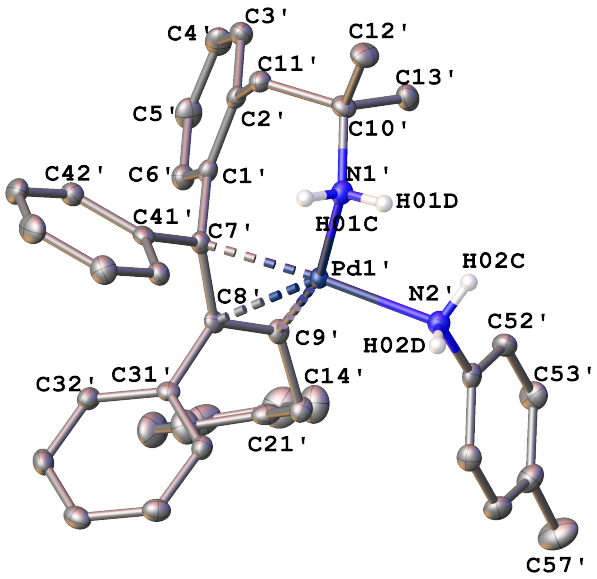

Figure S6. Thermal ellipsoid plot (50 % probability) of the cation of one (A') of the two independent molecules of complex *syn*-**3b**·CH_2Cl_2 along with the labeling scheme. The solvent molecule and the hydrogen atoms bonded to carbon have been omitted for clarity. Selected bond lengths (Å) and angles (deg): Pd(1')–N(1') = 2.130(2), Pd(1')–N(2') = 2.163(2), Pd(1')–C(7') = 2.117(2), Pd(1')–C(8') = 2.134(2), Pd(1')–C(9') = 2.165(2), C(7')–C(8') = 1.452(3), C(8')–C(9') = 1.413(3); N(1')–Pd(1')–N(2') = 88.94(8), C(7')–C(8')–C(9') = 117.5(2), C(8')–C(9')–C(14') = 124.0(2).

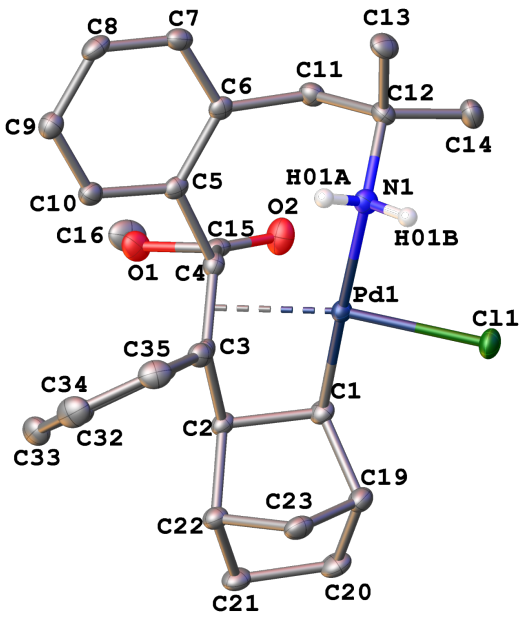

Figure S7. Thermal ellipsoid plot (50 % probability) of **7d**·1/2CH_2Cl_2 along with the labeling scheme. The solvent molecule and the hydrogen atoms bonded to carbon have been omitted for clarity. Selected bond lengths (Å) and angles (deg): Pd(1)–N(1) = 2.219(3), Pd(1)–Cl(1) = 2.3439(8), Pd(1)–C(1) = 2.041(3), Pd(1)–C(3) = 2.177(3), Pd(1)–C(4) = 2.170(3), Pd(1)–X = 2.058, C(1)–C(2) = 1.544(4), C(2)–C(3) = 1.534(4), C(3)–C(4) = 1.400(4), C(4)–C(5) = 1.511(4); N(1)–Pd(1)–Cl(1) = 86.31(7), Cl(1)–Pd(1)–C(1) = 92.68(9), C(1)–Pd(1)–X = 76.7, X–Pd(1)–N(1) = 104.3, C(2)–C(3)–C(4) = 118.3(3), C(3)–C(4)–C(5) = 123.3(3). X represents the midpoint of the double bond C(3)–C(4).

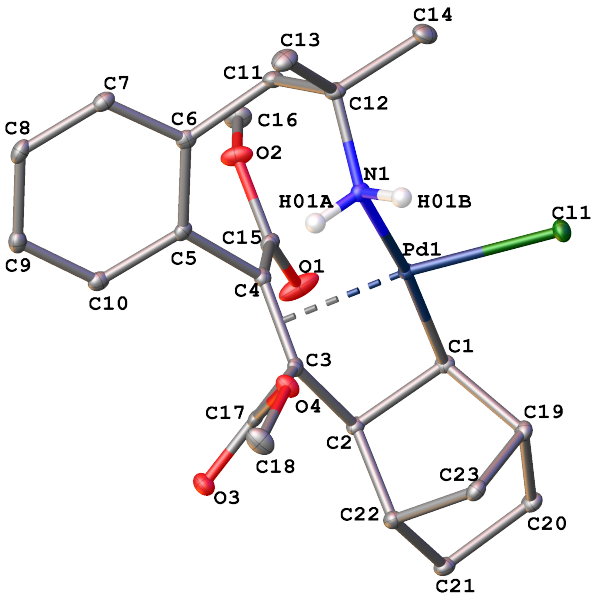

Figure S8. Thermal ellipsoid plot (30 % probability) of **7f** along with the labeling scheme. The hydrogen atoms bonded to carbon have been omitted for clarity. Selected bond lengths (Å) and angles (deg): Pd(1)–N(1) = 2.2240(16), Pd(1)–Cl(1) = 2.3363(5), Pd(1)–C(1) = 2.0583(18), Pd(1)–C(3) = 2.1355(18), Pd(1)–C(4) = 2.2042(18), Pd(1)–X = 2.053, C(1)–C(2) = 1.547(3), C(2)–C(3) = 1.534(2), C(3)–C(4) = 1.405(3), C(4)–C(5) = 1.515(3); N(1)–Pd(1)–Cl(1) = 89.49(5), Cl(1)–Pd(1)–C(1) = 92.99(5), C(1)–Pd(1)–X = 77.6, X–Pd(1)–N(1) = 99.7, C(2)–C(3)–C(4) = 121.82(16), C(3)–C(4)–C(5) = 121.20(17). X represents the midpoint of the double bond C(3)–C(4).

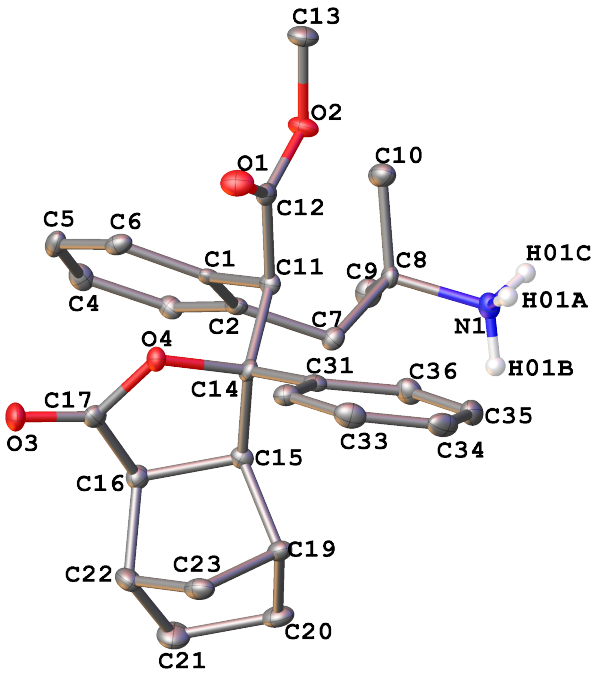

Figure S9. Thermal ellipsoid plot (50 % probability) of the cation of **9d** along with the labeling scheme. The hydrogen atoms bonded to carbon have been omitted for clarity. Selected bond lengths (Å) and angles (deg): N(1)–C(8) = 1.517(3), C(11)–C(12) = 1.523(3), C(11)–C(14) = 1.554(3), C(14)–O(4) = 1.461(3), C(17)–O(3) = 1.213(3), C(17)–O(4) = 1.338(3), C(16)–C(17) = 1.505(3); C(1)–C(11)–C(12) = 110.01(19), C(11)–C(14)–O(4) = 108.07(18), C(14)–O(4)–C(17) = 112.77(17), O(4)–C(17)–C(16) = 111.8(2), C(17)–C(16)–C(15) = 104.35(19), C(16)–C(15)–C(14) = 104.38(18), C(15)–C(14)–O(4) = 105.06(17).

Table S5. Hydrogen bonds for complex *anti*-**1b** (Å and deg).

D–H···A	d(D–H)	d(H···A)	d(D···A)	<(DHA)
N(1)–H(01A)···Cl(1)#1	0.85(2)	2.57(2)	3.339(2)	151(3)

Symmetry transformations used to generate equivalent atoms: #1 -x+1,-y+2,-z+1

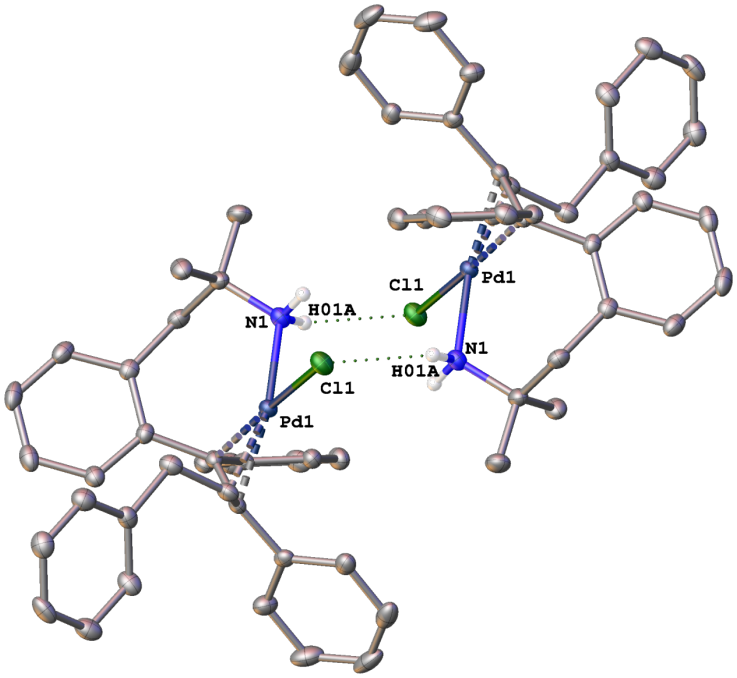

Figure S10. Thermal ellipsoid plot (50 % probability) of complex *anti*-**1b** showing the dimers formed through hydrogen bonds.

Table S6. Hydrogen bonds for complex *syn*-**1b** (Å and deg).

D–H···A	d(D–H)	d(H···A)	d(D···A)	<(DHA)
N(1)–H(01B)···Cl(1)#1	0.845(17)	2.71(2)	3.3336(15)	131.3(18)

Symmetry transformations used to generate equivalent atoms: #1 -x,-y+2,-z+1

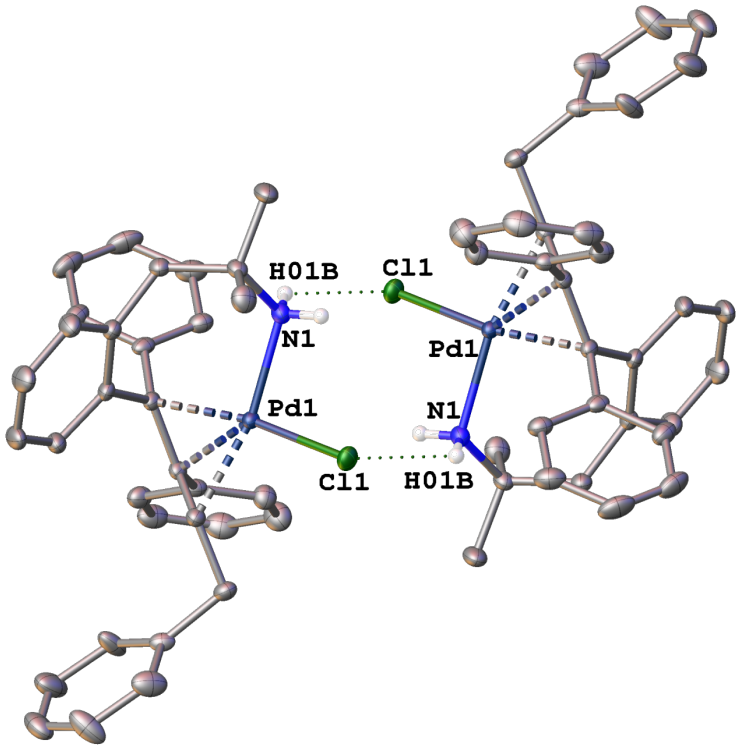

Figure S11. Thermal ellipsoid plot (50 % probability) of complex *syn*-**1b** showing the dimers formed through hydrogen bonds.

Table S7. Hydrogen bonds for complex *anti*-**2a**·CH_2Cl_2 (Å and deg).

D–H...A	d(D–H)	d(H···A)	d(D···A)	<(DHA)
C(99)–H(99B)···Br(1)#1	0.99	2.79	3.725(4)	157.6
C(99)–H(99A)···O(4)#1	0.99	2.53	3.343(4)	139.4
C(3)–H(3)···O(3)#2	0.95	2.44	3.344(3)	160.0
N(1)–H(01A)···Br(1)#1	0.91	2.72	3.472(2)	140.2

Symmetry transformations used to generate equivalent atoms:

#1 -x+3/2,y+1/2,-z+1/2 #2 x,y+1,z

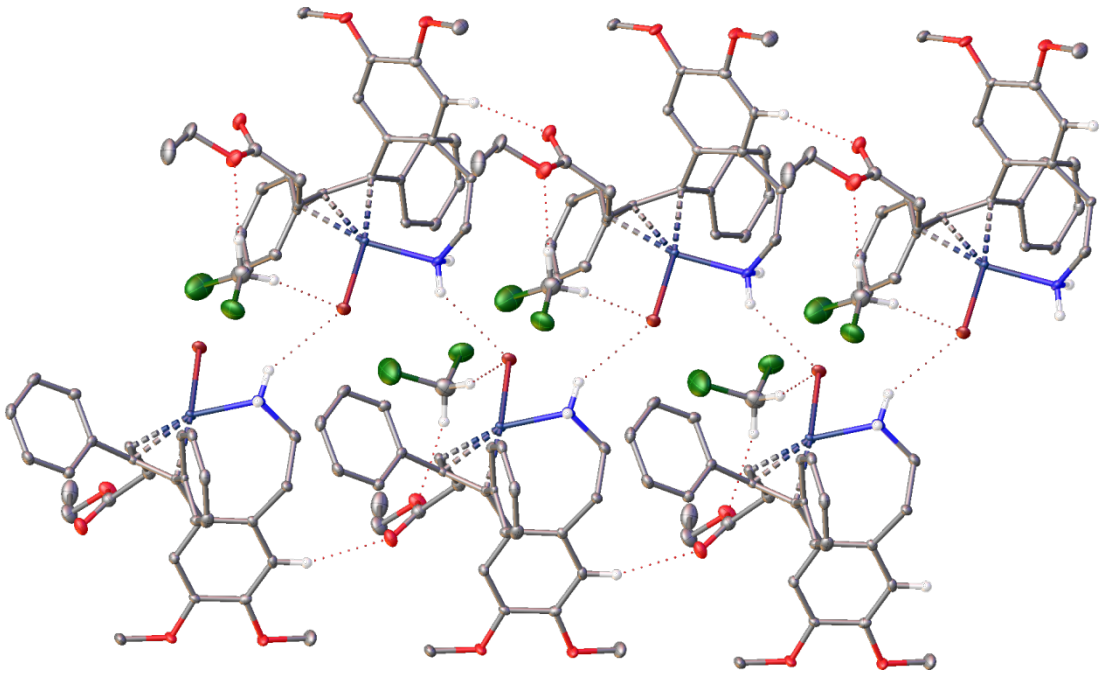

Figure S12. X-ray packing view (50 % probability) of *anti*-**2a**·CH_2Cl_2 showing the double chains parallel to the *b* axis formed through hydrogen bonds.

Table S8. Hydrogen bonds for complex *syn*-**2a** (Å and deg).

D–H···A	d(D–H)	d(H···A)	d(D···A)	<(DHA)
N(1)–H(01A)···Br(1)	0.82(3)	2.93(4)	3.297(3)	110(3)
N(1)–H(01B)···Br(1)#1	0.81(3)	2.71(3)	3.481(4)	160(4)

Symmetry transformations used to generate equivalent atoms: #1 x-1/2,-y+3/2,-z+2

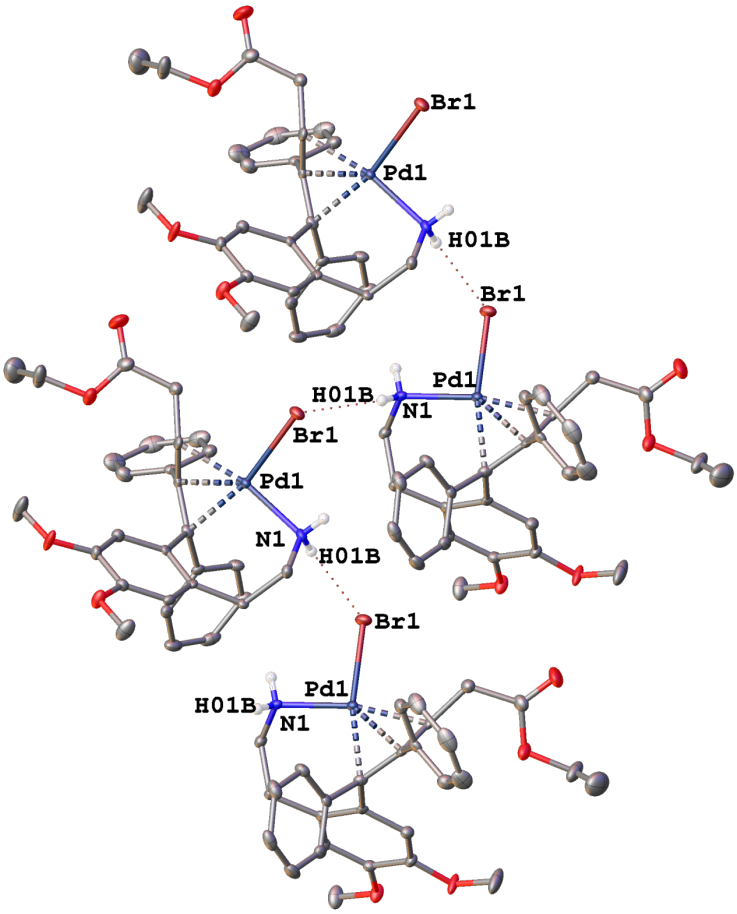

Figure S13. X-ray packing view (50 % probability) of *syn*-**2a** showing the *zigzag* chains parallel to the *a* axis formed through hydrogen bonds.

Table S9. Hydrogen bonds for complex *anti*-**2b**·$CHCl_3$ (Å and deg).

D–H···A	d(D–H)	d(H···A)	d(D···A)	<(DHA)
N(1)–H(01B)···Cl(1)#1	0.837(18)	2.69(2)	3.402(2)	144(3)
C(34)–H(34)···O(1)#2	0.95	2.42	3.350(4)	168.1

Symmetry transformations used to generate equivalent atoms:

#1 -x+1,-y+1,-z+1 #2 -x+1,-y+1,-z+2

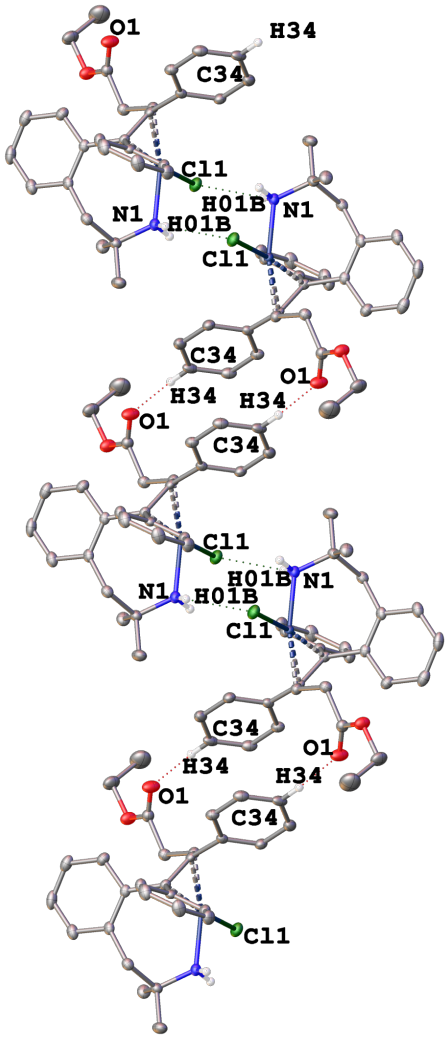

Figure S14. X-ray packing view (50 % probability) of *anti*-**2b**·$CHCl_3$ showing the *zigzag* chains parallel to the *c* axis formed through hydrogen bonds.

Table S10. Hydrogen bonds for complex *syn*-**2b** (Å and deg).

D–H...A	d(D–H)	d(H···A)	d(D···A)	<(DHA)
N(1)–H(01A)···Cl(1)#1	0.844(19)	2.61(2)	3.3340(19)	145(2)
C(42)–H(42)···O(2)#2	0.95	2.57	3.462(3)	155.9

Symmetry transformations used to generate equivalent atoms: #1 -x+2,-y,-z+1 #2 x-1,y,z

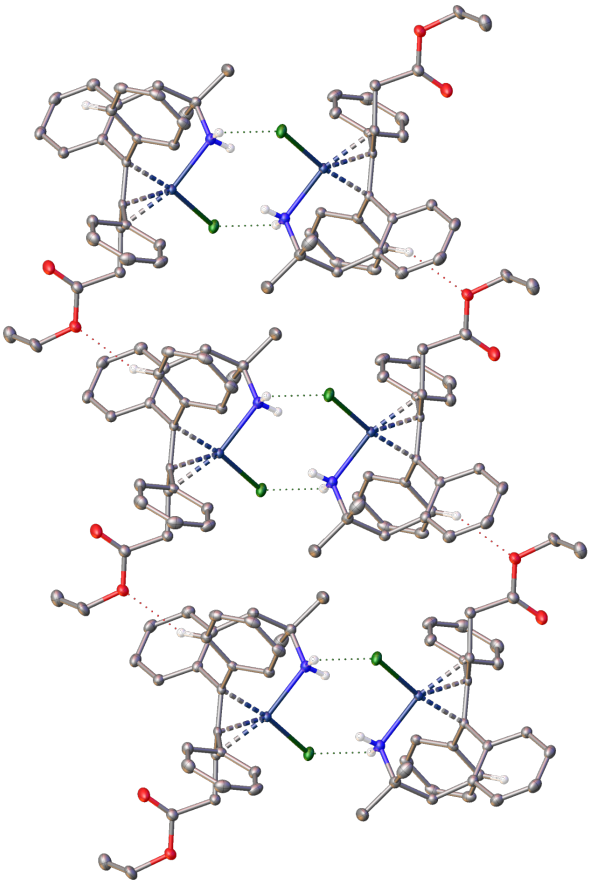

Figure S15. X-ray packing view (50 % probability) of *syn*-**2b** showing the double chains parallel to the *a* axis formed through hydrogen bonds.

Table S11. Hydrogen bonds for complex *syn*-**3b**·CH_2Cl_2 (Å and deg).

D–H···A	d(D–H)	d(H···A)	d(D···A)	<(DHA)
N(1)–H(01A)···O(2)	0.86(3)	2.30(3)	3.143(3)	170(3)
N(2)–H(02A)···O(1)	0.89(3)	2.09(4)	2.925(3)	155(3)
N(1')–H(01D)···O(6)#1	0.81(3)	2.35(3)	3.153(3)	172(3)
N(2')–H(02C)···O(5)#1	0.86(3)	2.16(3)	2.942(3)	153(3)
N(2')–H(02D)···O(6)#2	0.80(3)	2.42(3)	3.200(3)	165(3)

Symmetry transformations used to generate equivalent atoms: #1 -x+1,-y,-z #2 x+1,y,z

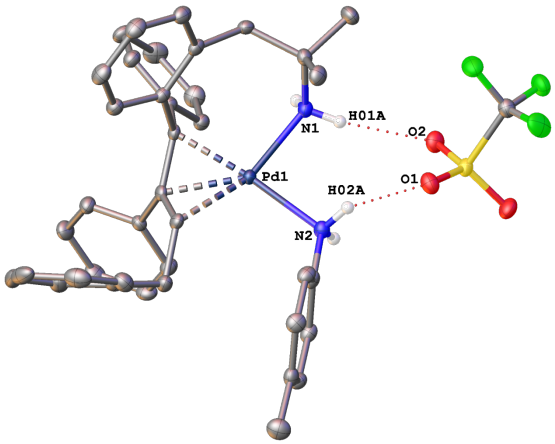

Figure S16. Thermal ellipsoid plot (50 % probability) of *syn*-**3b**·CH_2Cl_2 (molecule A) showing the hydrogen bonds between the cation and the triflate group.

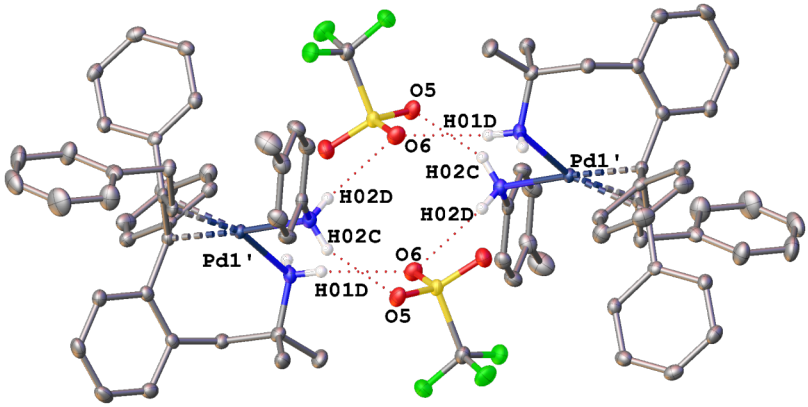

Figure S17. Thermal ellipsoid plot (50 % probability) of **3b**·CH_2Cl_2 (molecule A') showing the dimers formed through hydrogen bonds.

Table S12. Hydrogen bonds for compound **6b**·H_2O (Å and deg).

D–H···A	d(D–H)	d(H···A)	d(D···A)	<(DHA)
O(4)–H(04A)···O(3)#1	0.87(2)	1.89(2)	2.760(2)	177(2)
N(1)–H(01B)···O(4)#2	0.907(19)	1.85(2)	2.753(2)	171(2)
N(1)–H(01A)···O(1)#3	0.905(19)	1.95(2)	2.854(2)	176(2)
O(4)–H(04B)···O(1)	0.86(2)	1.99(2)	2.788(2)	154(3)
N(1)–H(01C)···O(2)	0.93(3)	1.94(3)	2.855(2)	164(2)

Symmetry transformations used to generate equivalent atoms:

#1 -x,y+1/2,-z+1/2 #2 x,-y+3/2,z-1/2 #3 -x,y-1/2,-z+1/2

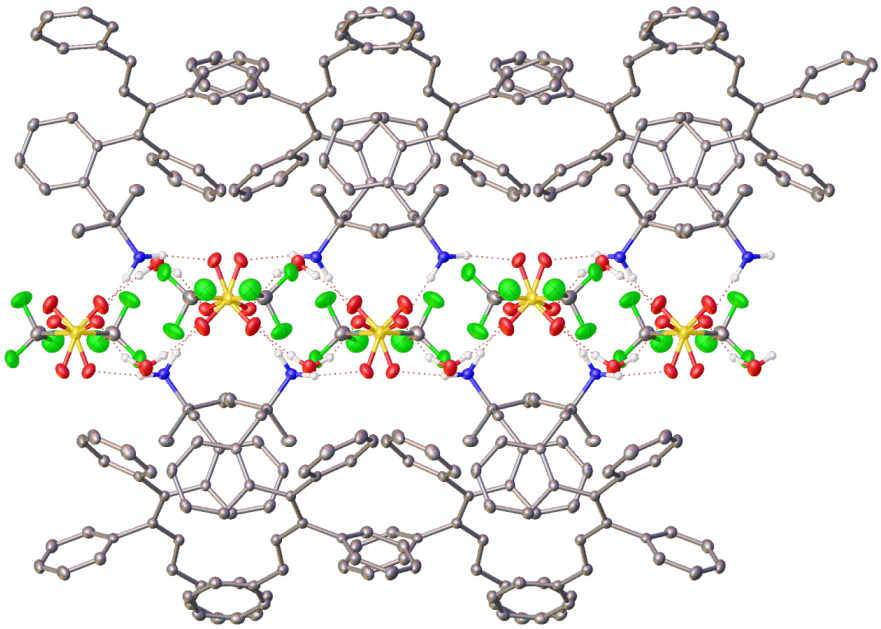

Figure S18. X-ray packing view (50 % probability) of **6b**·H_2O showing the double chains parallel to the *b* axis formed through hydrogen bonds.

Table S13. Hydrogen bonds for compound **7c**·$CHCl_3$ (Å and deg).

D–H···A	d(D–H)	d(H···A)	d(D···A)	<(DHA)
C(99)–H(99)···Cl(1)#1	1.00	2.43	3.409(2)	167.4

Symmetry transformations used to generate equivalent atoms: #1 x+1/2,-y+1/2,z-1/2

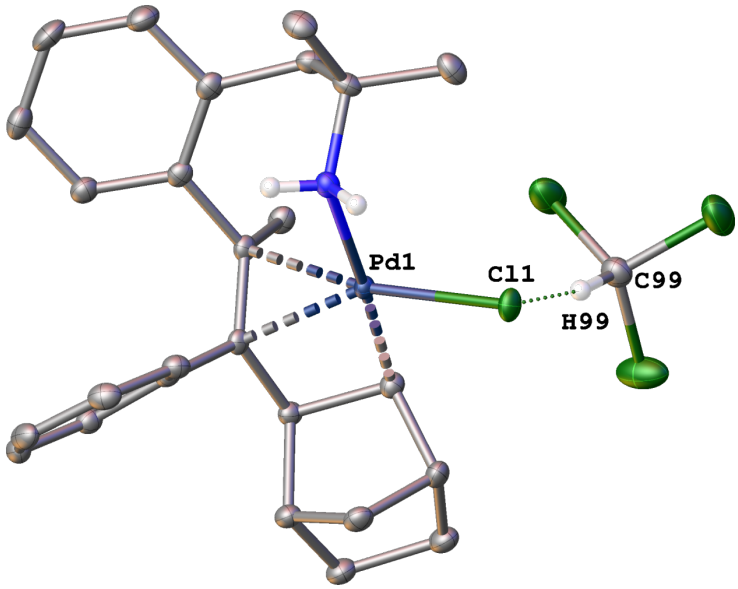

Figure S19. Thermal ellipsoid plot (50 % probability) of **7c**·$CHCl_3$ showing the hydrogen bond between complex **7c** and the crystallization solvent.

Table S14. Hydrogen bonds for compound **7d**·1/2$CHCl_3$ (Å and deg).

D–H···A	d(D–H)	d(H···A)	d(D···A)	<(DHA)
C(11)–H(11B)···O(2)	0.99	2.46	3.391(4)	156.7

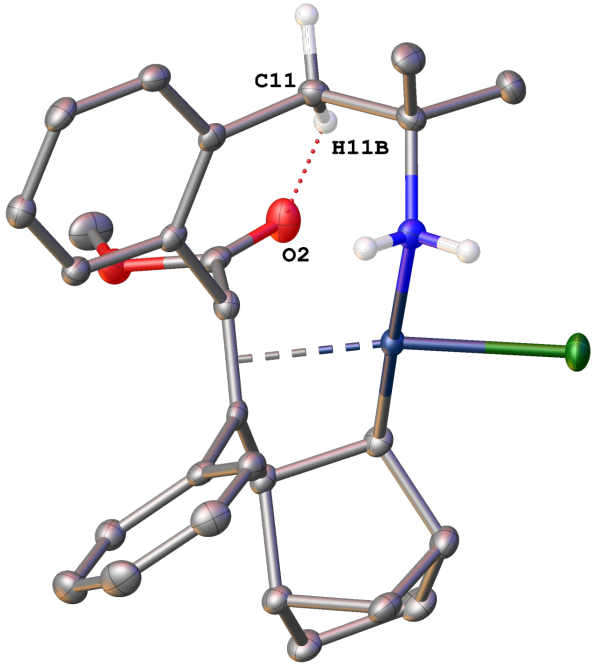

Figure S20. Thermal ellipsoid plot (50 % probability) of **7d**·1/2$CHCl_3$ showing the intramolecular hydrogen bond.

Table S15. Hydrogen bonds for compound **7f** (Å and deg).

D–H···A	d(D–H)	d(H···A)	d(D···A)	<(DHA)
N(1)–H(01A)···O(4)	0.827(18)	2.36(2)	2.956(2)	129(2)
N(1)–H(01B)···Cl(1)#1	0.833(17)	2.80(2)	3.4396(18)	134.7(18)
C(11)–H(11A)···O(3)#2	0.99	2.59	3.495(2)	151.4
C(16)–H(16C)···O(3)#3	0.98	2.59	3.401(3)	140.3

Symmetry transformations used to generate equivalent atoms:

#1 -x+2,-y+2,-z #2 -x+3/2,y-1/2,-z+1/2 #3 -x+2,-y+2,-z+1

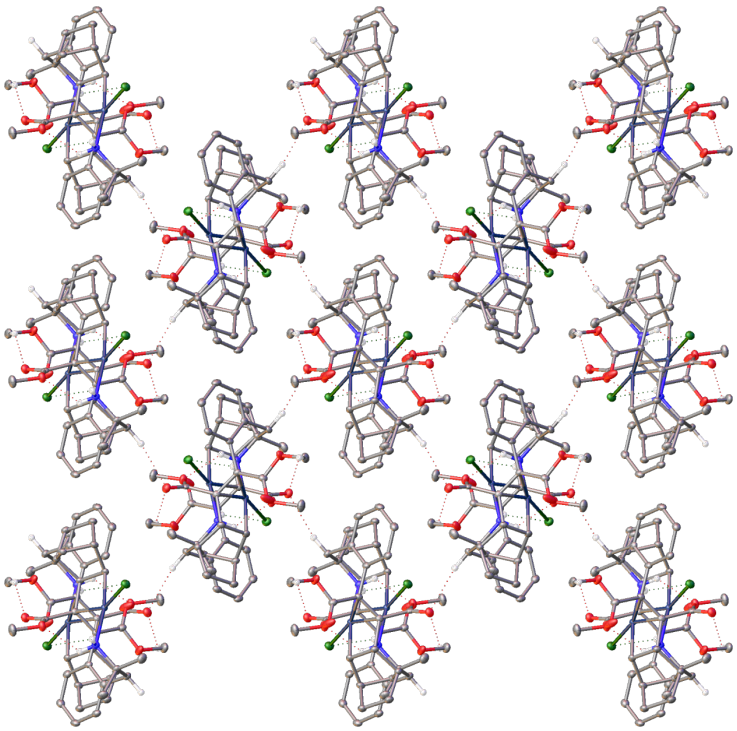

Figure S21. X-ray packing view (30 % probability) of **7f** showing the three-dimensional net, formed through hydrogen bonds, viewed down the crystallographic *c* axis.

Table S16. Hydrogen bonds for compound **8f** (Å and deg).

D–H···A	d(D–H)	d(H···A)	d(D···A)	<(DHA)
N(1)–H(01A)···O(2)	0.908(15)	2.005(16)	2.7930(16)	144.3(15)
N(1)–H(01B)···O(6)#1	0.897(16)	2.007(17)	2.7834(15)	144.0(17)
C(12)–H(12A)···O(6)#2	0.98	2.53	3.4215(19)	151.8
C(23)–H(23B)···O(5)#3	0.98	2.60	3.4925(18)	151.8
C(6)–H(6)···O(7)	0.95	2.56	3.4679(17)	159.3
C(21)–H(21B)···O(5)	0.98	2.46	3.2902(18)	141.8

Symmetry transformations used to generate equivalent atoms:

#1 x,y-1,z #2 -x,-y+1,-z #3 -x,-y+1,-z+1

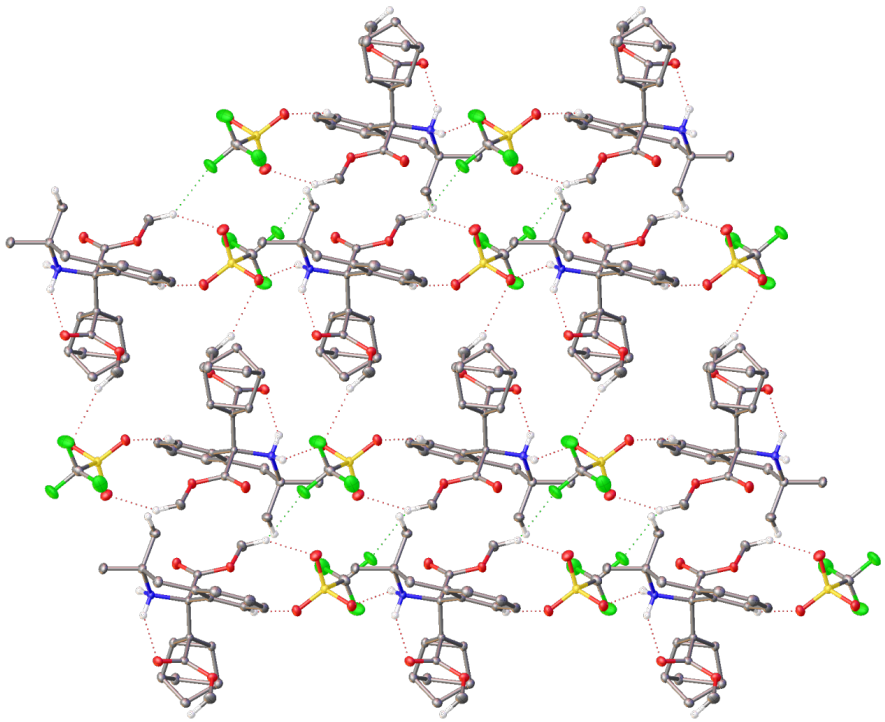

Figure S22. X-ray packing view (50 % probability) of **8f** showing the three-dimensional net, formed through hydrogen bonds, viewed down the crystallographic *a* axis.

Table S17. Hydrogen bonds for compound **9d** (Å and deg).

D–H···A	d(D–H)	d(H···A)	d(D···A)	<(DHA)
N(1)–H(01A)···O(3)#1	0.893(18)	2.09(2)	2.921(3)	154(3)
N(1)–H(01B)···O(1)#2	0.891(19)	2.28(2)	3.085(3)	150(3)
N(1)–H(01C)···O(6)#3	0.892(19)	1.913(19)	2.797(3)	171(3)
C(9)–H(9A)···F(3)#4	0.98	2.43	3.354(3)	158.0
C(9)–H(9B)···O(1)#2	0.98	2.57	3.384(3)	140.5
C(10)–H(10A)···O(3)#1	0.98	2.43	3.209(3)	136.6

Symmetry transformations used to generate equivalent atoms:

#1 -x+3/2,y+1/2,z #2 x+1/2,-y+1/2,-z #3 -x+2,-y+1,-z #4 x,-y+1/2,z-1/2

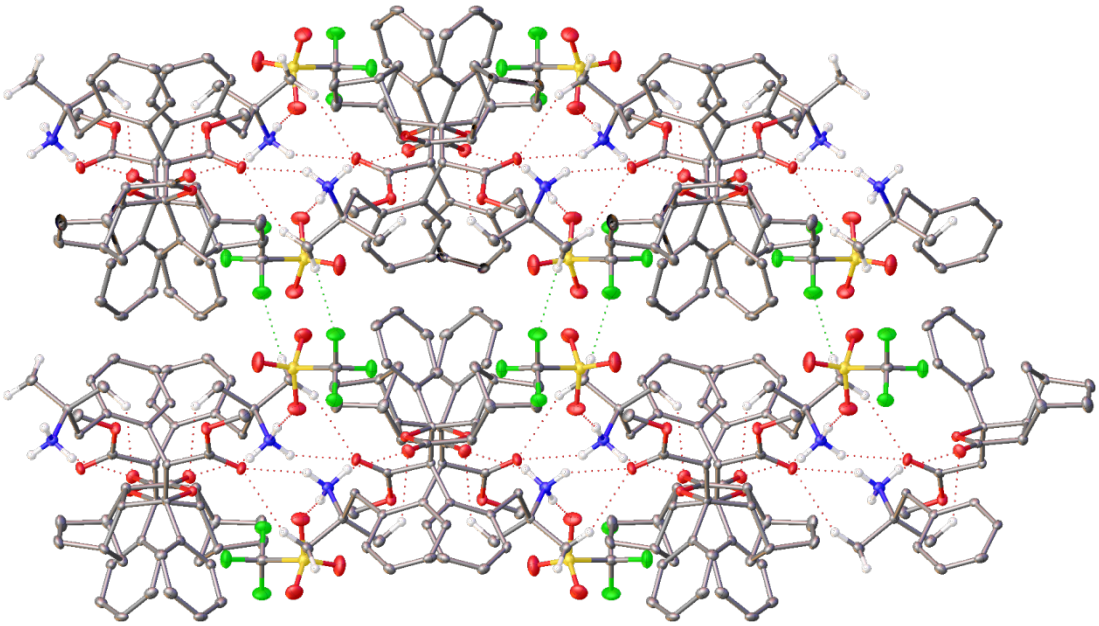

Figure S23. X-ray packing view (50 % probability) of **9d** showing showing the three-dimensional net, formed through hydrogen bonds, viewed down the crystallographic *b* axis.

Table S18. Hydrogen bonds for compound **9f**·Et_2O (Å and deg).

D–H···A	d(D–H)	d(H···A)	d(D···A)	<(DHA)
N(1)–H(01B)···O(9)	0.87(2)	2.06(2)	2.916(2)	167.1(19)
C(7)–H(7A)···O(6)	0.99	2.37	3.1974(19)	140.1
N(1)–H(01A)···O(3)#1	0.91(2)	1.94(2)	2.8063(19)	158.7(16)
N(1)–H(01C)···O(83)#2	0.90(2)	2.19(2)	2.9997(18)	150.0(18)
C(9)–H(9A)···O(7)#3	0.98	2.52	3.398(2)	148.3
C(81)–H(81C)···O(8)#4	0.98	2.57	3.468(3)	153.1

Symmetry transformations used to generate equivalent atoms:

#1 x+1/2,-y+1/2,z-1/2 #2 x,y,z-1 #3 x-1,y,z #4 x,y,z+1

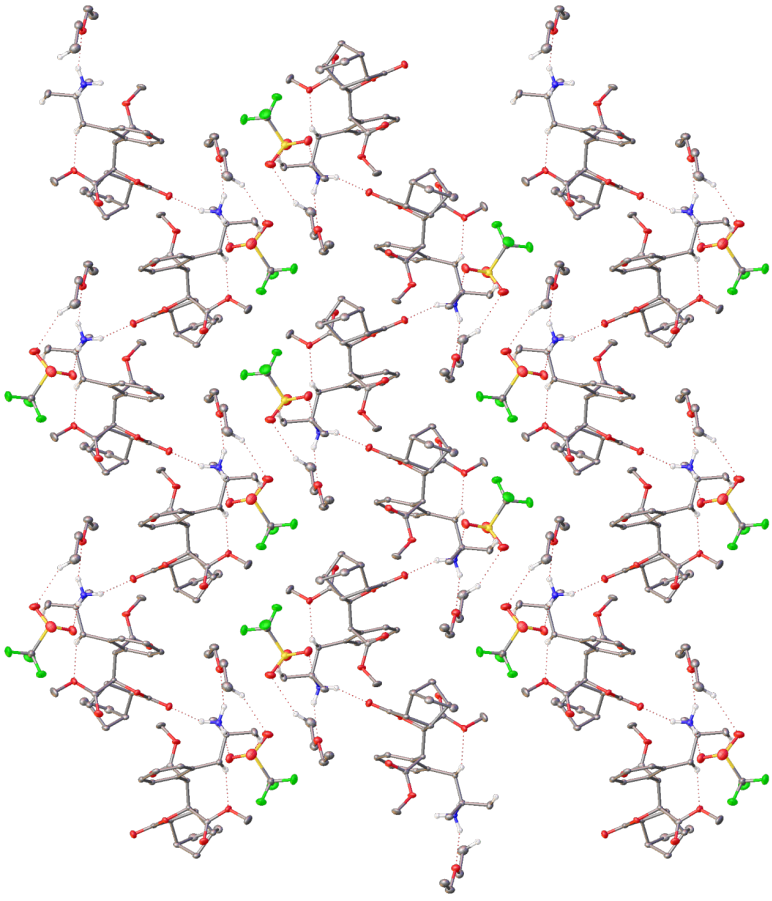

Figure S24. X-ray packing view (50 % probability) of **9f**·Et_2O showing the layers paralel to the ab plane, viewed down the crystallographic *c* axis.

Table S19. Hydrogen bonds for compound **10c**·H_2O (Å and deg).

D–H···A	d(D-H)	d(H···A)	d(D···A)	<(DHA)
C(7)–H(7A)···O(1)	0.99	2.49	3.389(2)	150.7
N(1)–H(01A)···O(1)	0.922(16)	2.226(18)	3.064(2)	150.8(19)
N(1)–H(01A)···O(4)	0.922(16)	2.53(2)	3.104(2)	120.8(17)
N(1)–H(01B)···O(99)#1	0.918(16)	1.867(17)	2.774(2)	169(2)
N(1)–H(01C)···O(3)#1	0.926(16)	2.014(17)	2.912(2)	163(2)
O(2)–H(2)···O(4)	0.84	1.87	2.710(2)	173.1
O(99)–H(99A)···O(5)#2	0.842(10)	2.158(15)	2.890(2)	145(2)
O(99)–H(99B)···O(1)	0.843(9)	2.114(14)	2.881(2)	151(2)

Symmetry transformations used to generate equivalent atoms:

#1 -x+1,-y,-z+1 #2 x+1,y,z

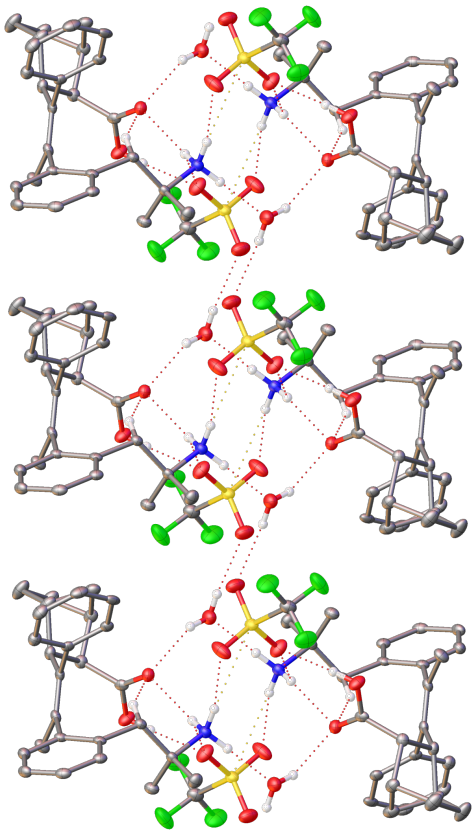

Figure S25. X-ray packing view (50 % probability) of **10c**·H_2O showing the double chains paralel to the *a* axis formed through hydrogen bonds.

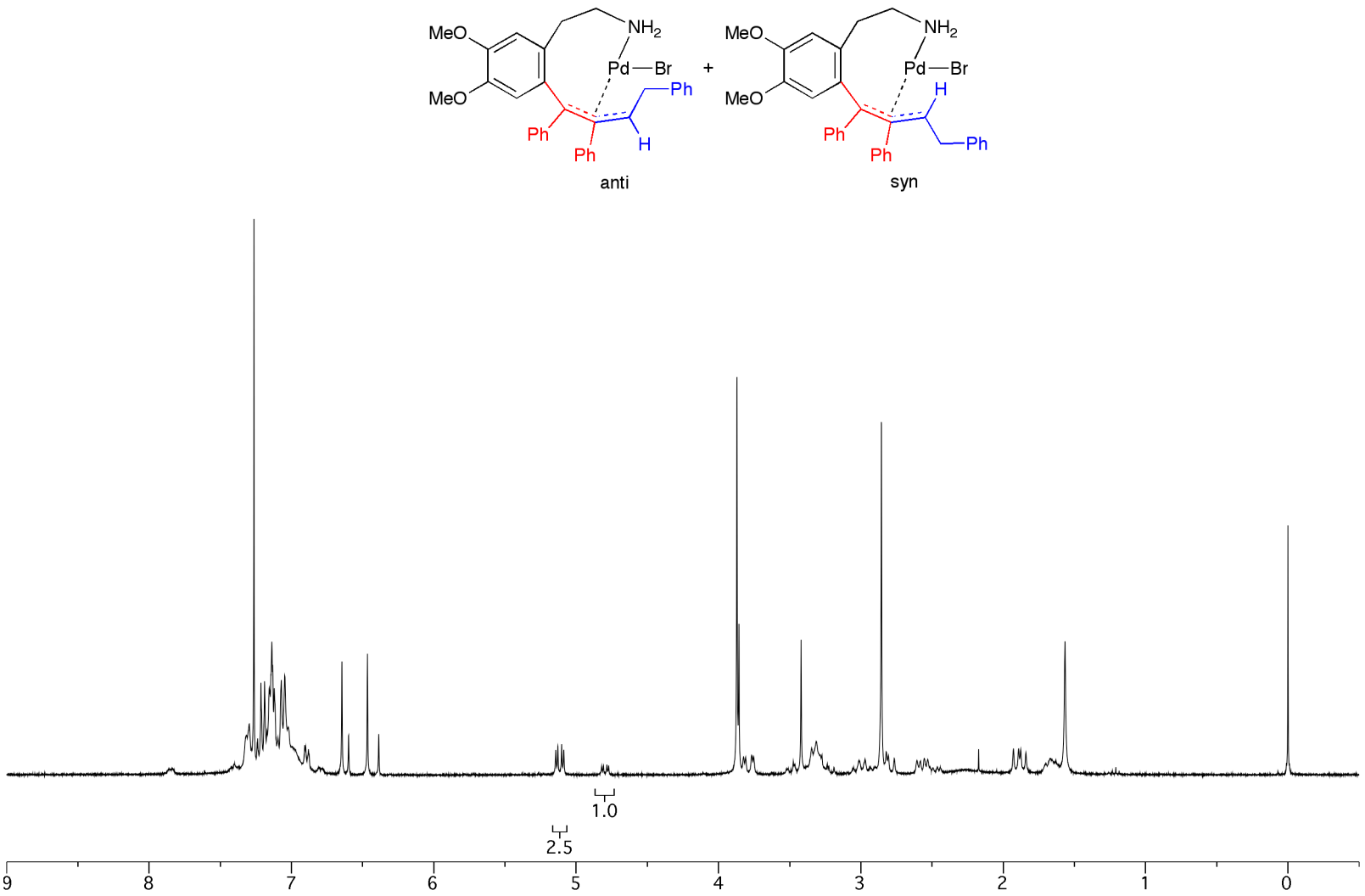

Figure S26. ^{1}H NMR spectrum of a 2.5:1 mixture of *anti/syn*-**1a** (300.1 MHz, $CDCl_3$, 25 ºC)

(From left to right, the asteriks indicate the signals corresponding to $CHCl_3$, and H_2O)

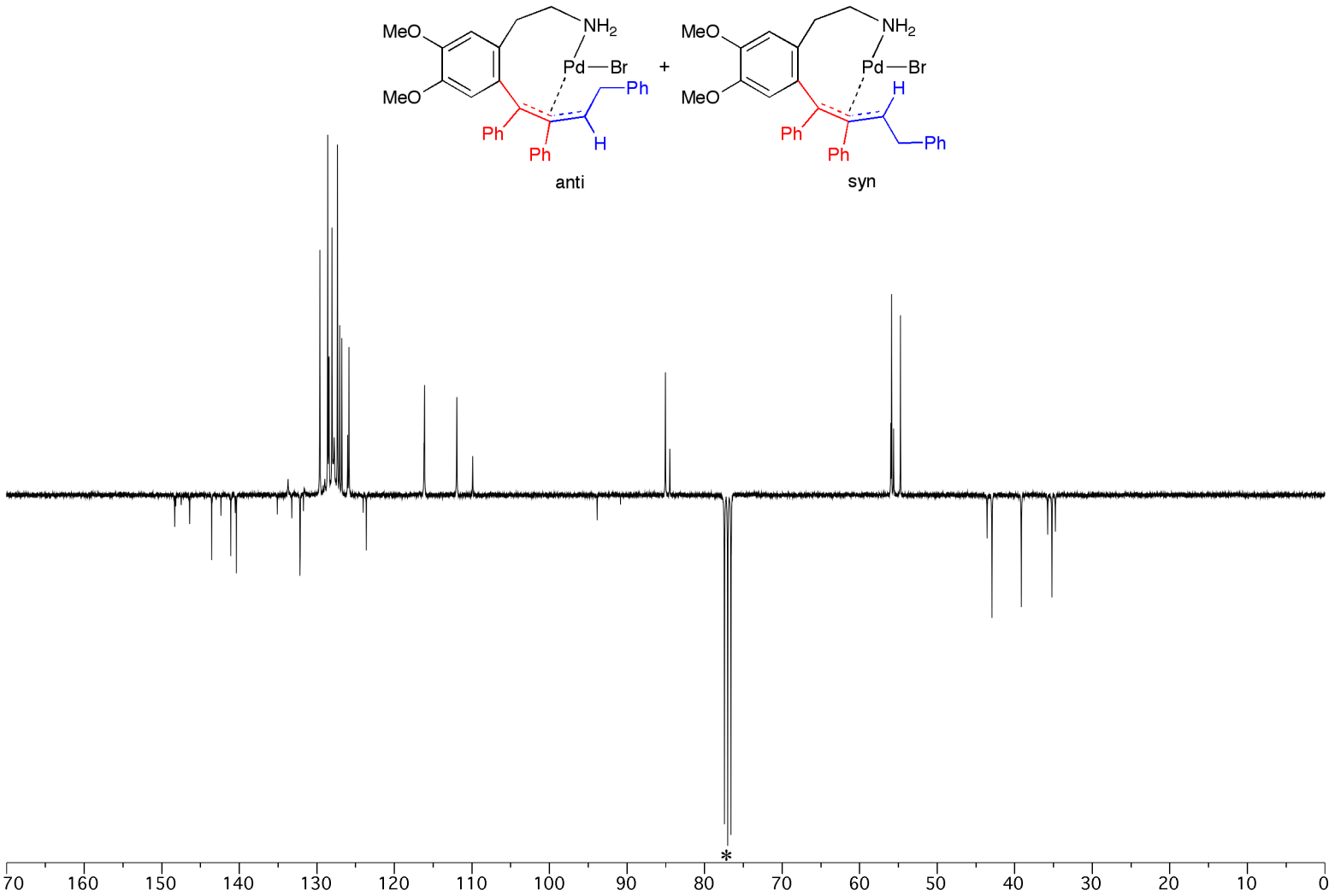

Figure S27. $^{13}C\{^{1}H\}$ APT NMR spectrum of 2.5:1 mixture of *anti/syn*-**1a** (75.5 MHz, $CDCl_3$, 25 ºC)

(The asterik indicates the signal corresponding to $CDCl_3$)

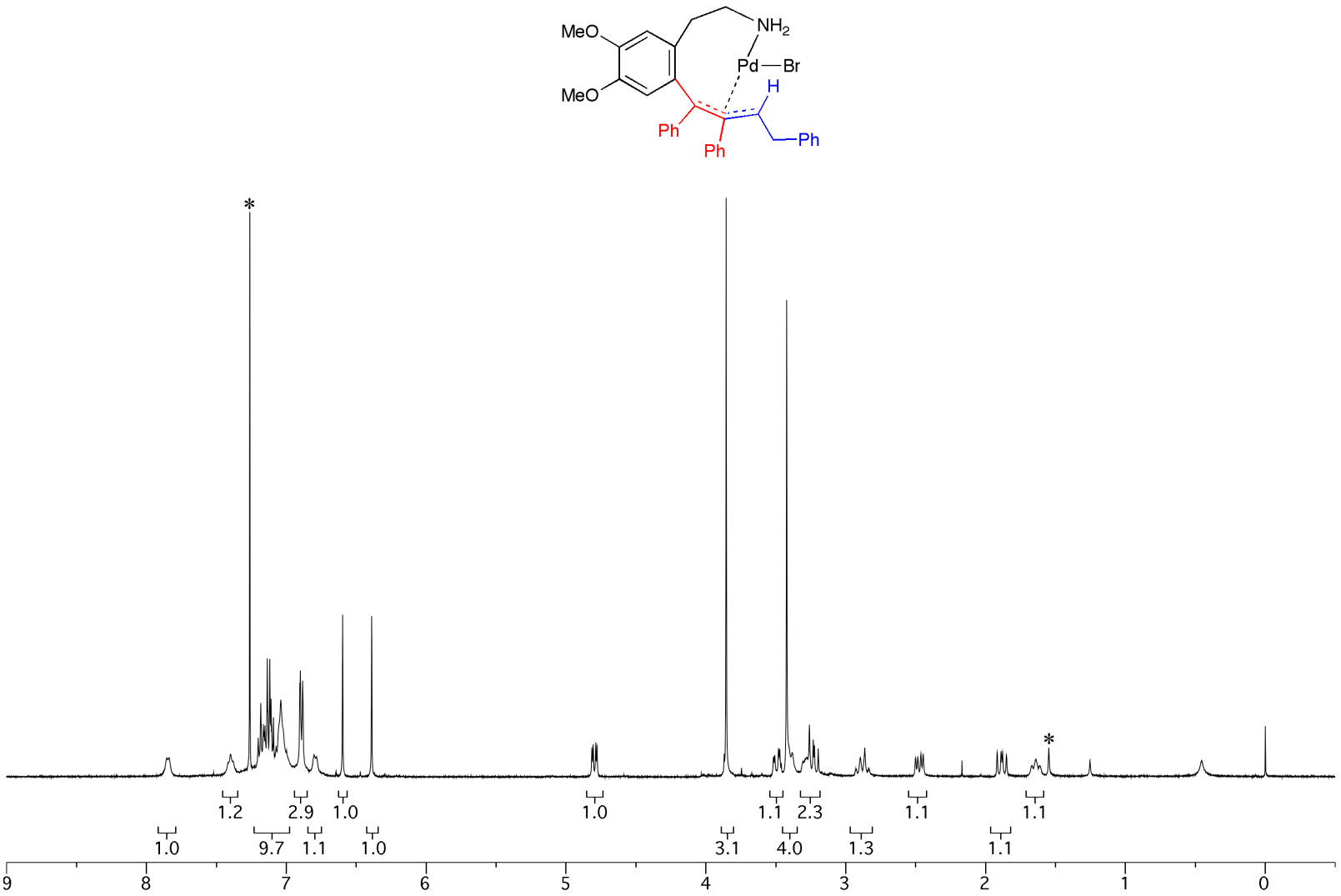

Figure S28. ^{1}H NMR spectrum of *syn*-**1a** (400.9 MHz, $CDCl_3$, 25 ºC)

(From left to right, the asteriks indicate the signals corresponding to $CHCl_3$, and H_2O)

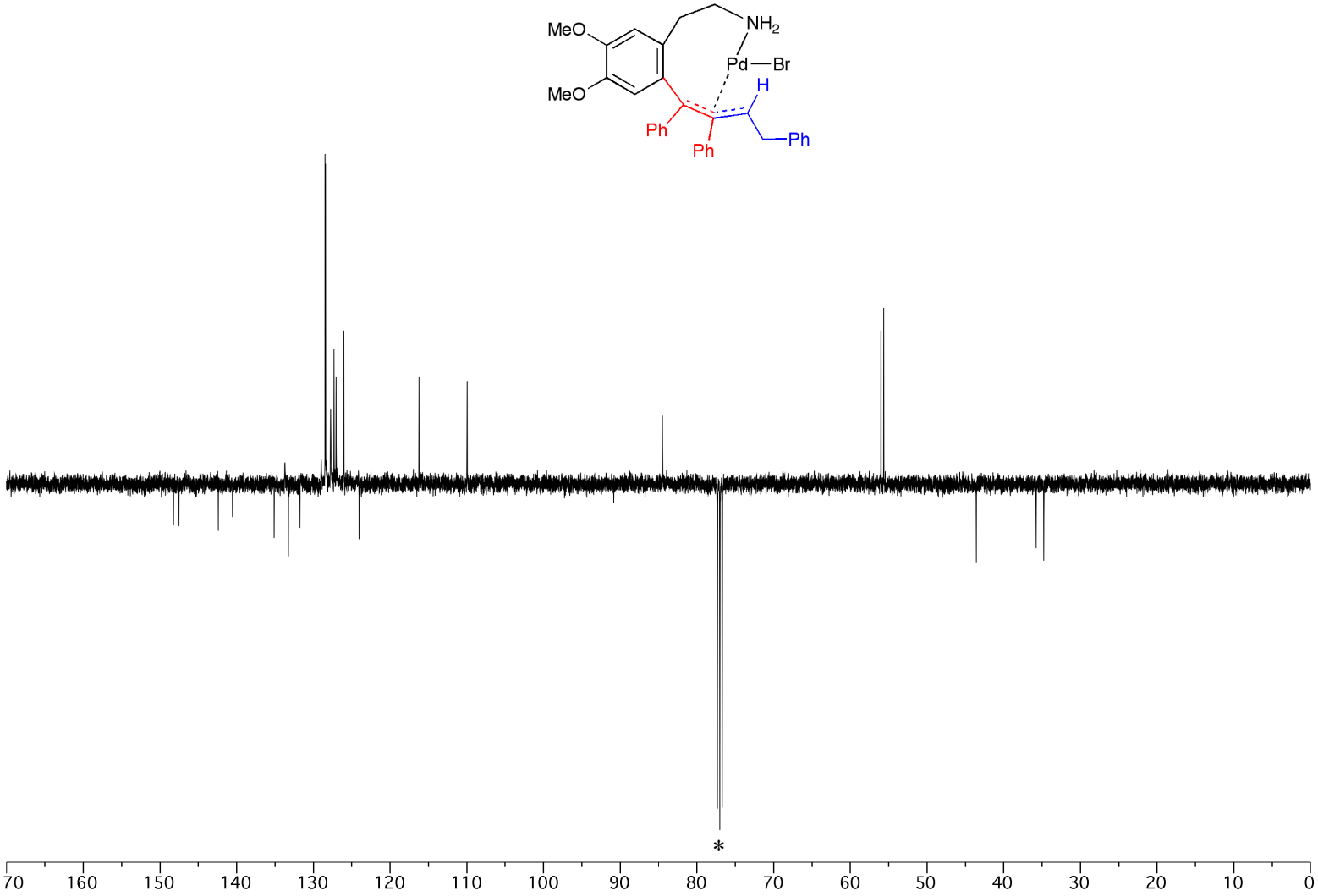

Figure S29. $^{13}C\{^{1}H\}$ APT NMR spectrum of *syn*-**1a** (100.8 MHz, $CDCl_3$, 25 ºC)

(The asterik indicates the signal corresponding to $CDCl_3$)

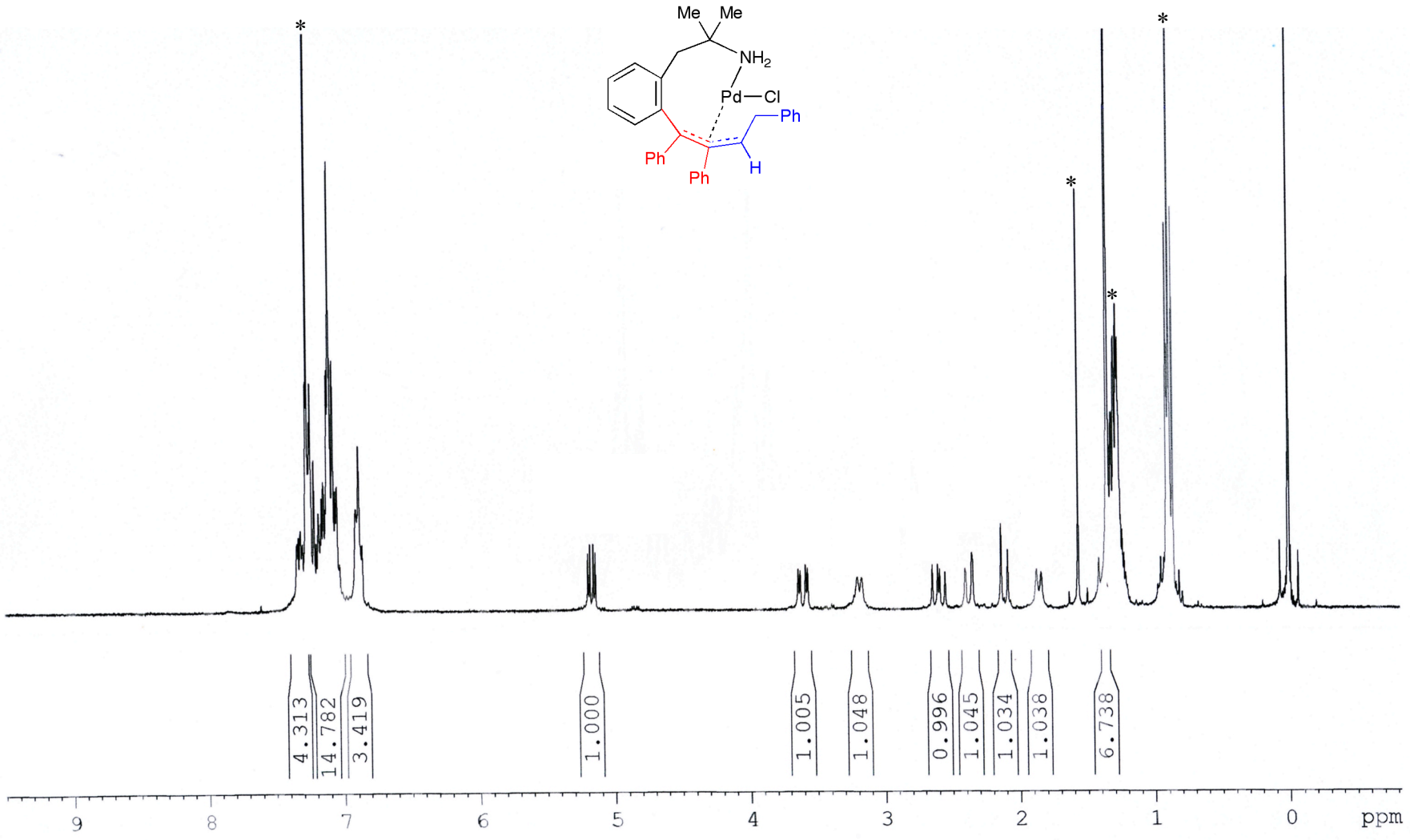

Figure S30. ^{1}H NMR spectrum of *anti*-**1b** (300.1 MHz, $CDCl_3$, 25 ºC)

(From left to right, the asteriks indicate the signals corresponding to $CHCl_3$, H_2O, and *n*-pentane)

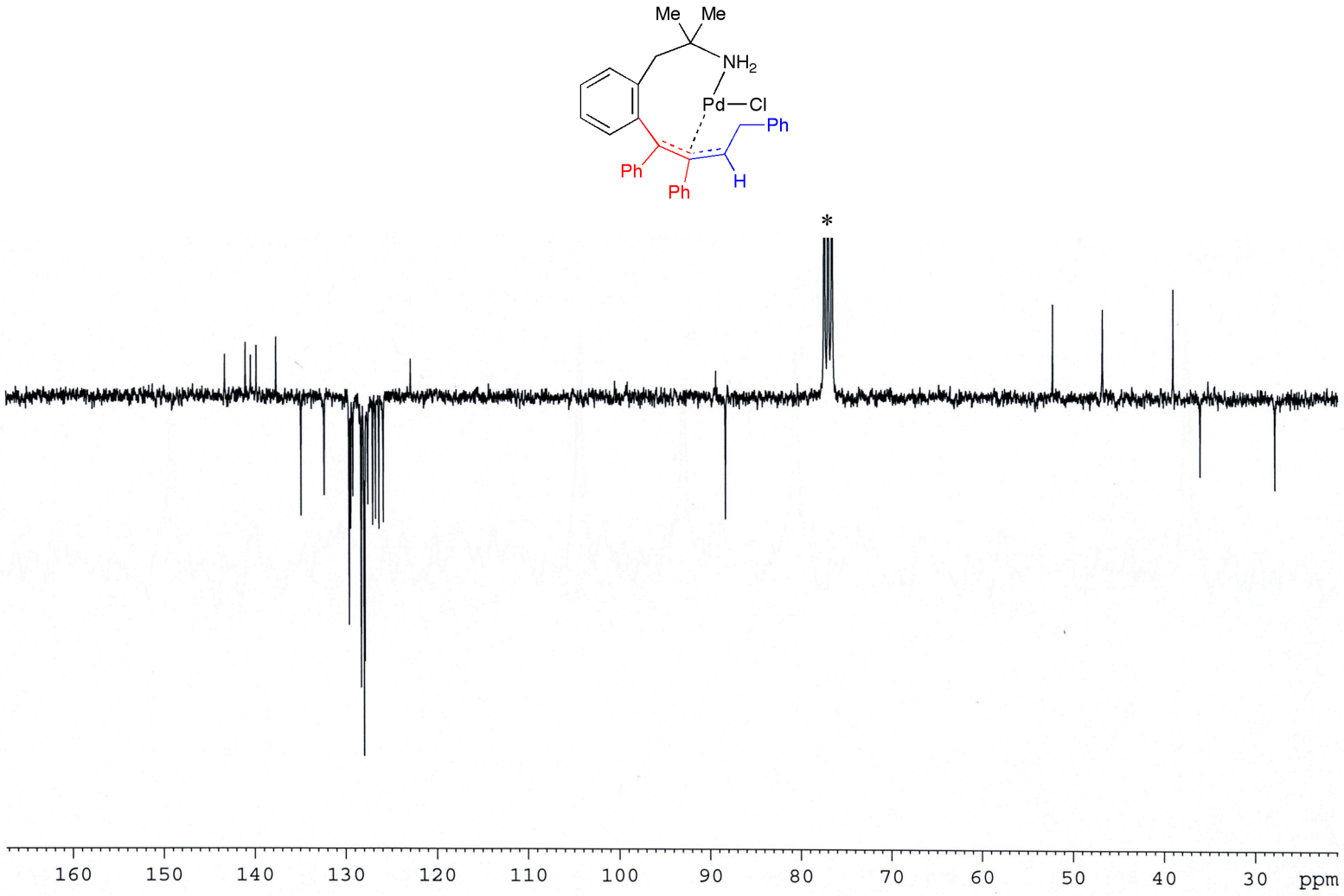

Figure S31. $^{13}C\{^{1}H\}$ APT NMR spectrum of *anti*-**1b** (75.5 MHz, $CDCl_3$, 25 ºC)

(The asterik indicates the signal corresponding to $CDCl_3$)

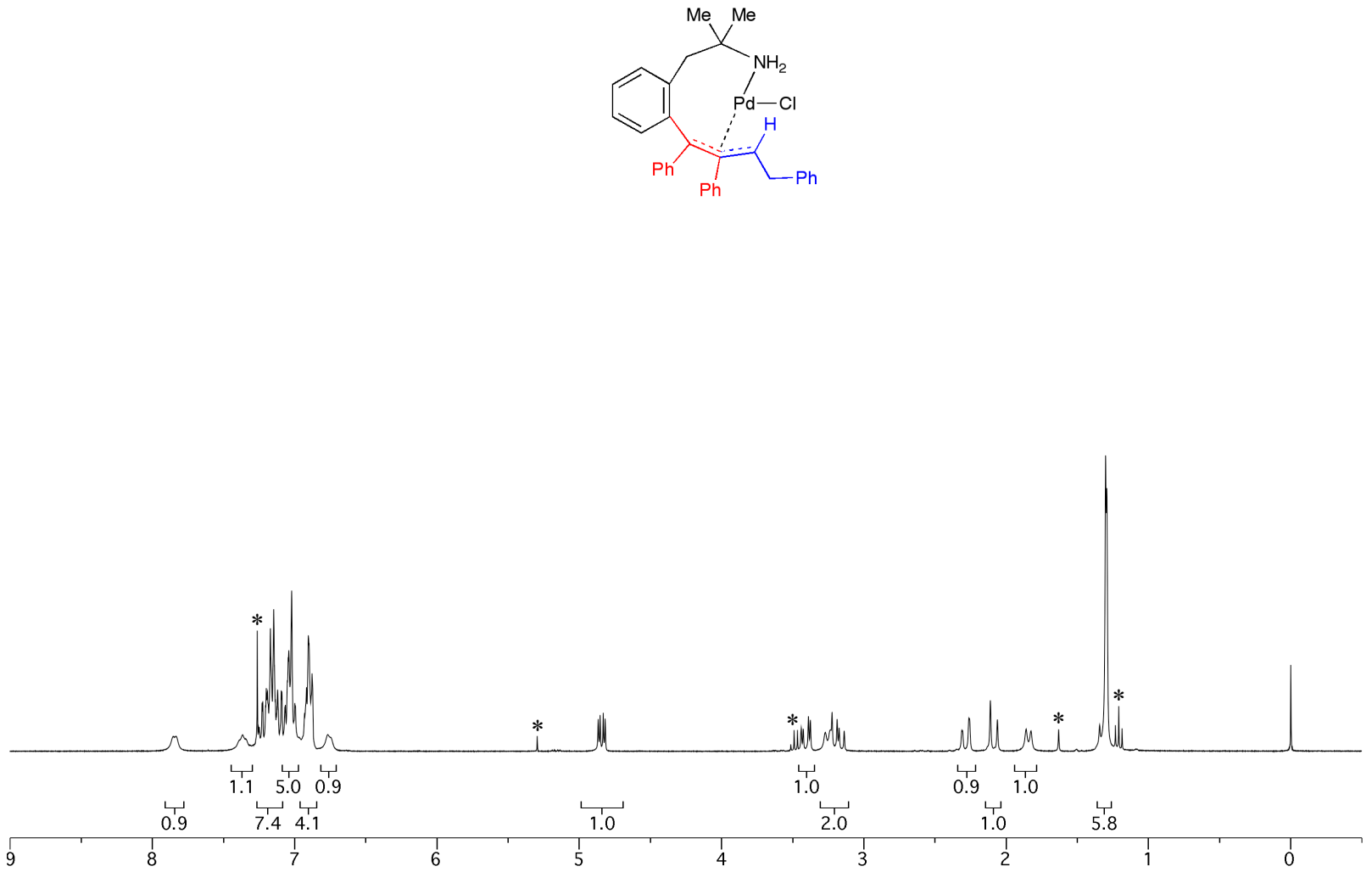

Figure S32. ^{1}H NMR spectrum of *syn*-**1b** (300.1 MHz, $CDCl_3$, 25 ºC)

(From left to right, the asteriks indicate the signals corresponding to $CHCl_3$, CH_2Cl_2, Et_2O, H_2O, and Et_2O)

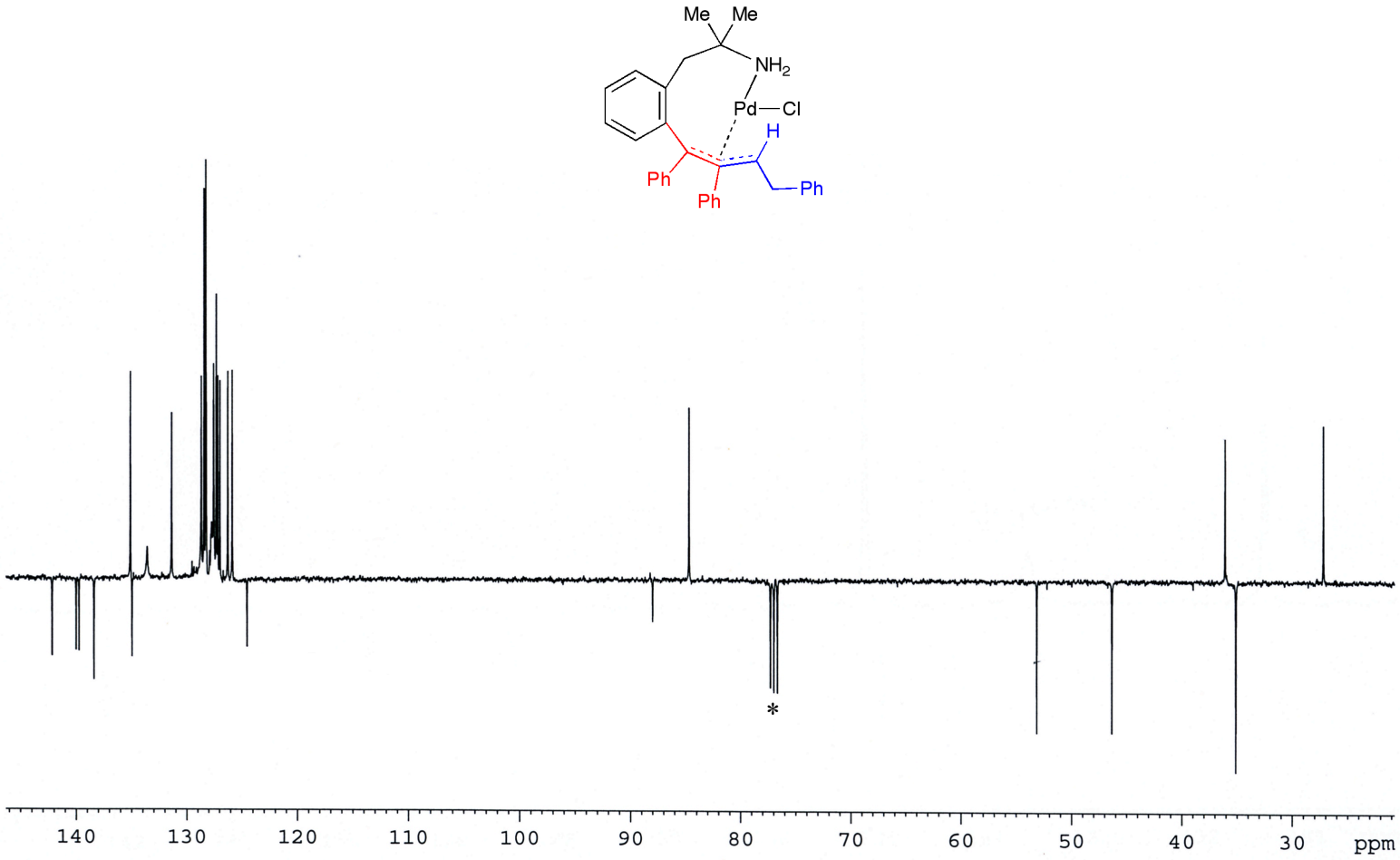

Figure S33. $^{13}C\{^{1}H\}$ APT NMR spectrum of *syn*-**1b** (100.8 MHz, $CDCl_3$, 25 ºC)

(The asterik indicates the signal corresponding to $CDCl_3$)

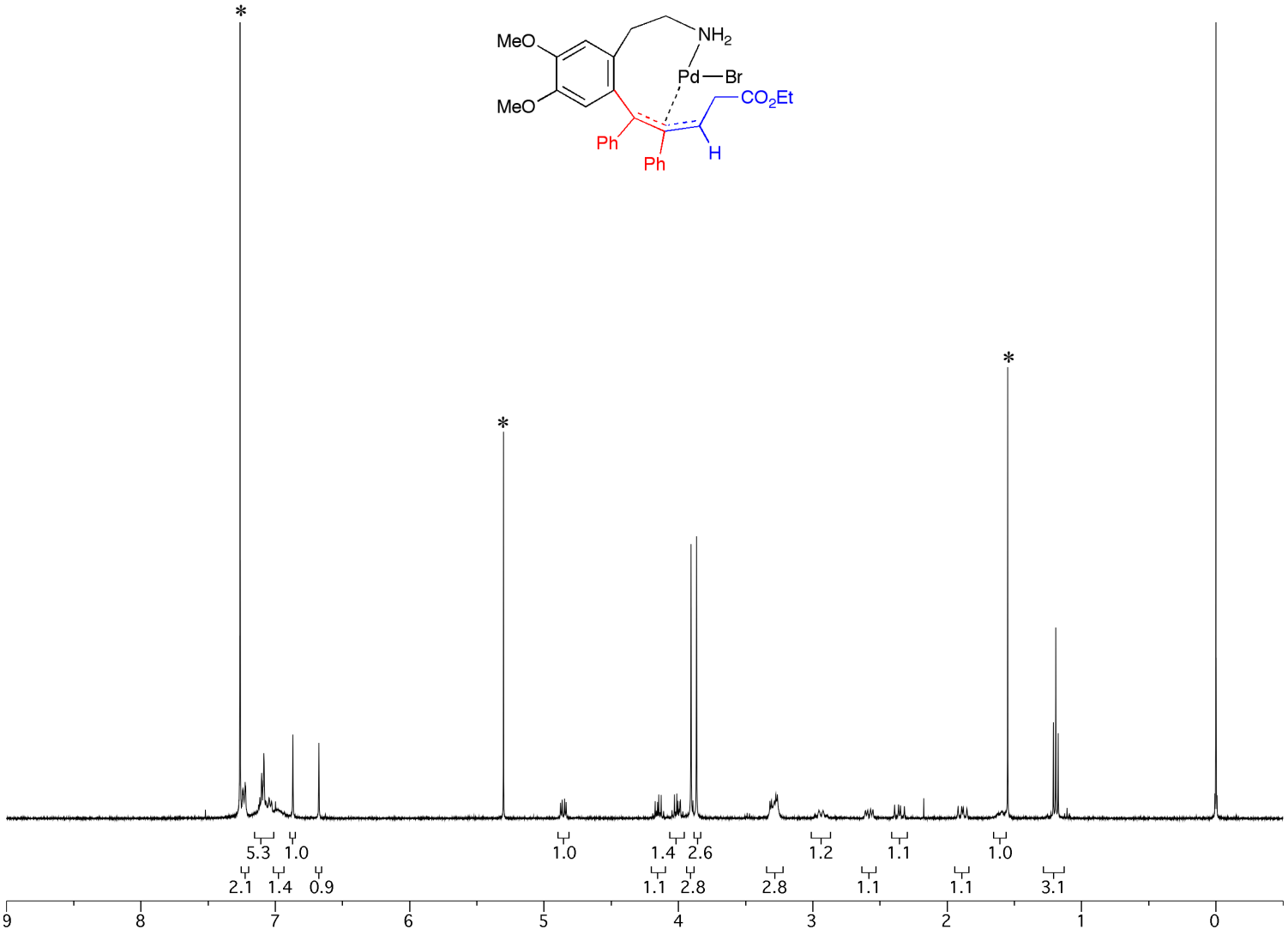

Figure S34. ^{1}H NMR spectrum of *anti*-**2a** (400.9 MHz, $CDCl_3$, 25 ºC)

(From left to right, the asteriks indicate the signals corresponding to $CHCl_3$, CH_2Cl_2, and H_2O)

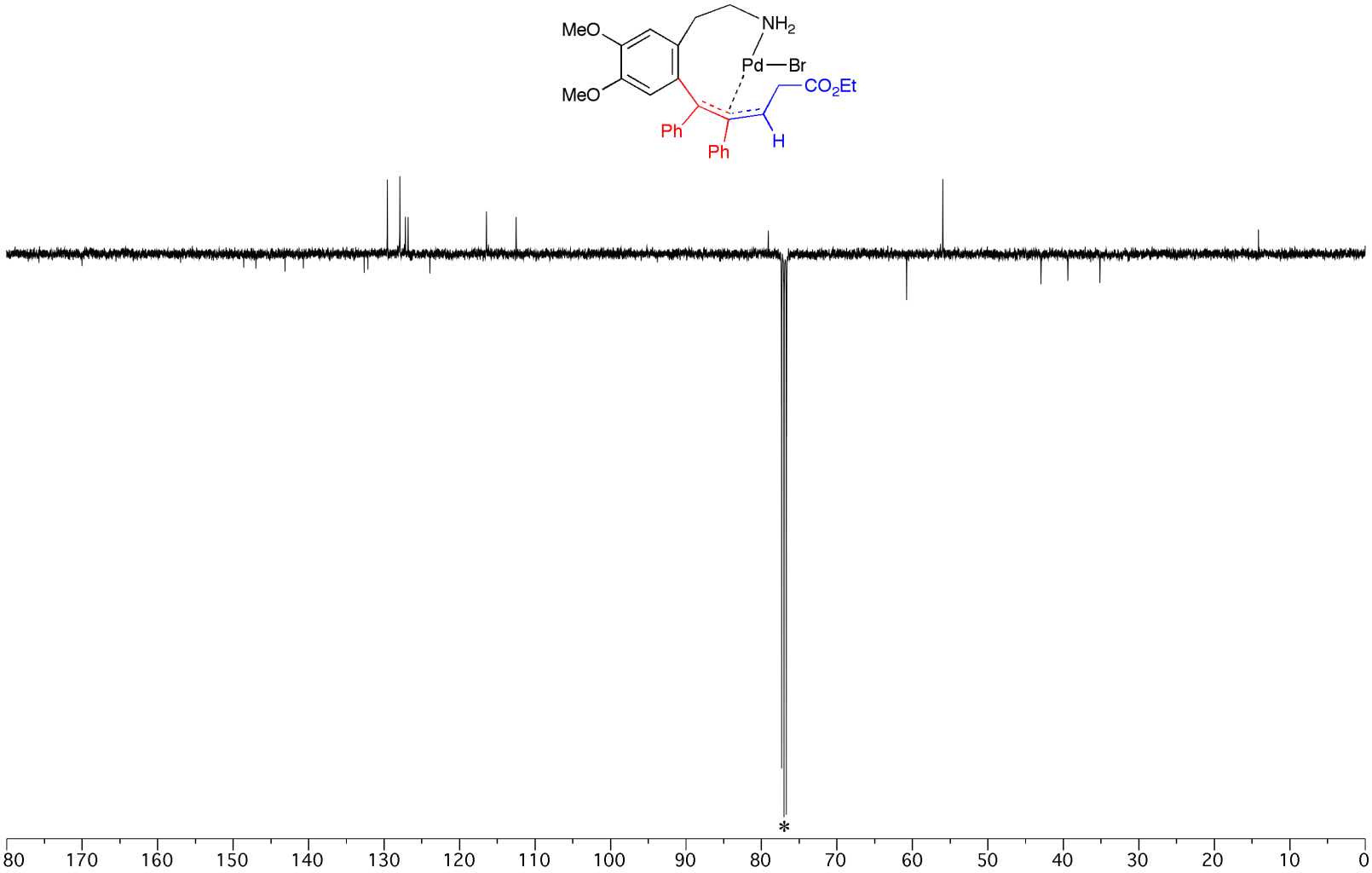

Figure S35. $^{13}C\{^{1}H\}$ APT NMR spectrum of *anti*-**2a** (100.8 MHz, $CDCl_3$, 25 ºC)

(The asterik indicates the signal corresponding to $CDCl_3$)

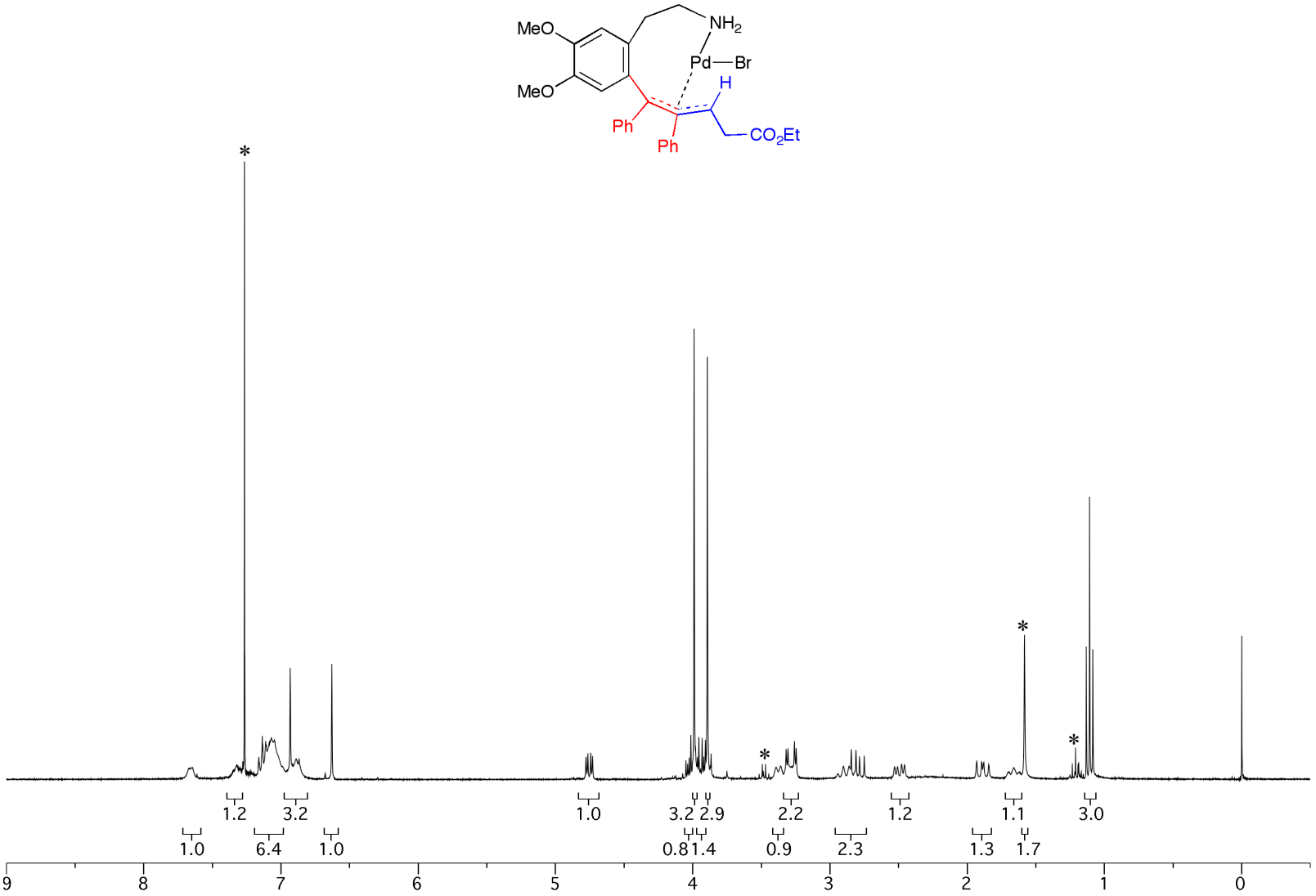

Figure S36. ^{1}H NMR spectrum of *syn*-**2a** (300.1 MHz, $CDCl_3$, 25 ºC)

(From left to right, the asteriks indicate the signals corresponding to $CHCl_3$, Et_2O, H_2O, and Et_2O)

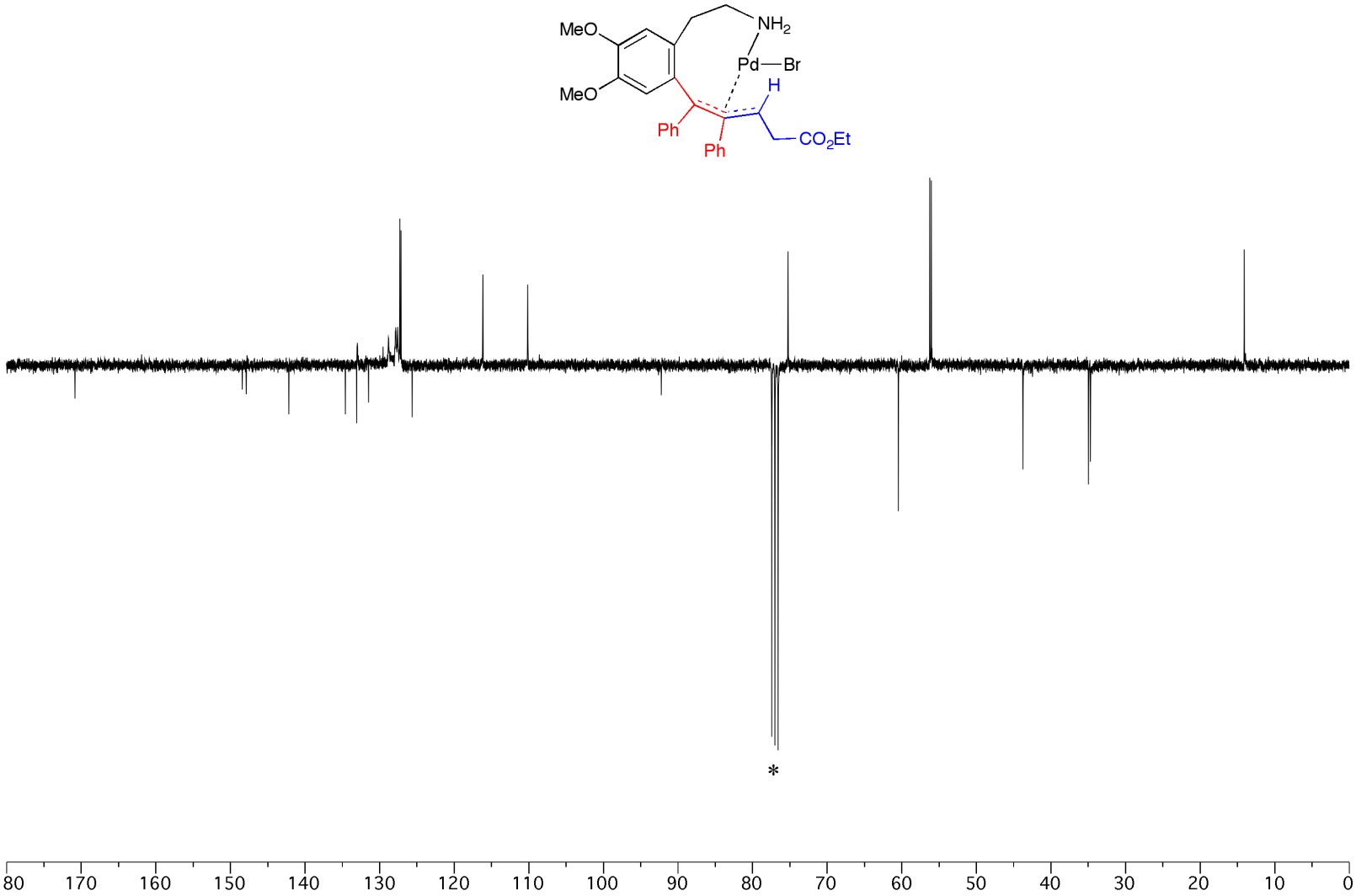

Figure S37. $^{13}C\{^{1}H\}$ APT NMR spectrum of *syn*-**2a** (75.5 MHz, $CDCl_3$, 25 ºC)

(The asterik indicates the signal corresponding to $CDCl_3$)

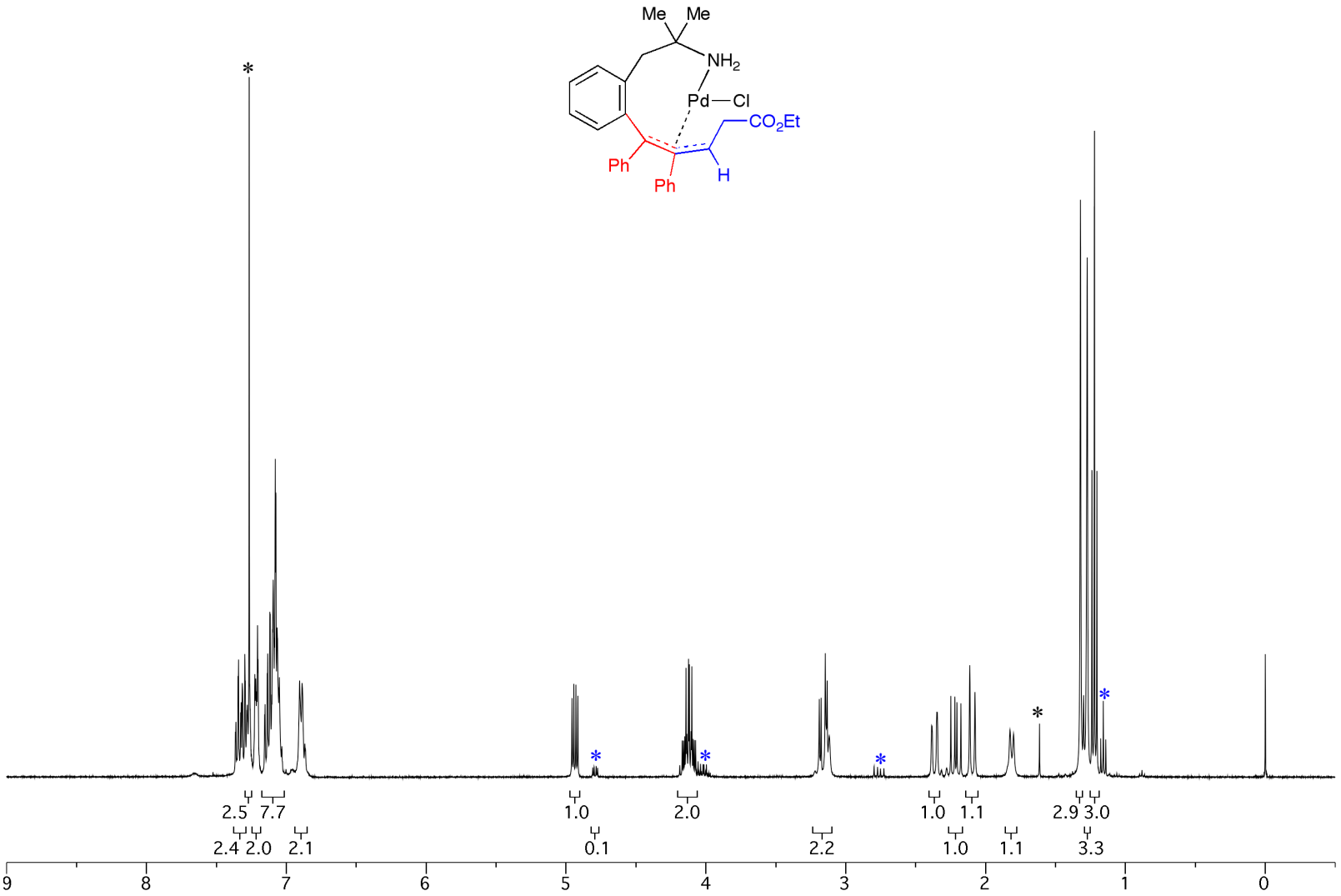

Figure S38. ^{1}H NMR spectrum of *anti*-**2b** (400.9 MHz, $CDCl_3$, 25 ºC)

(From left to right, the black asteriks indicate the signals corresponding to $CHCl_3$, and H_2O; the blue asteriks correspond to the *syn* isomer)

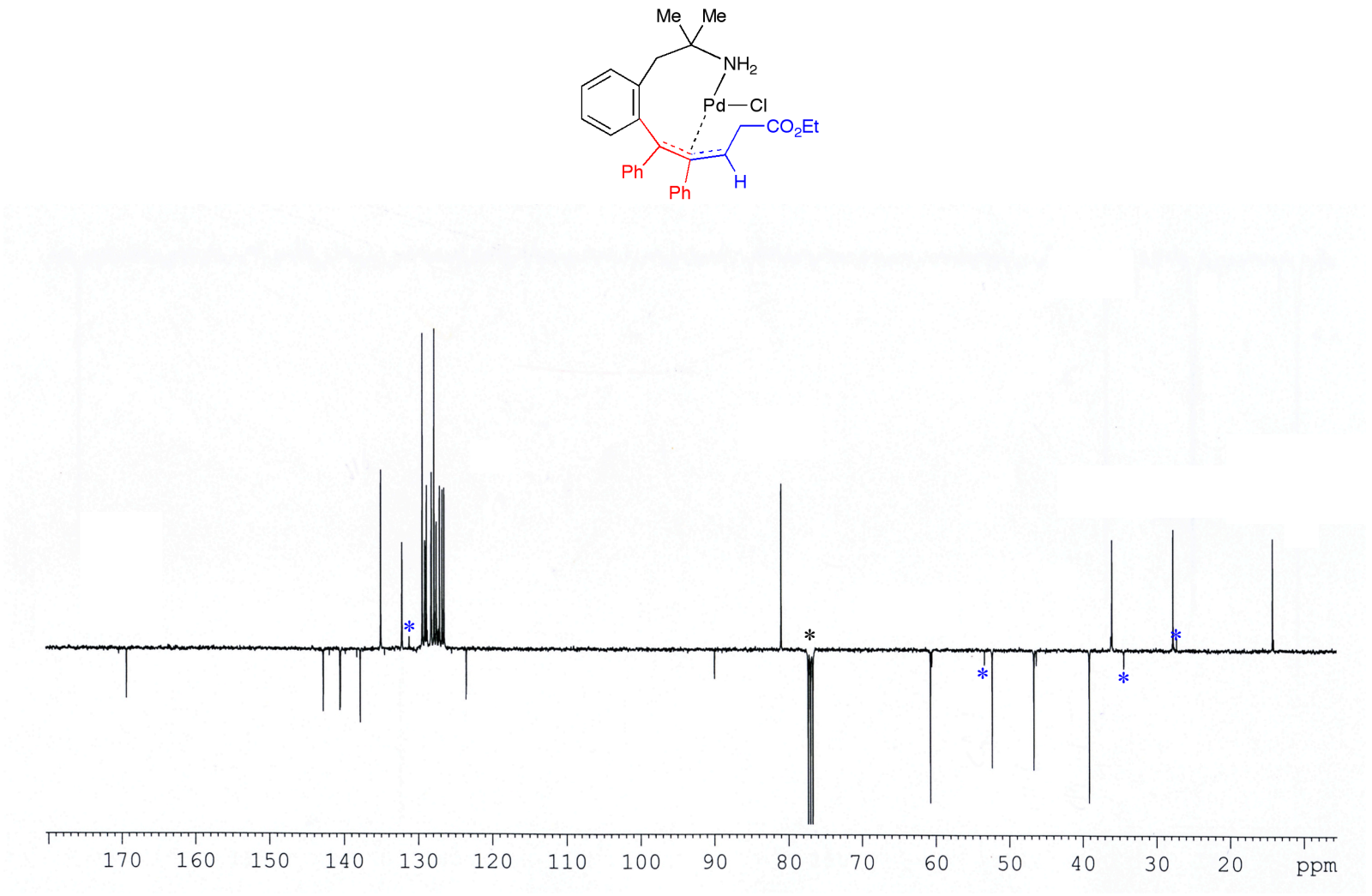

Figure S39. $^{13}C\{^{1}H\}$ APT NMR spectrum of *anti*-**2b** (100.8 MHz, $CDCl_3$, 25 ºC)

(The black asterik indicates the signal corresponding to $CDCl_3$; the blue asteriks correspond to the *syn* isomer)

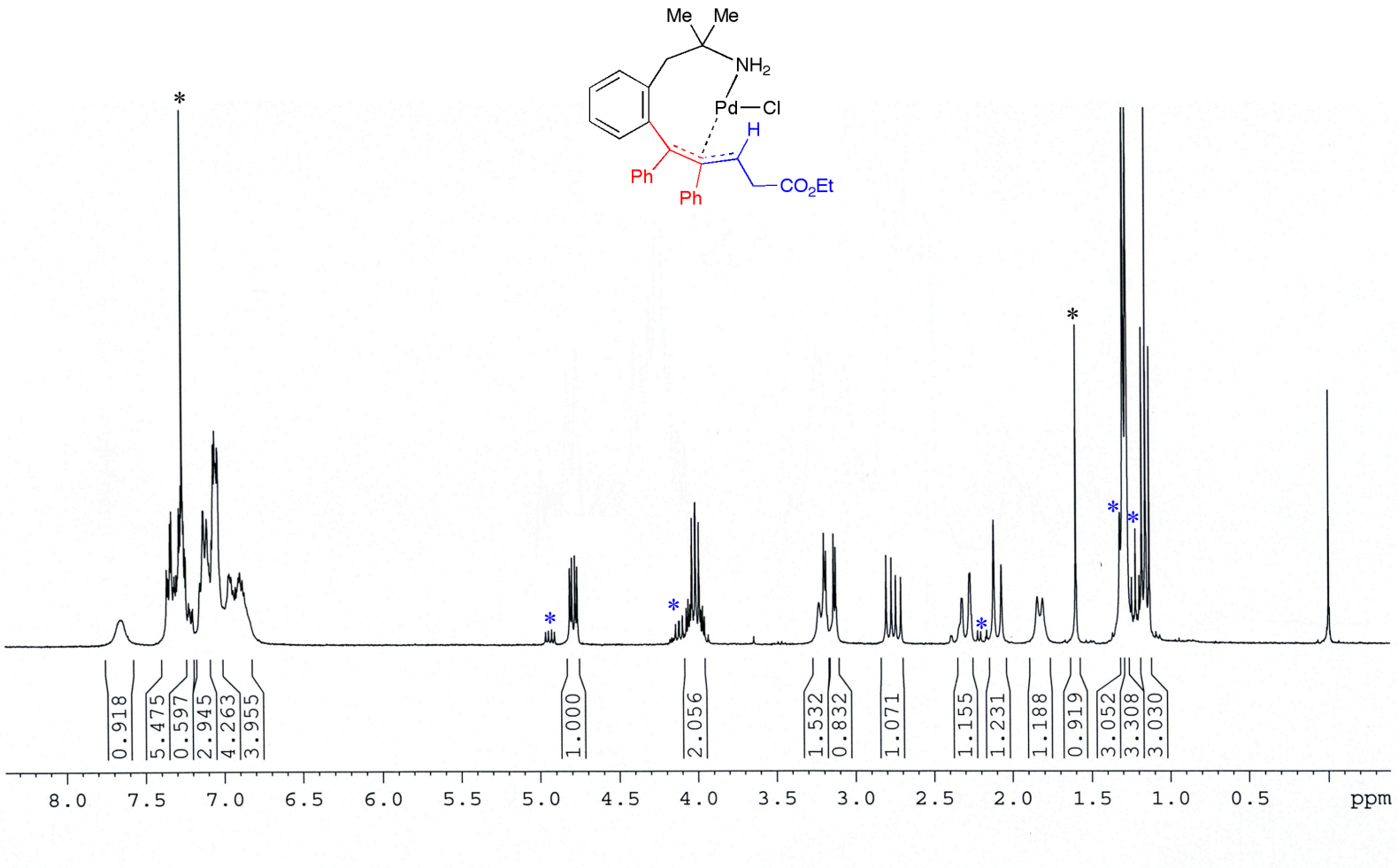

Figure S40. ^{1}H NMR spectrum of *syn*-**2b** (300.1 MHz, $CDCl_3$, 25 ºC)

(From left to right, the black asteriks indicate the signals corresponding to $CHCl_3$, and H_2O; the blue asteriks correspond to the *anti* isomer)

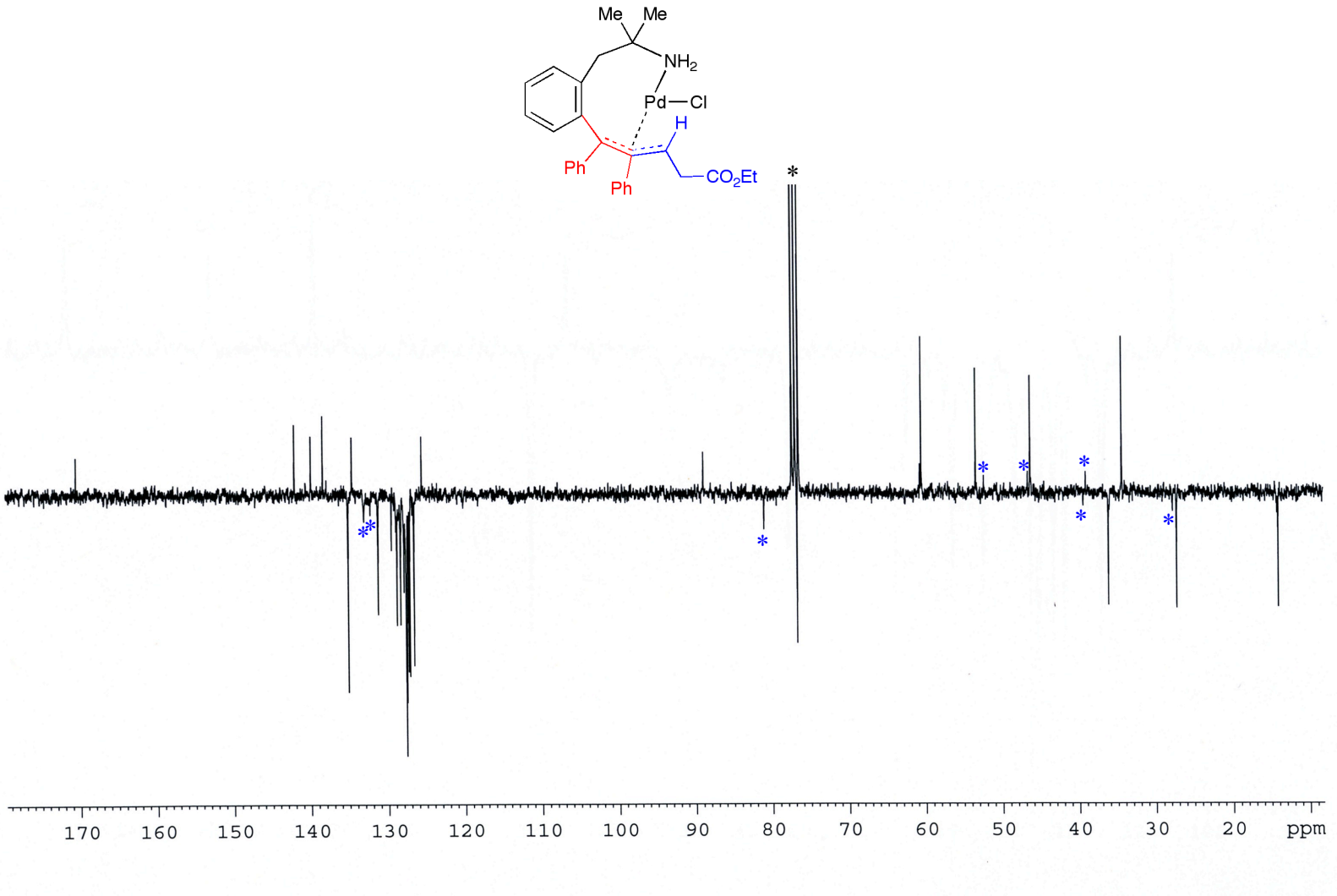

Figure S41. $^{13}C\{^{1}H\}$ APT NMR spectrum of *syn*-**2b** (75.5 MHz, $CDCl_3$, 25 ºC)

(The black asterik indicates the signal corresponding to $CDCl_3$; the blue asteriks correspond to the *anti* isomer)

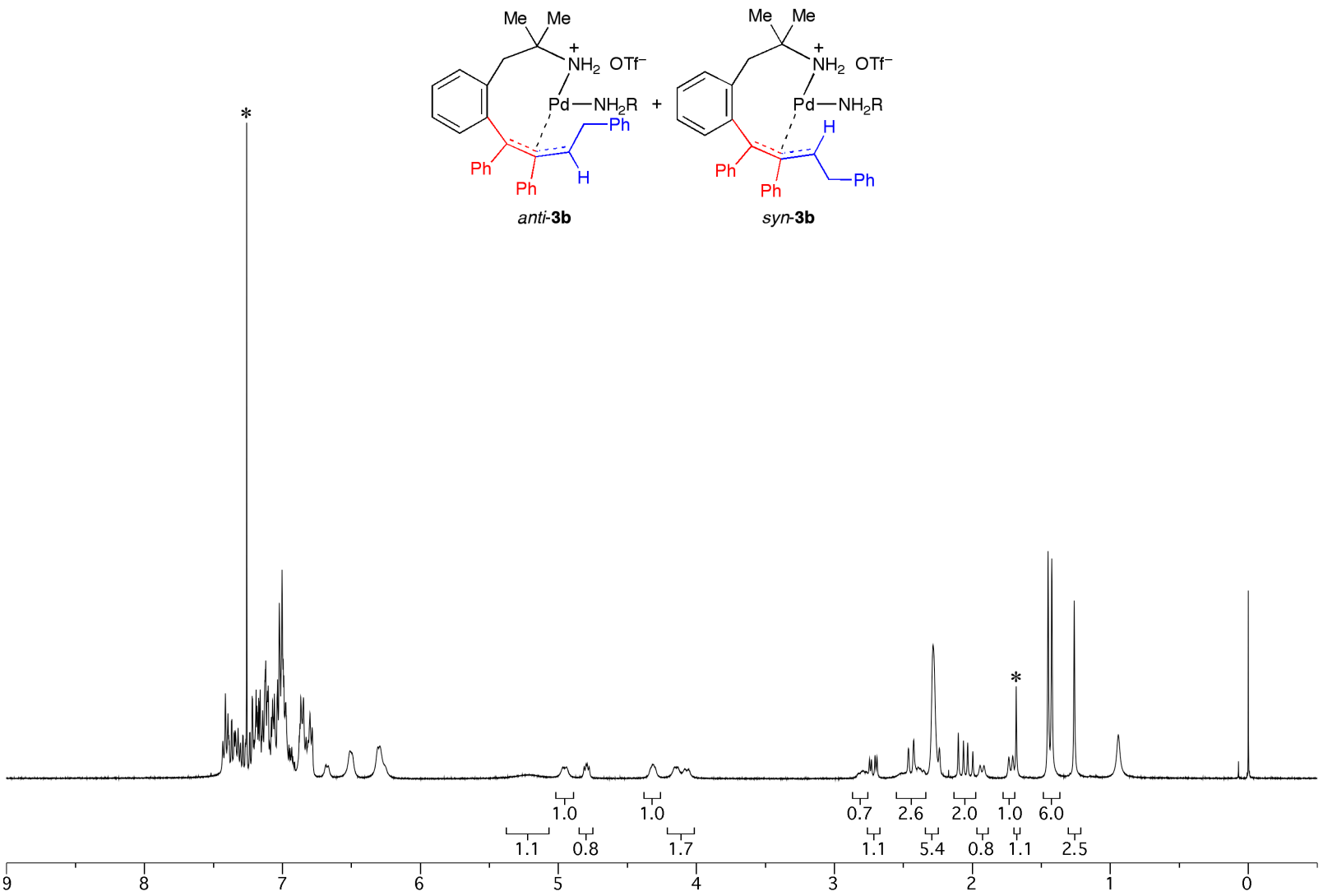

Figure S42. ^{1}H NMR spectrum of a 1:1.33 mixture of *anti*/*syn*-**3b** (400.9 MHz, $CDCl_3$, 25 ºC)

(From left to right, the black asteriks indicate the signals corresponding to $CHCl_3$, and H_2O)

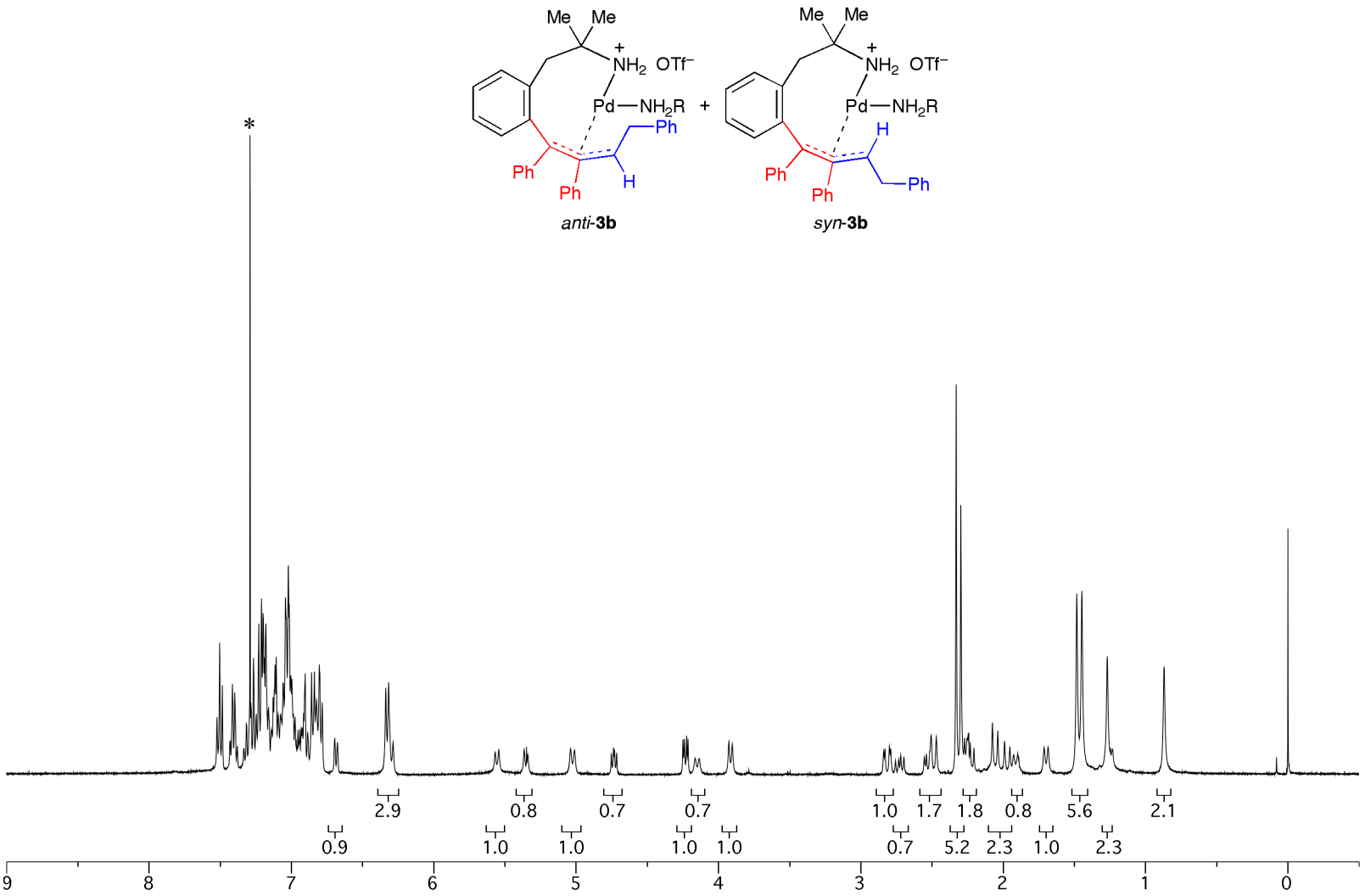

Figure S43. ^{1}H NMR spectrum of a 1:1.33 mixture of *anti*/*syn*-**3b** (400.9 MHz, $CDCl_3$, –40 ºC)

(From left to right, the black asterik indicates the signal corresponding to $CHCl_3$.)

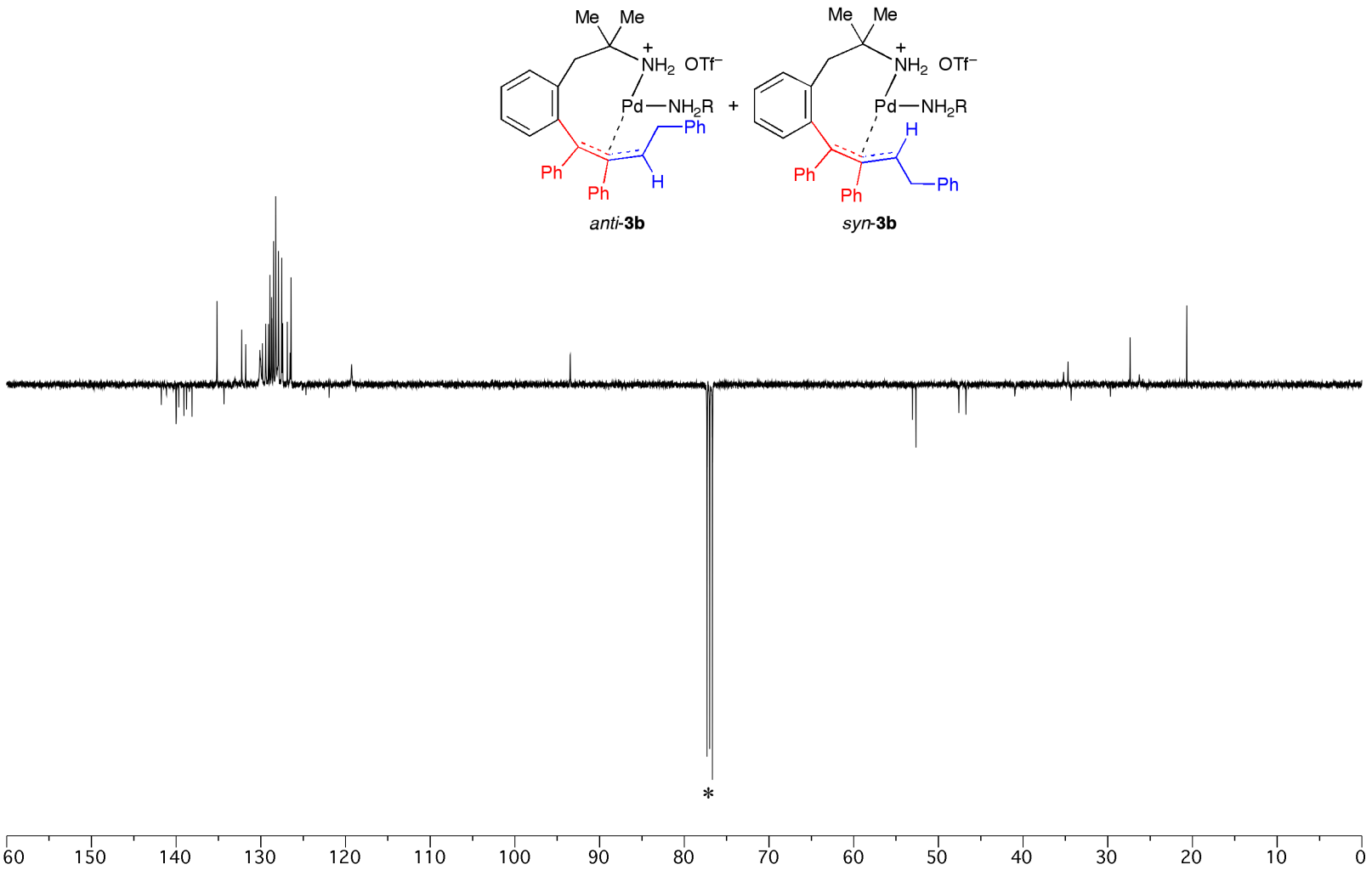

Figure S44. $^{13}C\{^{1}H\}$ APT NMR spectrum of a 1:1.33 mixture of *anti*/*syn*-**3b** (100.8 MHz, $CDCl_3$, 25 ºC)

(The black asterik indicates the signal corresponding to $CDCl_3$)

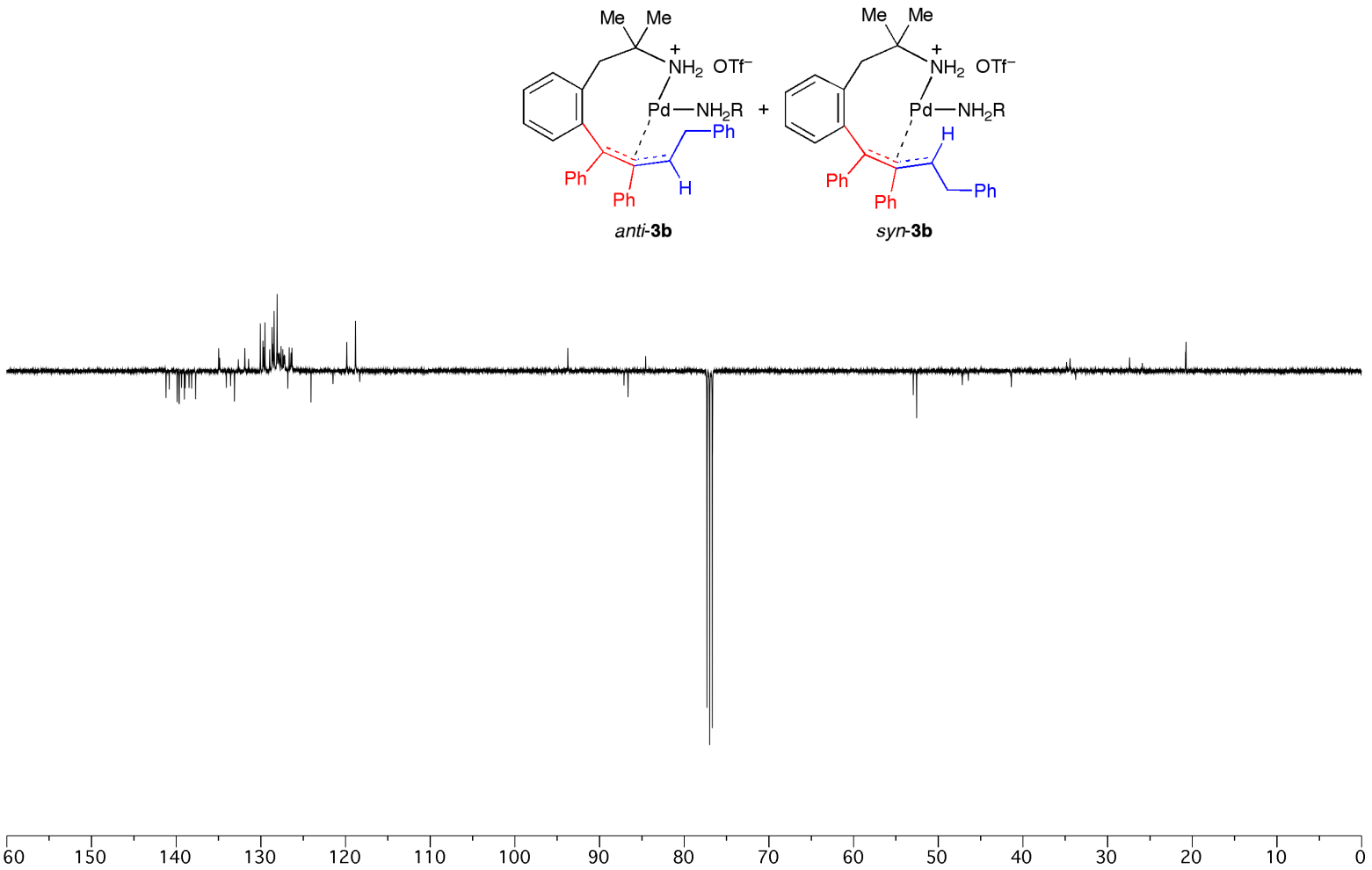

Figure S45. $^{13}C\{^{1}H\}$ APT NMR spectrum of a 1:1.33 mixture of *anti*/*syn*-**3b** (100.8 MHz, $CDCl_3$, –40 ºC)

(The black asterik indicates the signal corresponding to $CDCl_3$)

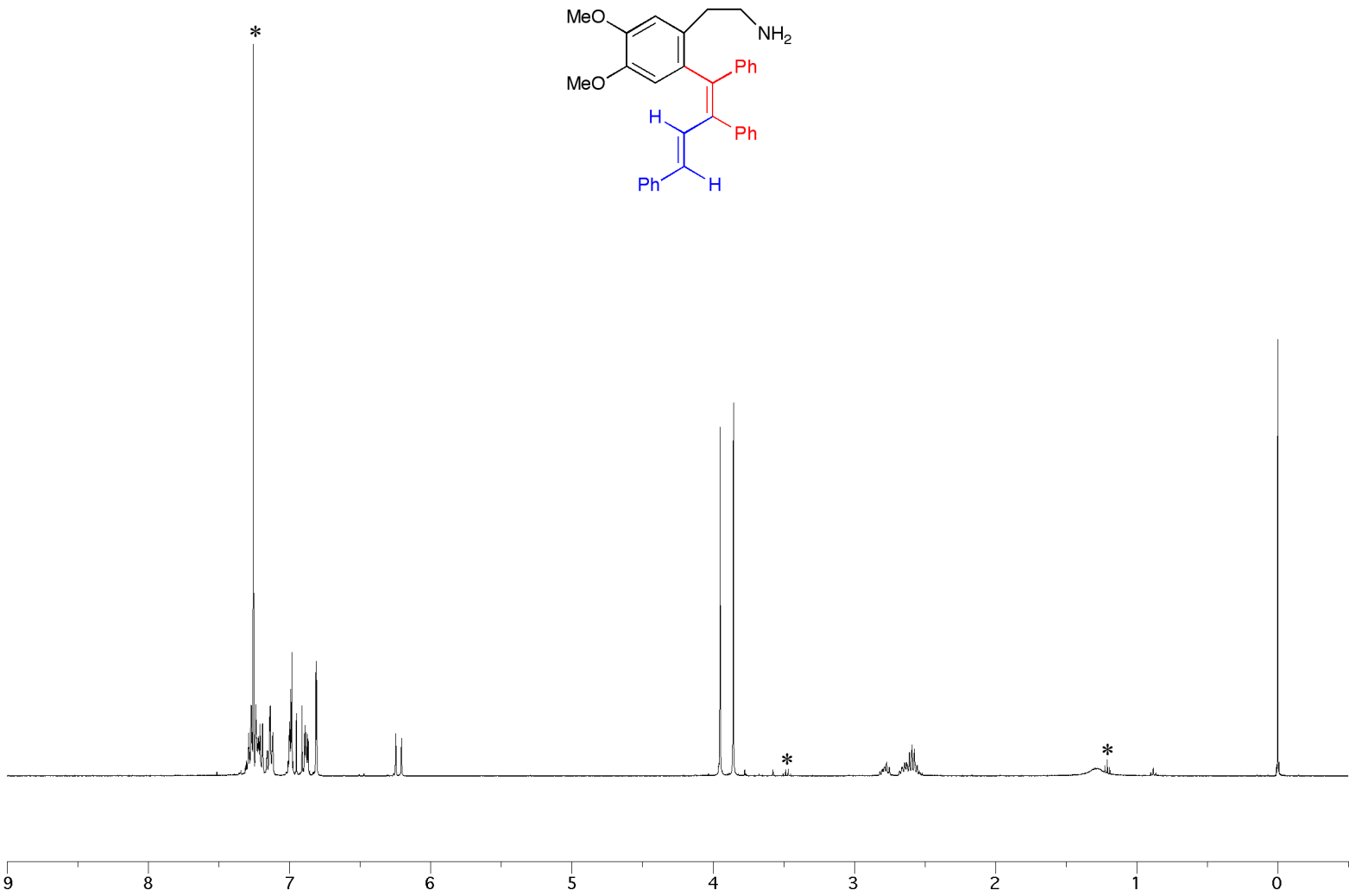

Figure S46. ^{1}H NMR spectrum of **4a**·1/2H_2O (400.9 MHz, $CDCl_3$, 25 ºC)

(From left to right, the asteriks indicate the signals corresponding to $CHCl_3$, and traces of Et_2O)

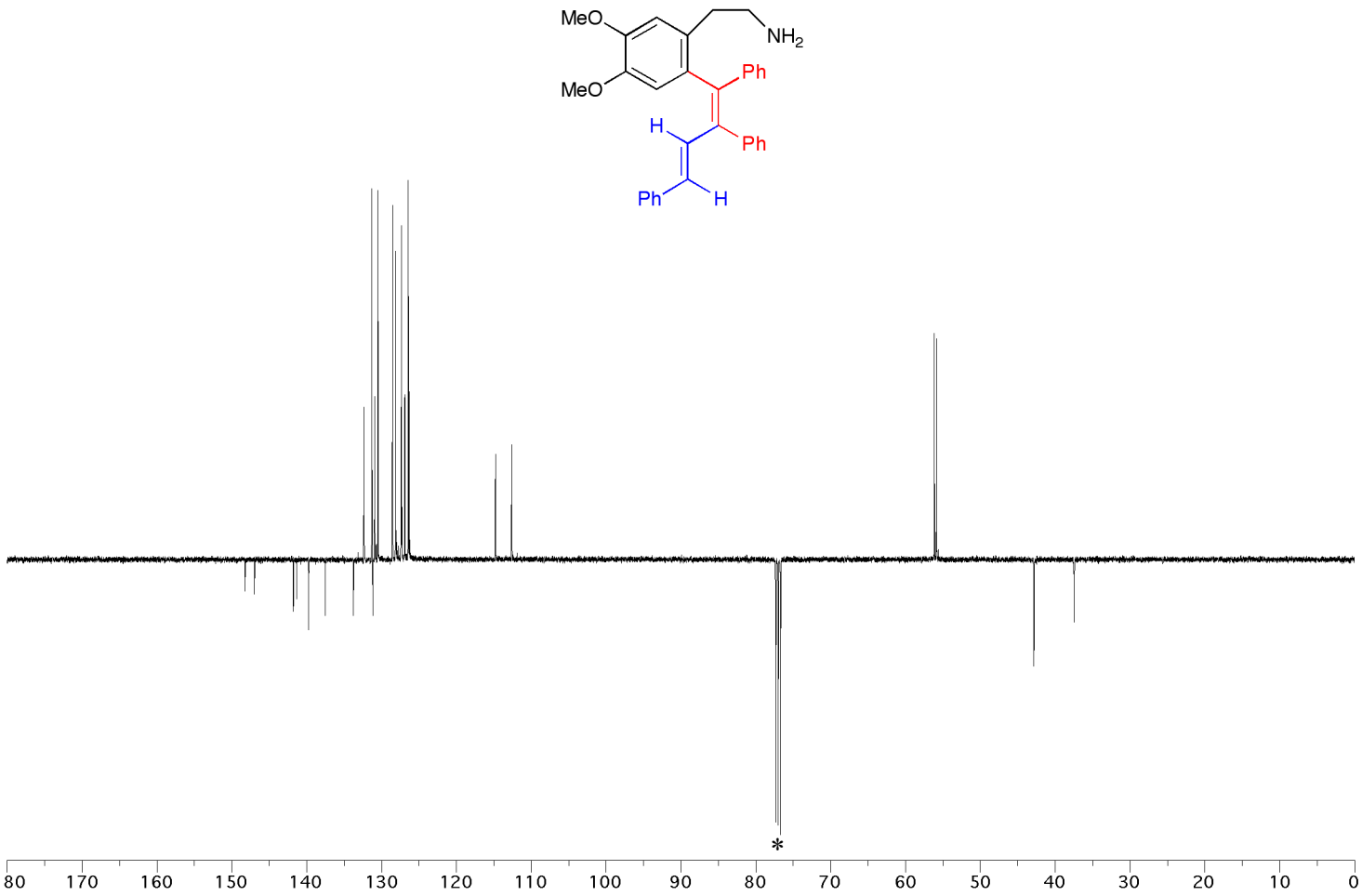

Figure S47. $^{13}C\{^{1}H\}$ APT NMR spectrum of **4a**·1/2H_2O (100.8 MHz, $CDCl_3$, 25 ºC)

(The asterik indicates the signal corresponding to $CDCl_3$)

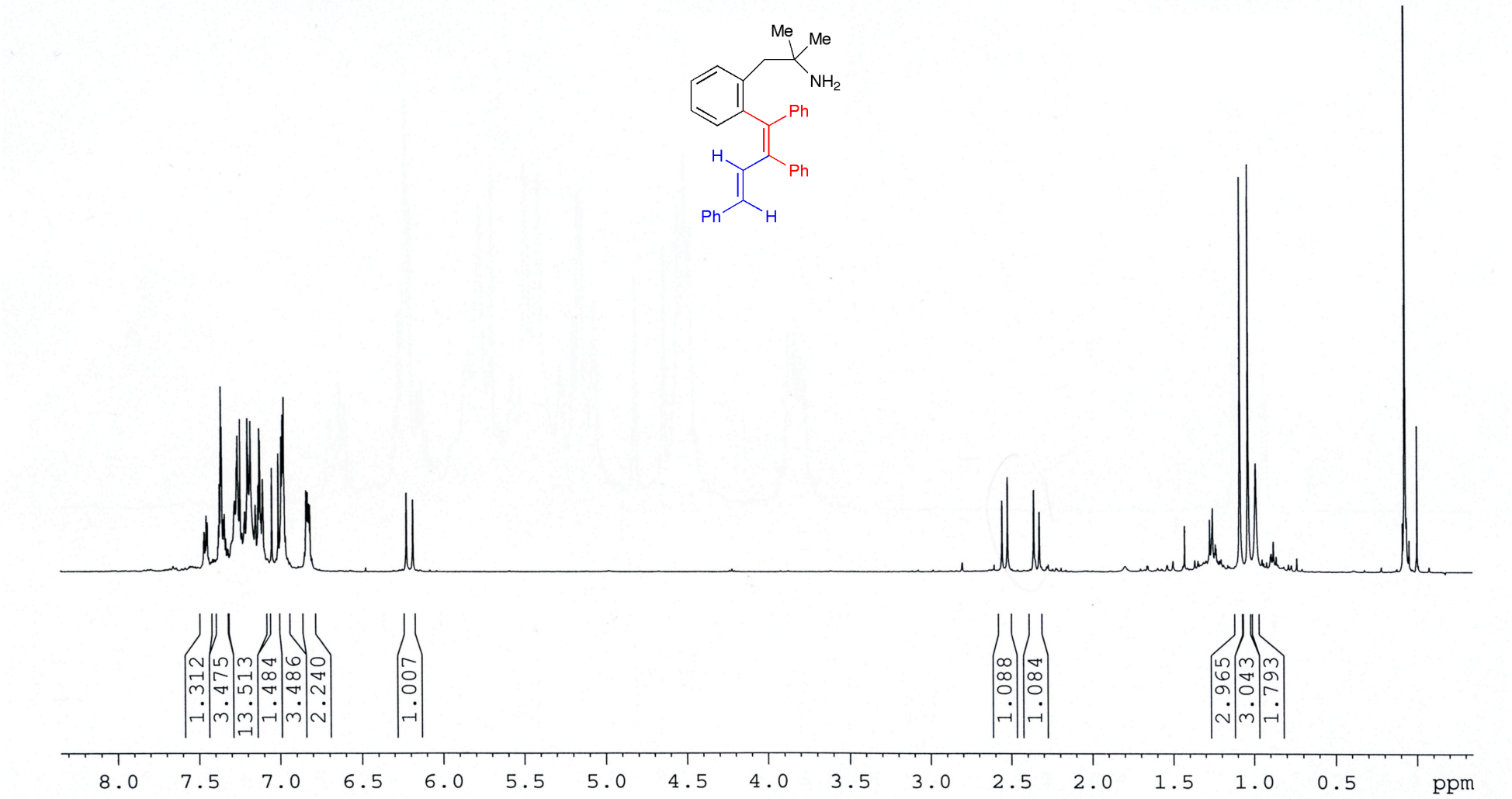

Figure S48. ^{1}H NMR spectrum of crude **4b** (400.9 MHz, $CDCl_3$, 25 ºC)

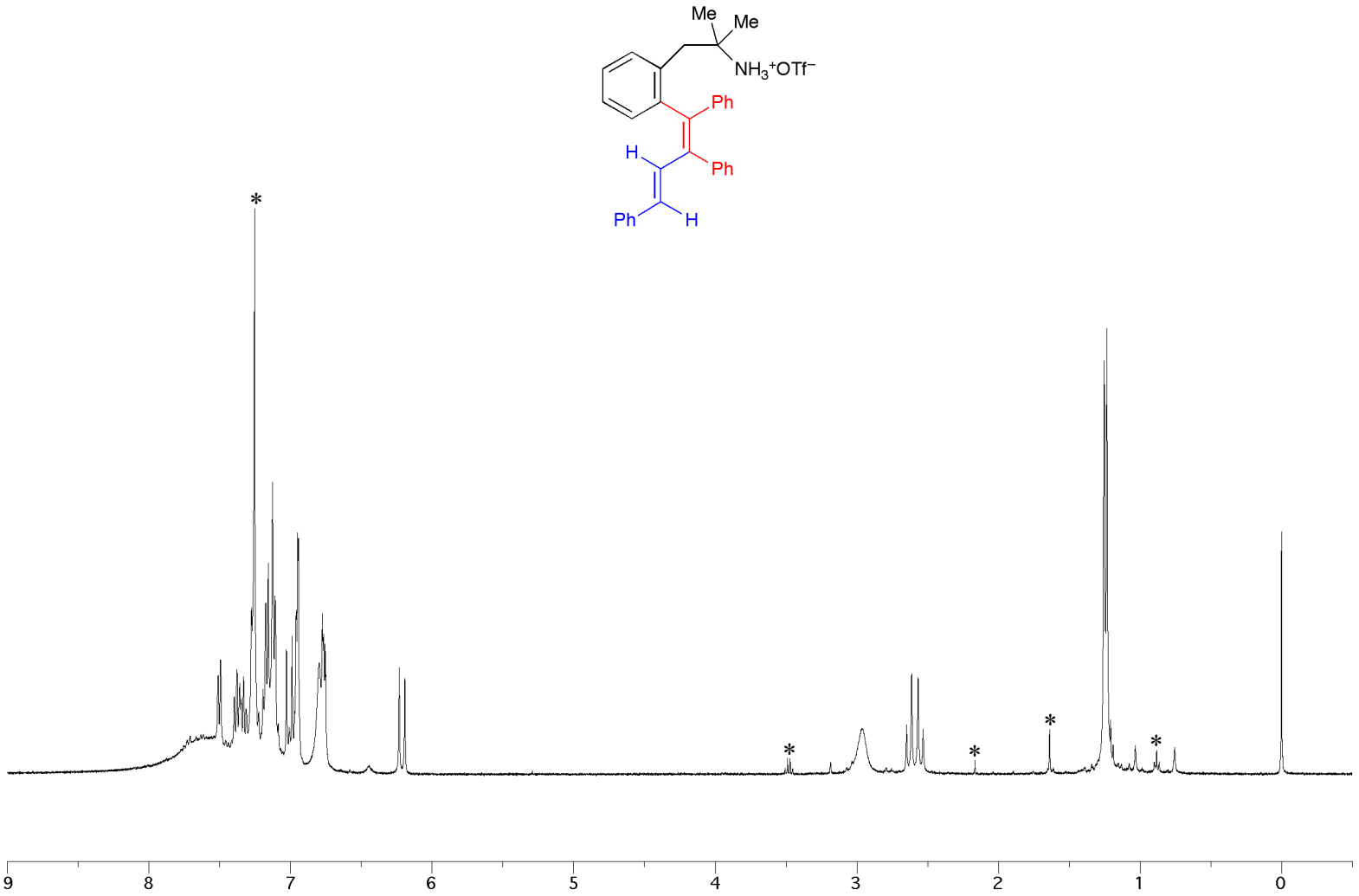

Figure S49. ^{1}H NMR spectrum of **5b**·H_2O (400.9 MHz, $CDCl_3$, 25 ºC)

(From left to right, the asteriks indicate the signals corresponding to $CHCl_3$, and traces of Et_2O, acetone, H_2O, and *n*-pentane)

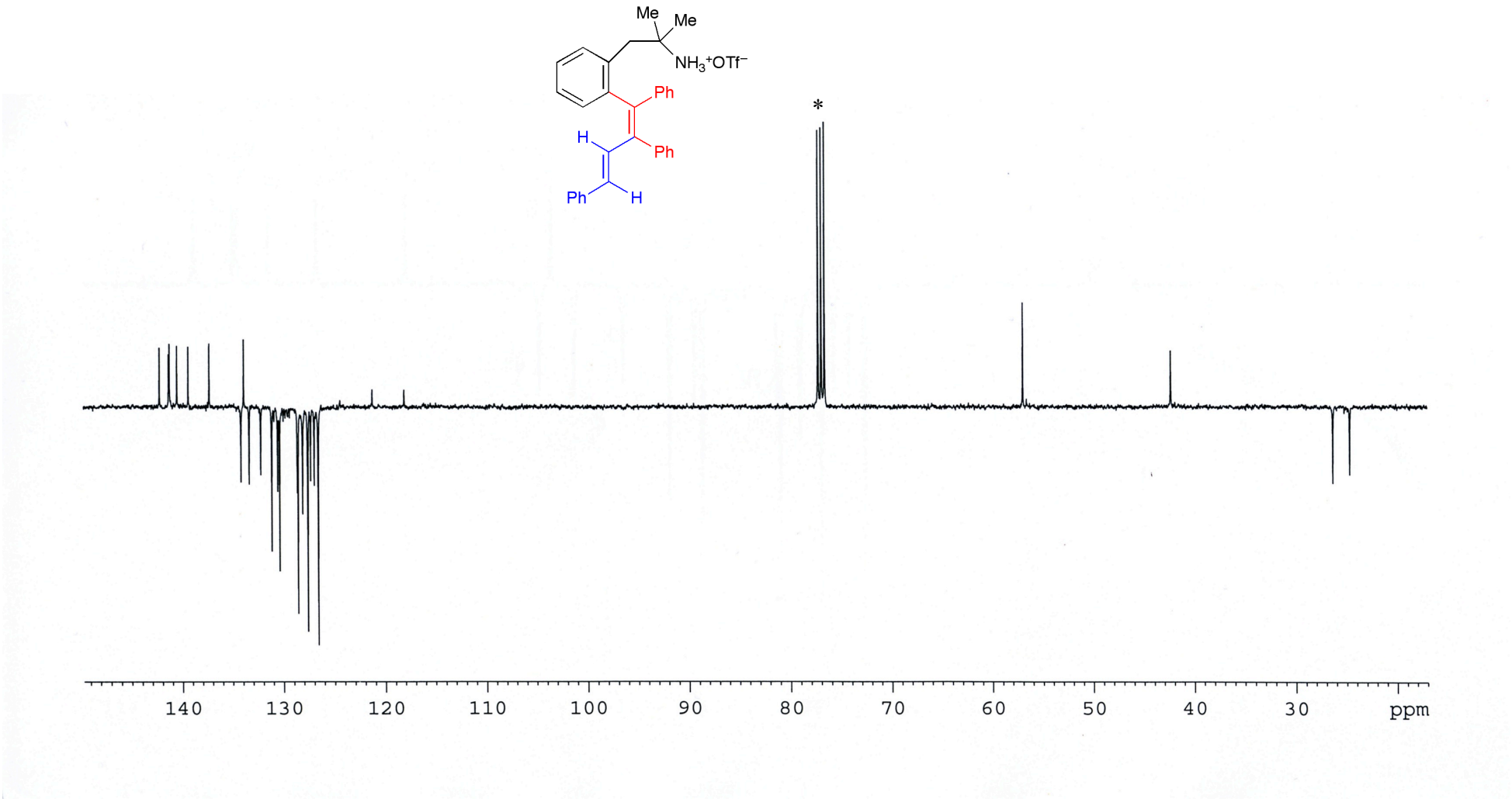

Figure S50. $^{13}C\{^{1}H\}$ APT NMR spectrum of **5b**·H_2O (100.8 MHz, $CDCl_3$, 25 ºC)

(The asterik indicates the signal corresponding to $CDCl_3$)

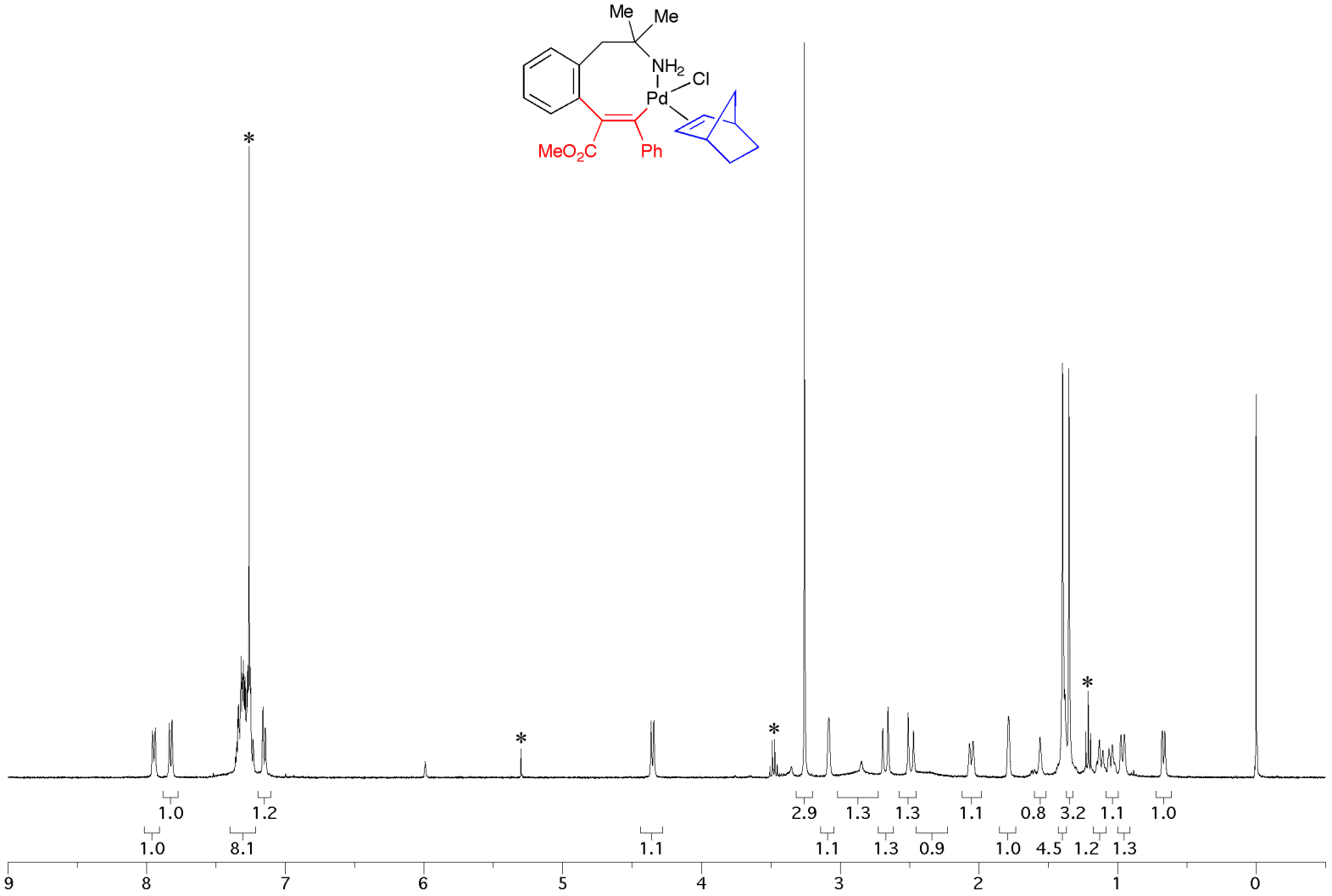

Figure S51. ^{1}H NMR spectrum of **6d** (400.9 MHz, $CDCl_3$, 25 ºC)

(From left to right, the asteriks indicate the signals corresponding to $CHCl_3$, CH_2Cl_2, and Et_2O)

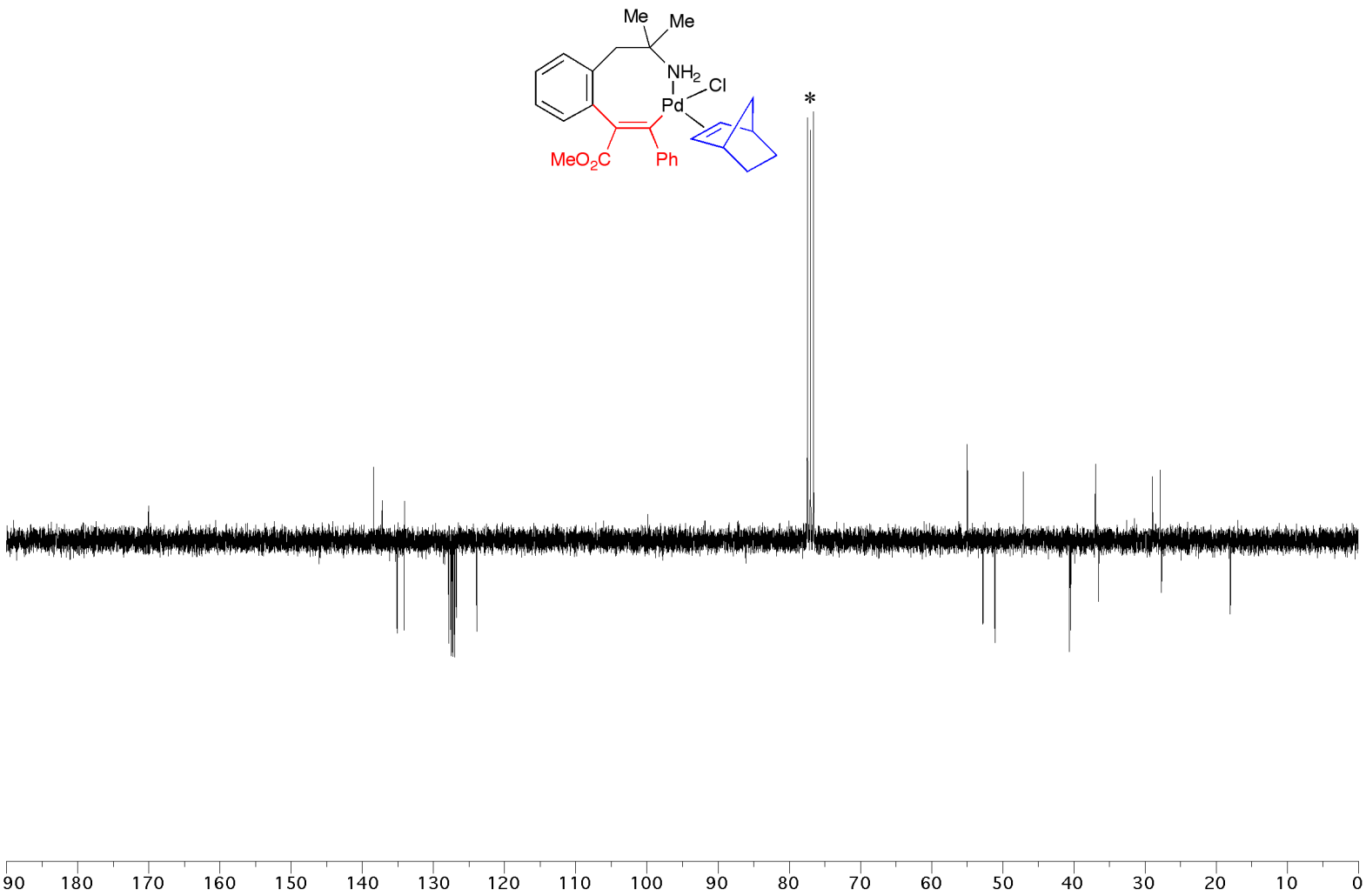

Figure S52. $^{13}C\{^{1}H\}$ APT NMR spectrum of **6d** (75.5 MHz, $CDCl_3$, 25 ºC)

(The asterik indicates the signal corresponding to $CDCl_3$)

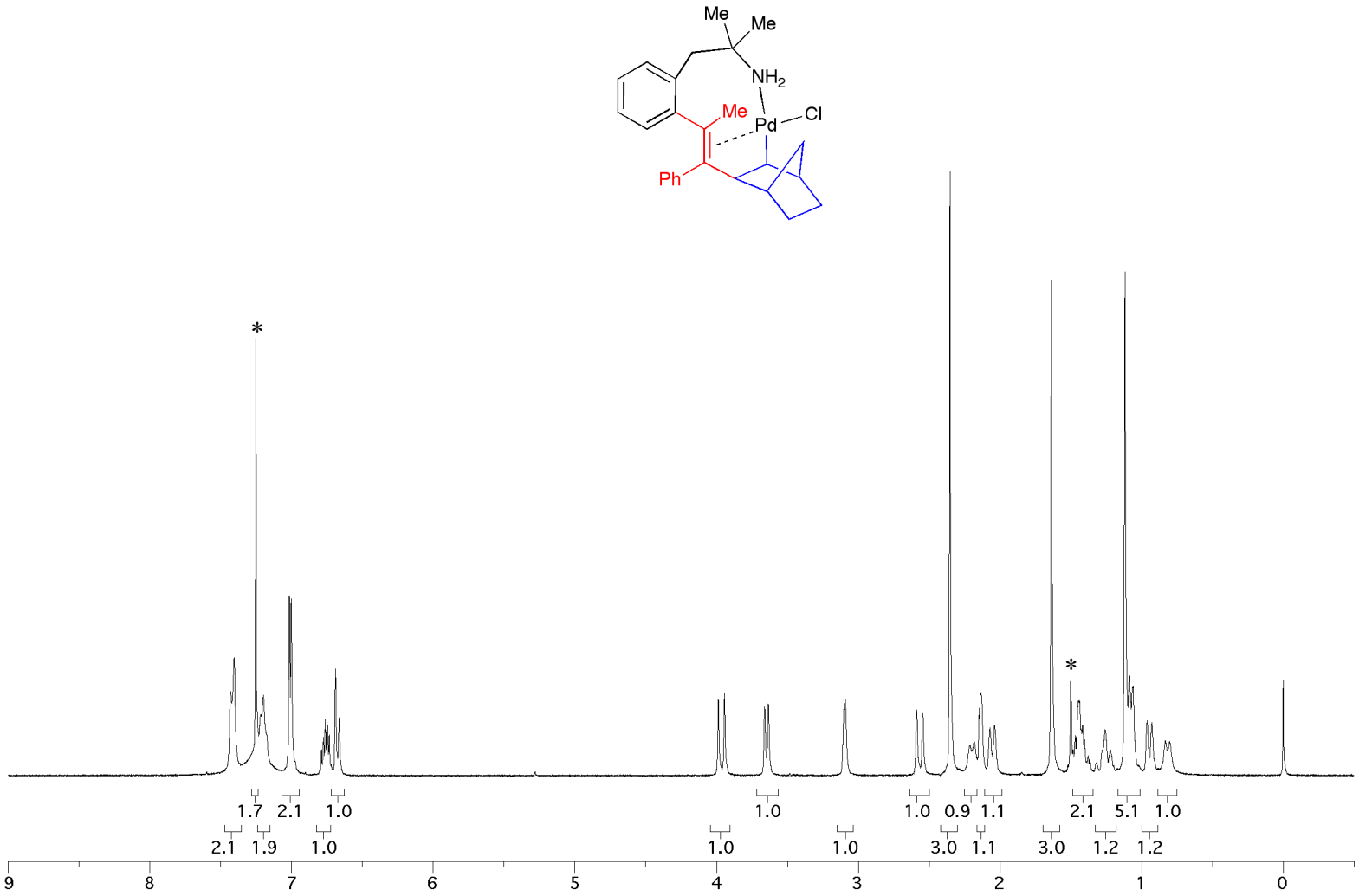

Figure S53. ^{1}H NMR spectrum of **7c**·$CHCl_3$ (300.1 MHz, $CDCl_3$, 25 ºC)

(From left to right, the asteriks indicate the signals corresponding to $CHCl_3$, and H_2O)

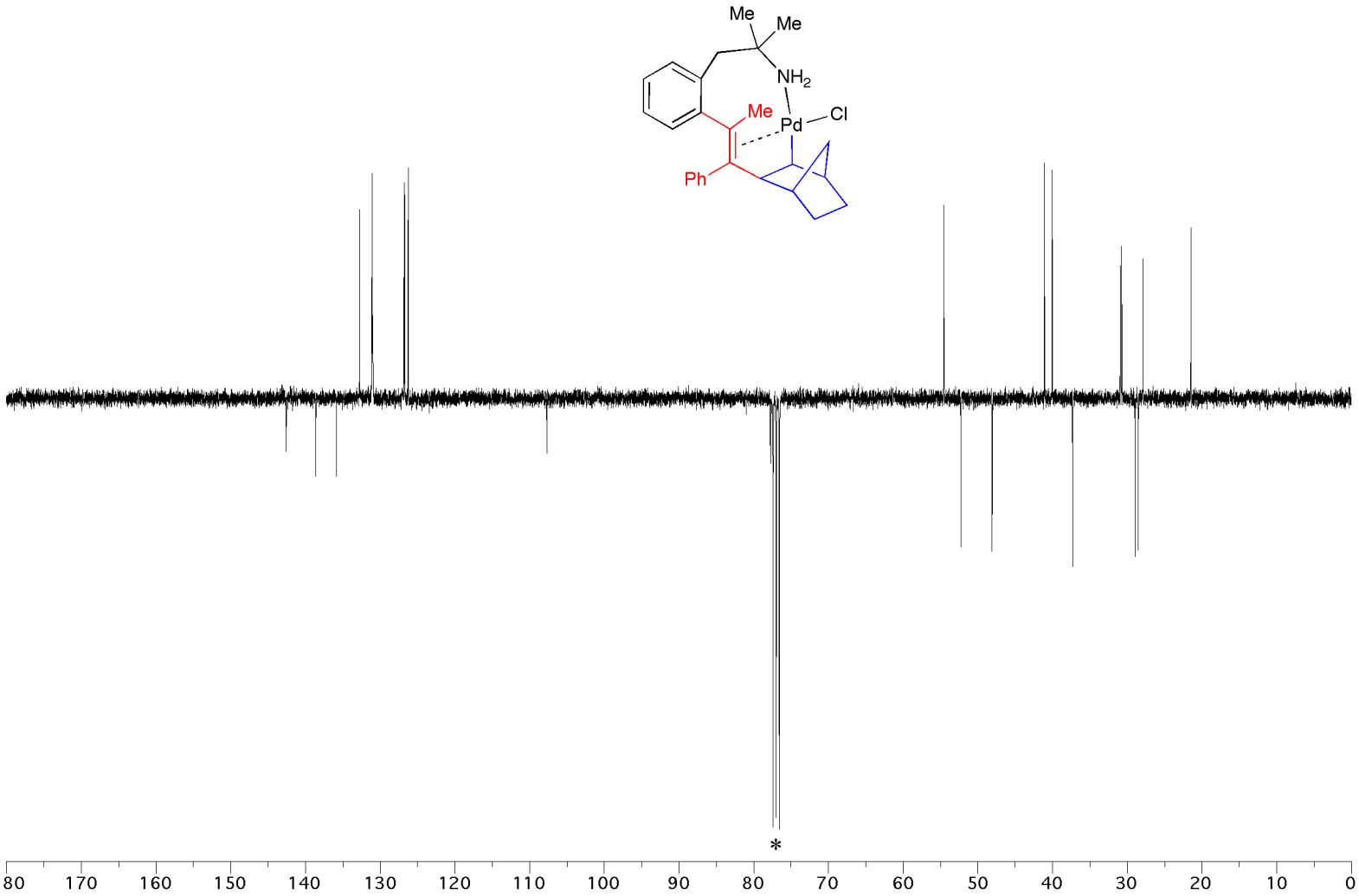

Figure S54. $^{13}C\{^{1}H\}$ APT NMR spectrum of **7c**·$CHCl_3$ (75.5 MHz, $CDCl_3$, 25 ºC)

(The asterik indicates the signal corresponding to $CDCl_3$)

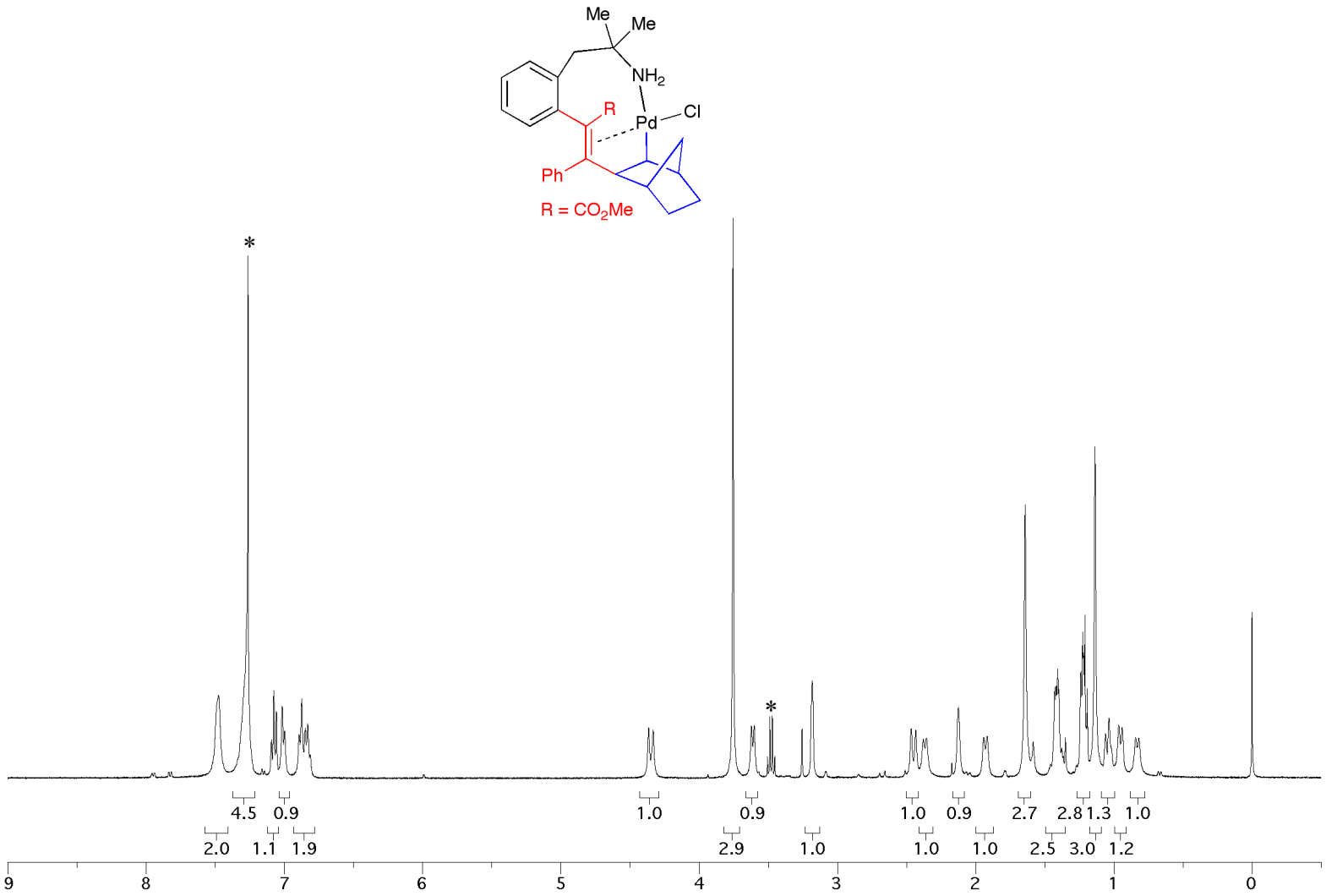

Figure S55. ^{1}H NMR spectrum of **7d**·1/2$CHCl_3$ (400.9 MHz, $CDCl_3$, 25 ºC)

(From left to right, the asteriks indicate the signals corresponding to $CHCl_3$, and Et_2O)

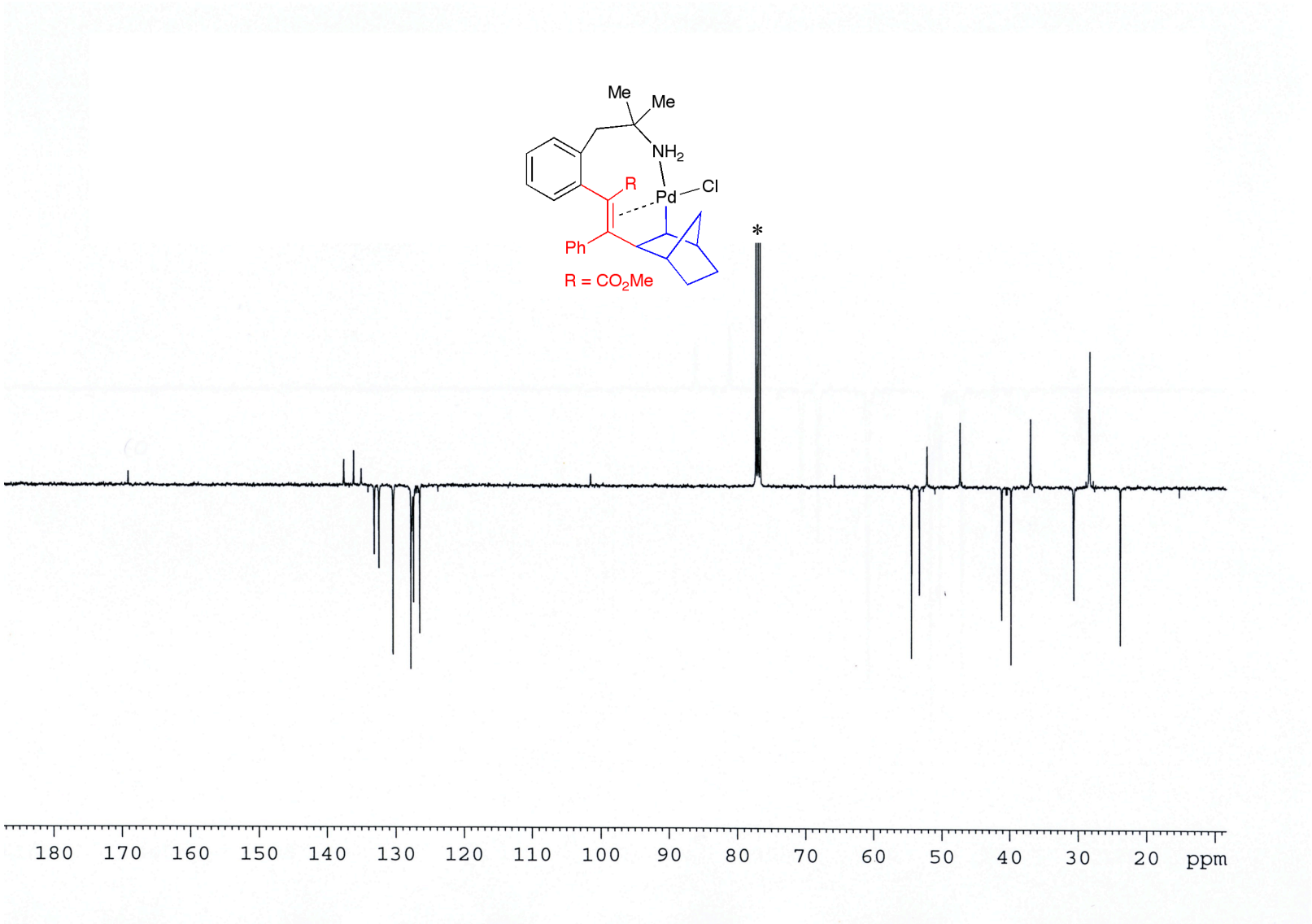

Figure S56. $^{13}C\{^{1}H\}$ APT NMR spectrum of **7d**·1/2$CHCl_3$ (100.8 MHz, $CDCl_3$, 25 ºC)

(The asterik indicates the signal corresponding to $CDCl_3$)

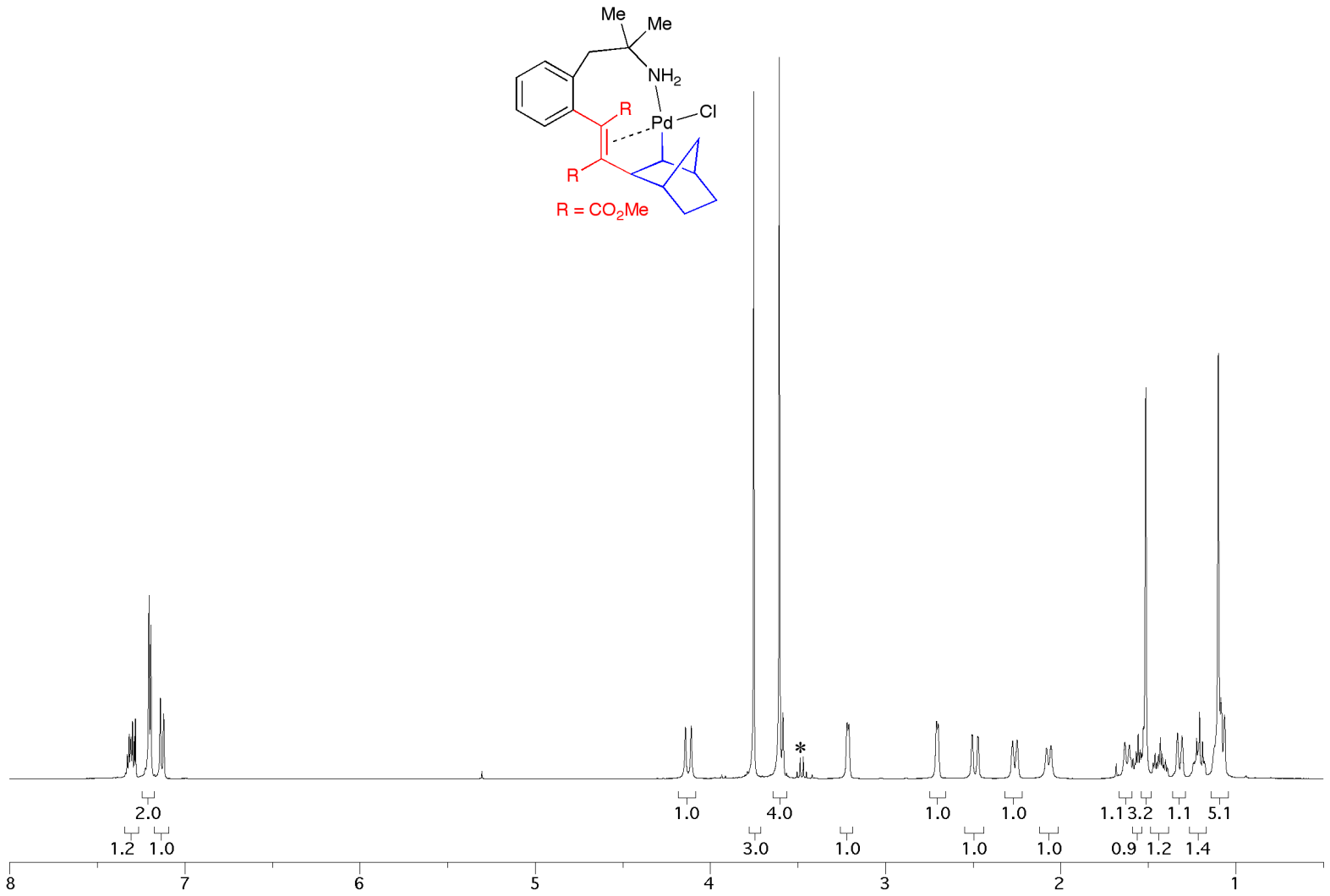

Figure S57. ^{1}H NMR spectrum of **7f** (400.9 MHz, $CDCl_3$, 25 ºC)

(The asterik indicates the signal corresponding to traces of Et_2O)

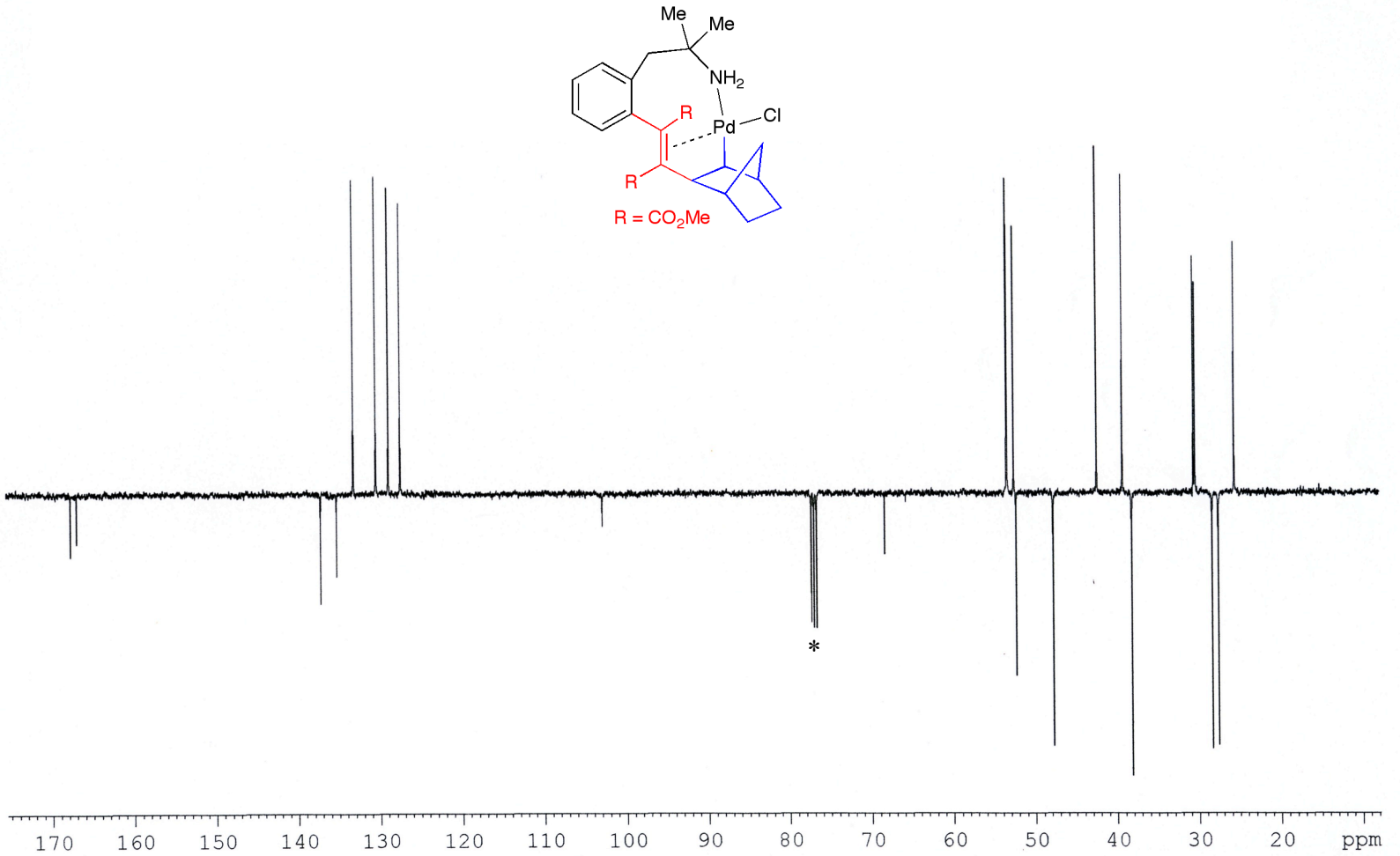

Figure S58. $^{13}C\{^{1}H\}$ APT NMR spectrum of **7f** (100.8 MHz, $CDCl_3$, 25 ºC)

(The asterik indicates the signal corresponding to $CDCl_3$)

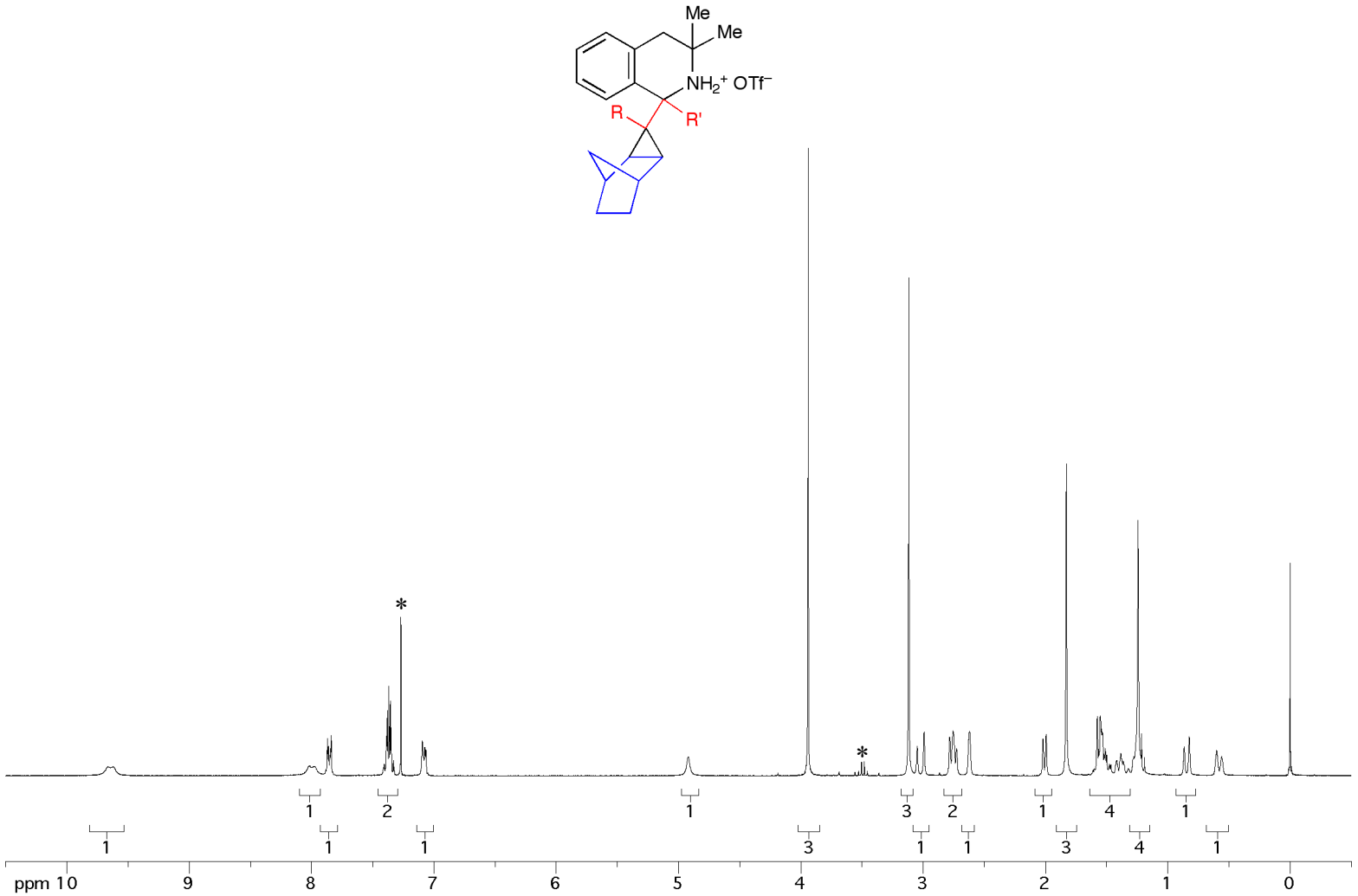

Figure S59. ^{1}H NMR spectrum of **8f** (300.1 MHz, $CDCl_3$, 25 ºC)

(From left to right, the asteriks indicate the signals corresponding to $CHCl_3$ and traces of Et_2O)

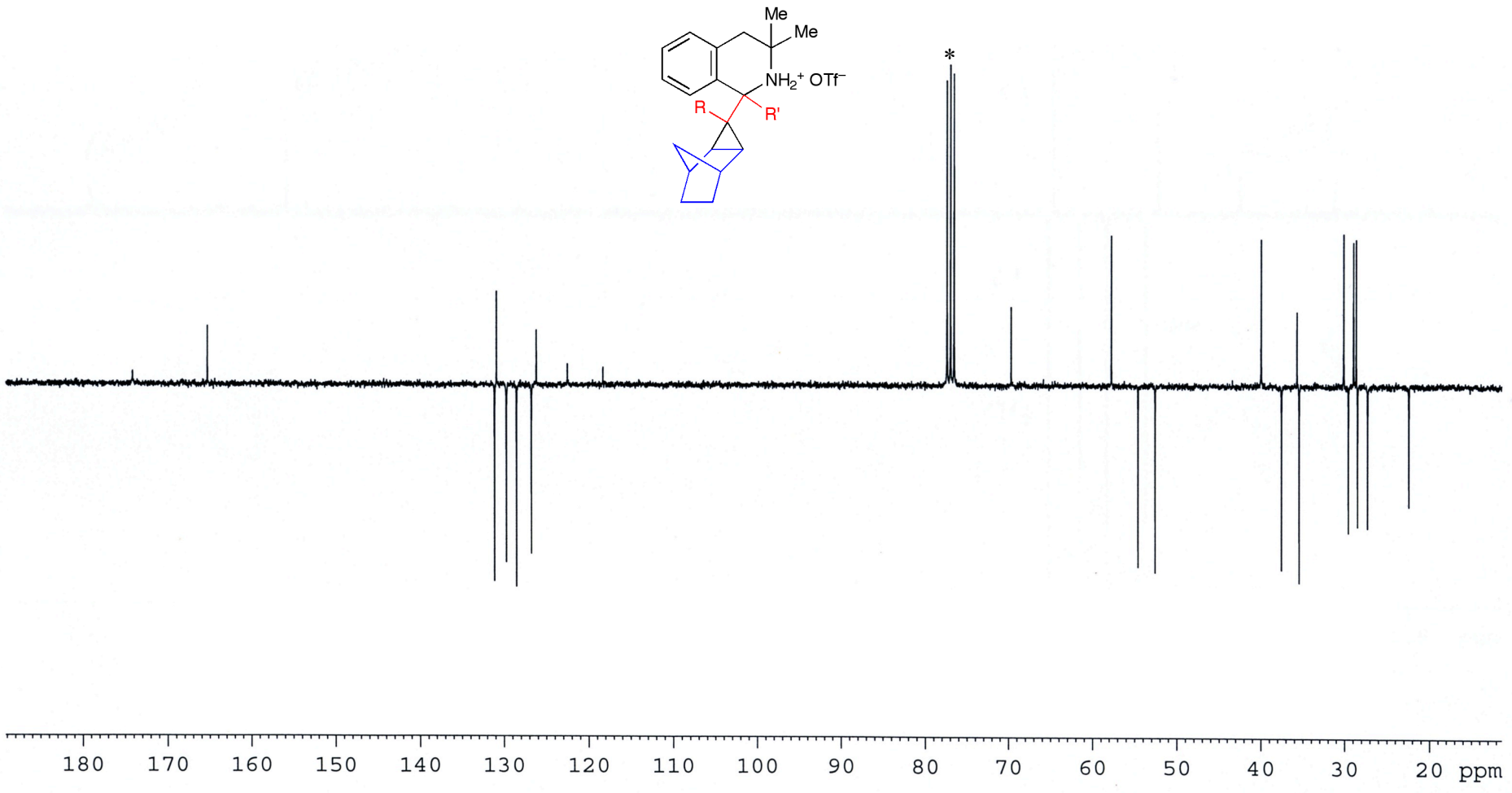

Figure S60. $^{13}C\{^{1}H\}$ APT NMR spectrum of **8f** (75.5 MHz, $CDCl_3$, 25 ºC)

(The asterik indicates the signal corresponding to $CDCl_3$)

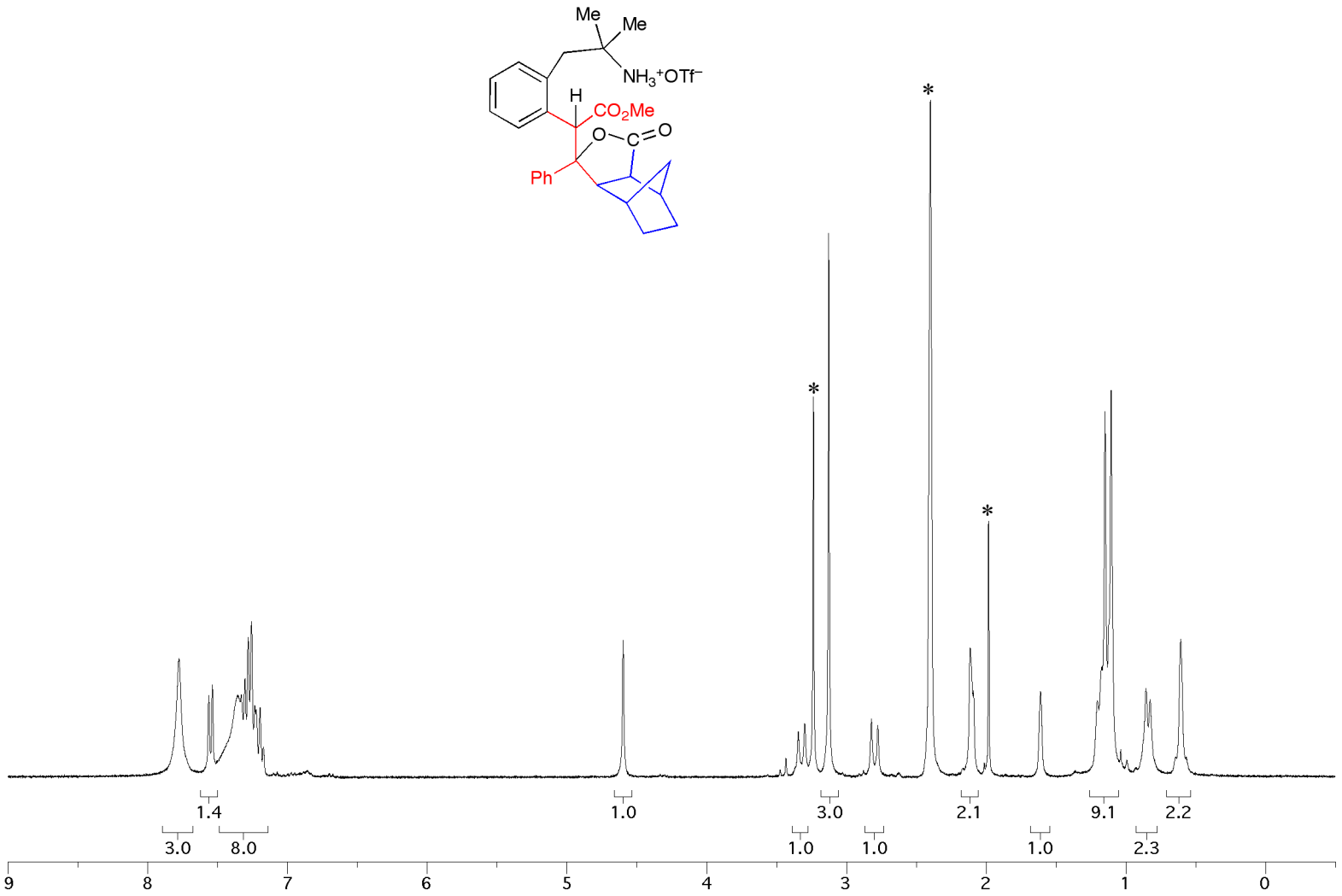

Figure S61. ^{1}H NMR spectrum of **9d** (300.1 MHz, DMSO-d_6, 25 ºC)

(From left to right, the asteriks indicate the signals corresponding to H_2O, deuterated DMSO, and acetone)

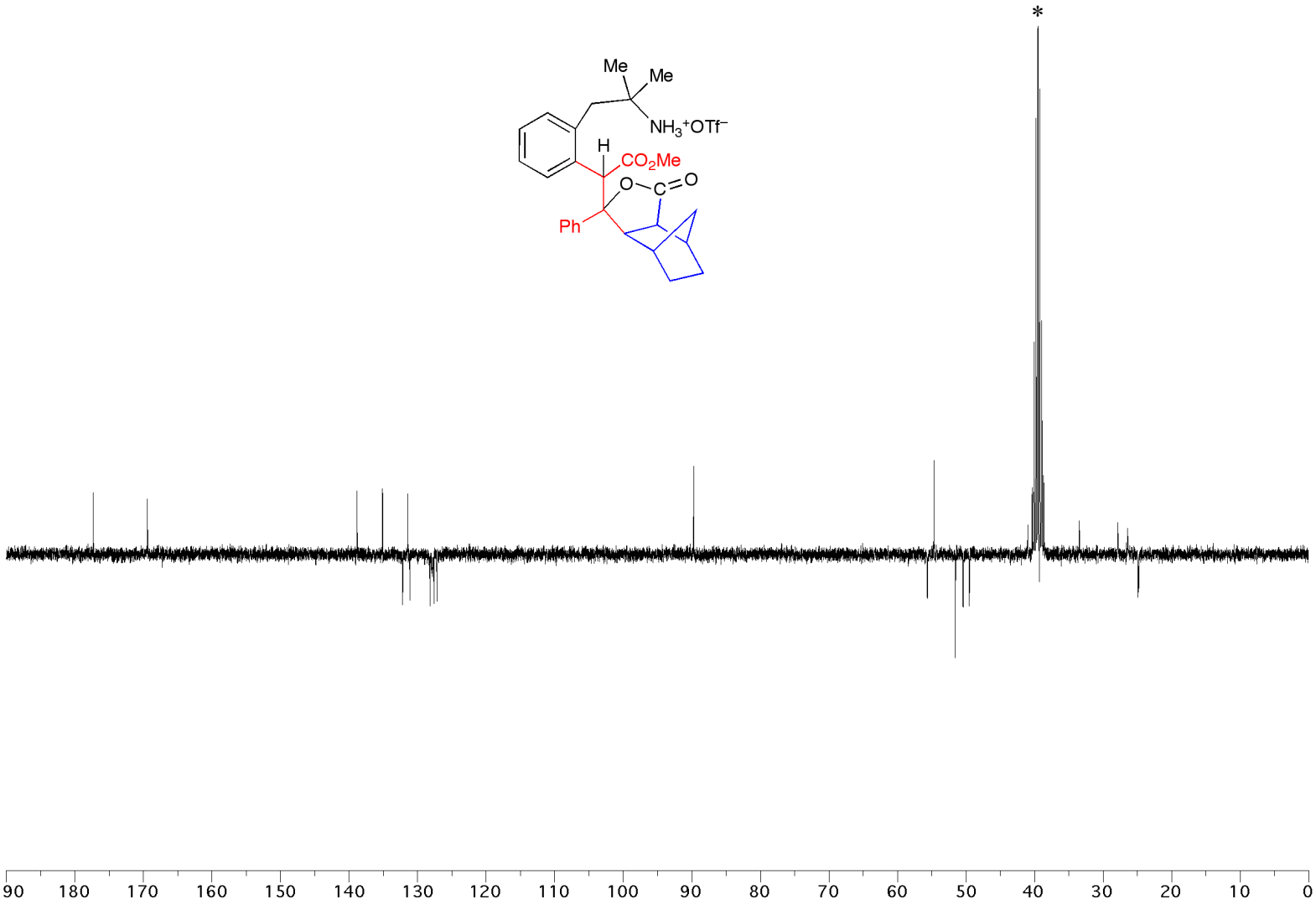

Figure S62. $^{13}C\{^{1}H\}$ APT NMR spectrum of **9d** (75.5 MHz, DMSO-d_6, 25 ºC)

(The asterik indicates the signal corresponding to DMSO-d_6)

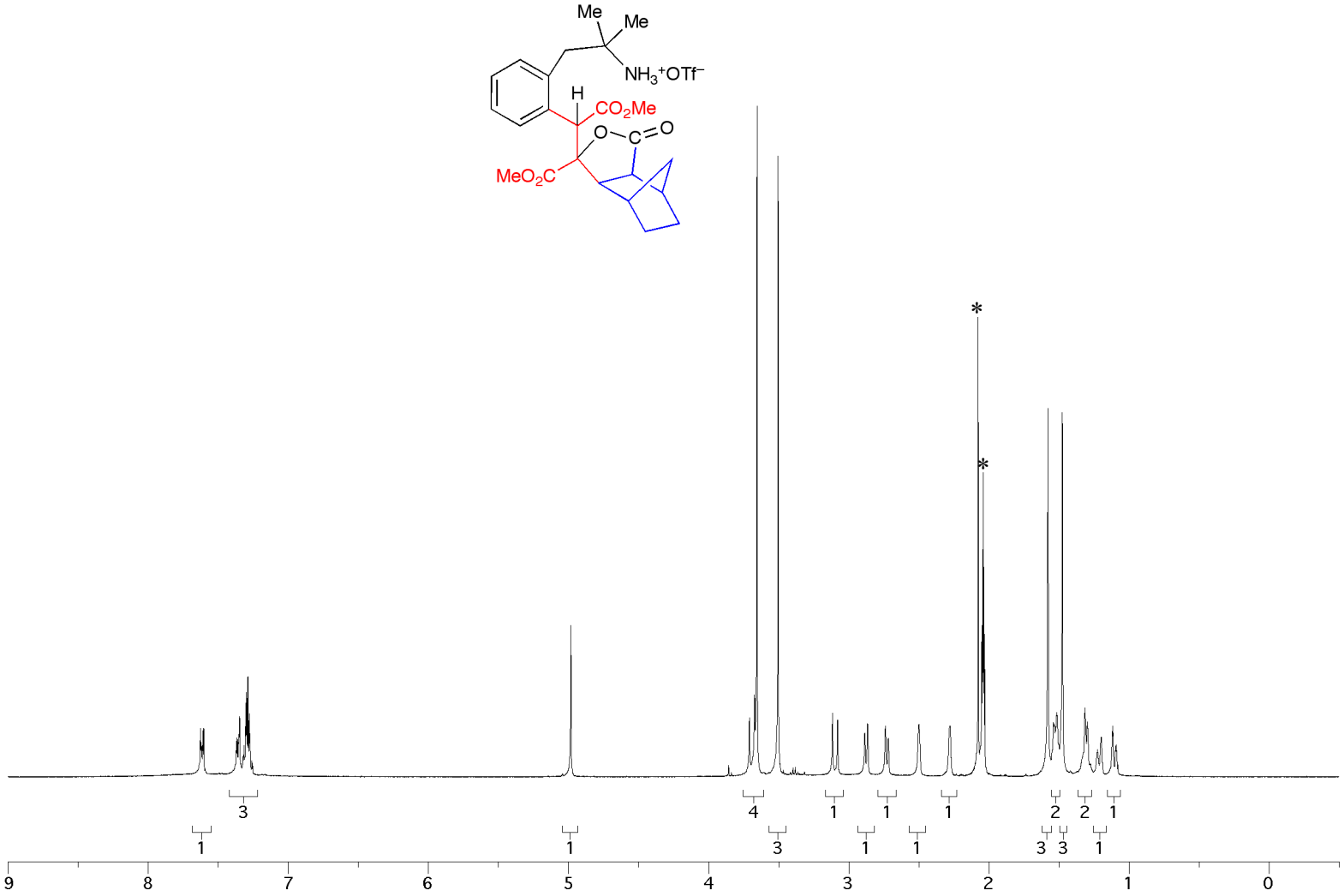

Figure S63. ^{1}H NMR spectrum of **9f** (400.9 MHz, acetone-d_6, 25 ºC)

(From left to right, the asteriks indicate the signals corresponding to deuterated acetone, and acetone)

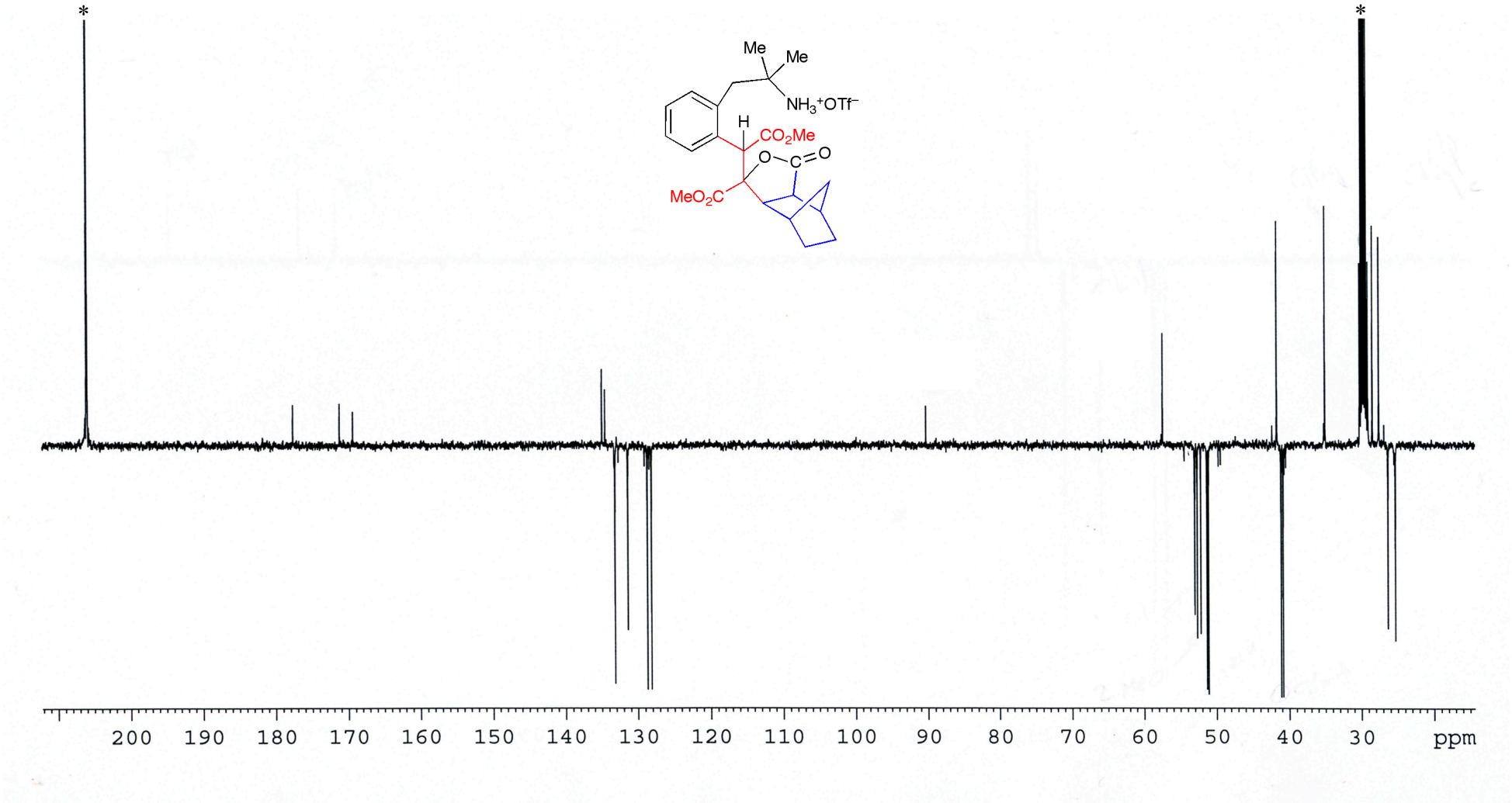

Figure S64. $^{13}C\{^{1}H\}$ APT NMR spectrum of **9f** (100.8 MHz, acetone-d_6, 25 ºC)

(The asteriks indicate the signals corresponding to acetone-d_6)

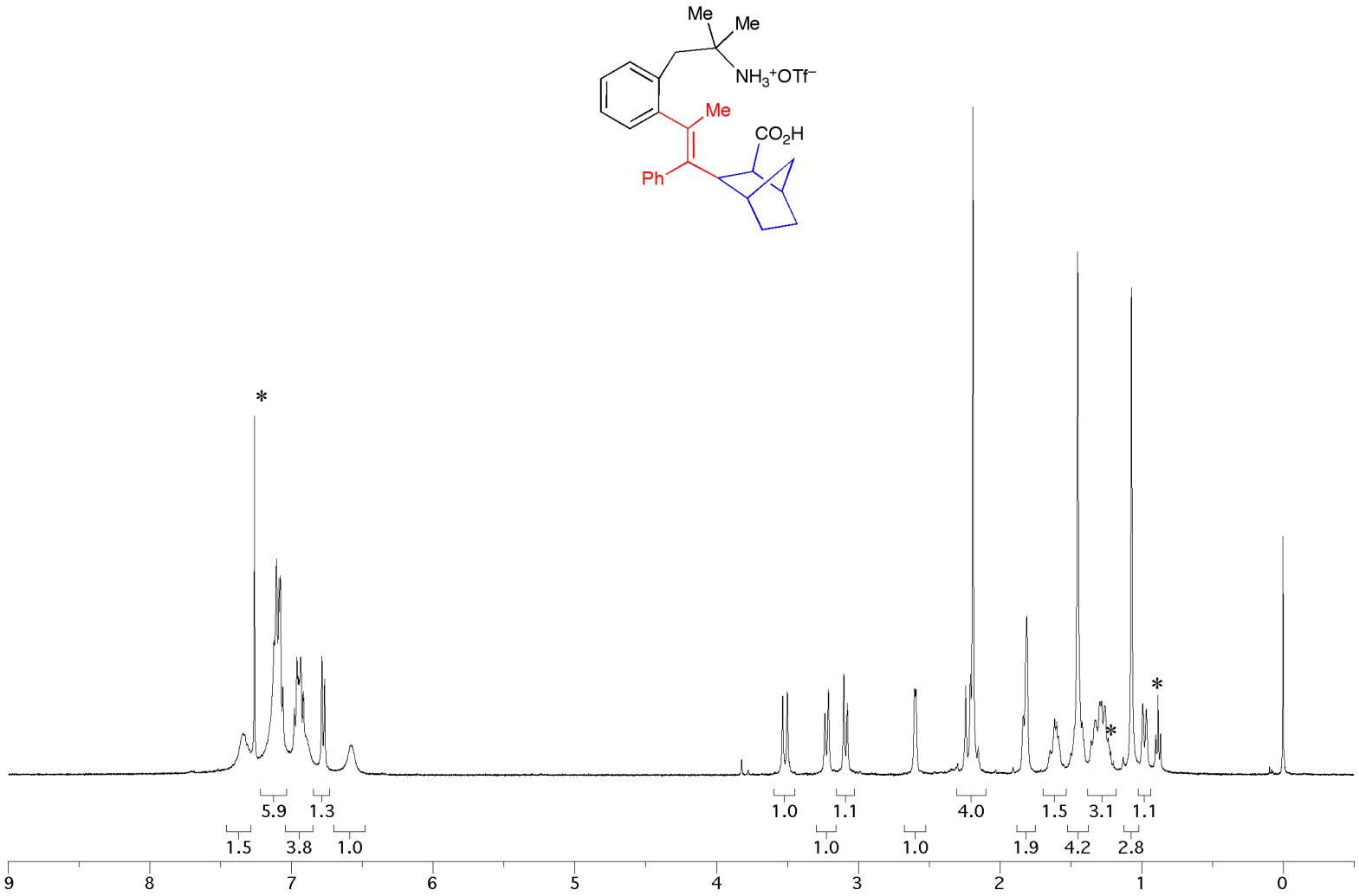

Figure S65. ^{1}H NMR spectrum of **10c** (400.9 MHz, $CDCl_3$, 25 ºC)

(From left to right, the asteriks indicate the signals corresponding to $CDCl_3$, and traces of *n*-pentane)

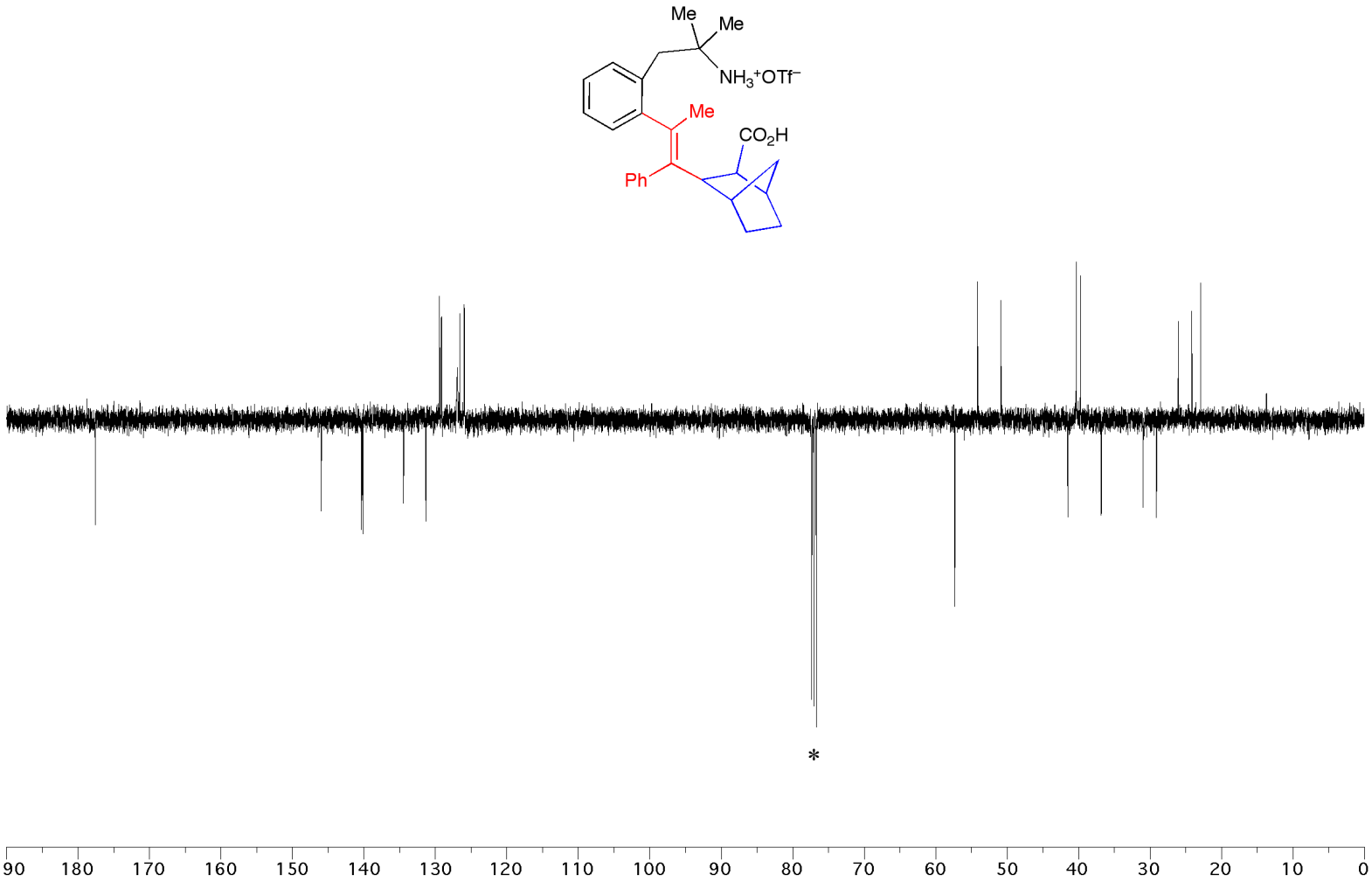

Figure S66. $^{13}C\{^{1}H\}$ APT NMR spectrum of **10c** (100.8 MHz, $CDCl_3$, 25 ºC)

(The asterik indicates the signal corresponding to $CDCl_3$)

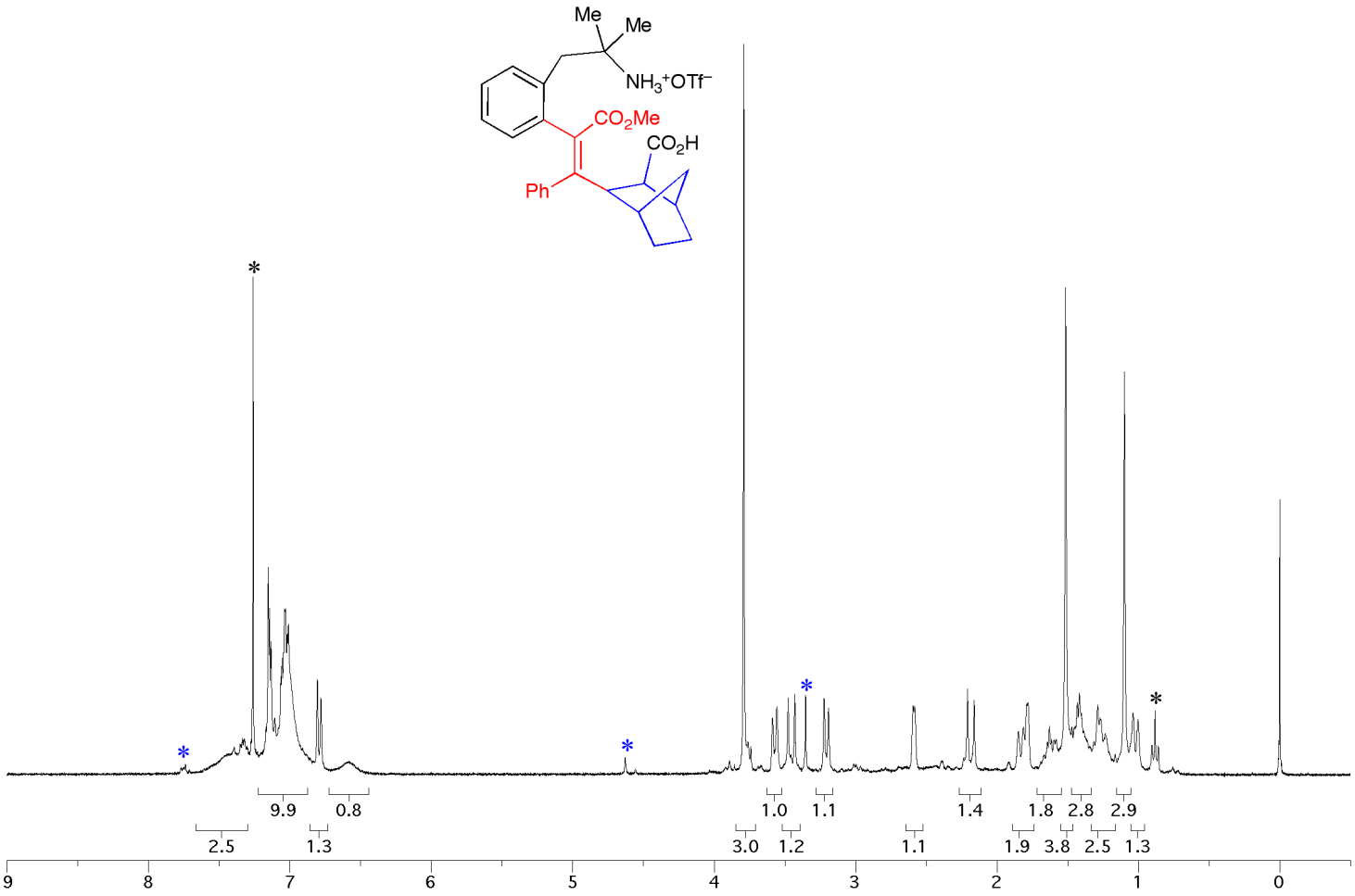

Figure S67. ^{1}H NMR spectrum of **10d** (300.1 MHz, $CDCl_3$, 25 ºC)

(From left to right, the black asteriks indicate the signals corresponding to $CDCl_3$, and traces of *n*-pentane. The blue asteriks correspond to traces of compound **9d**)

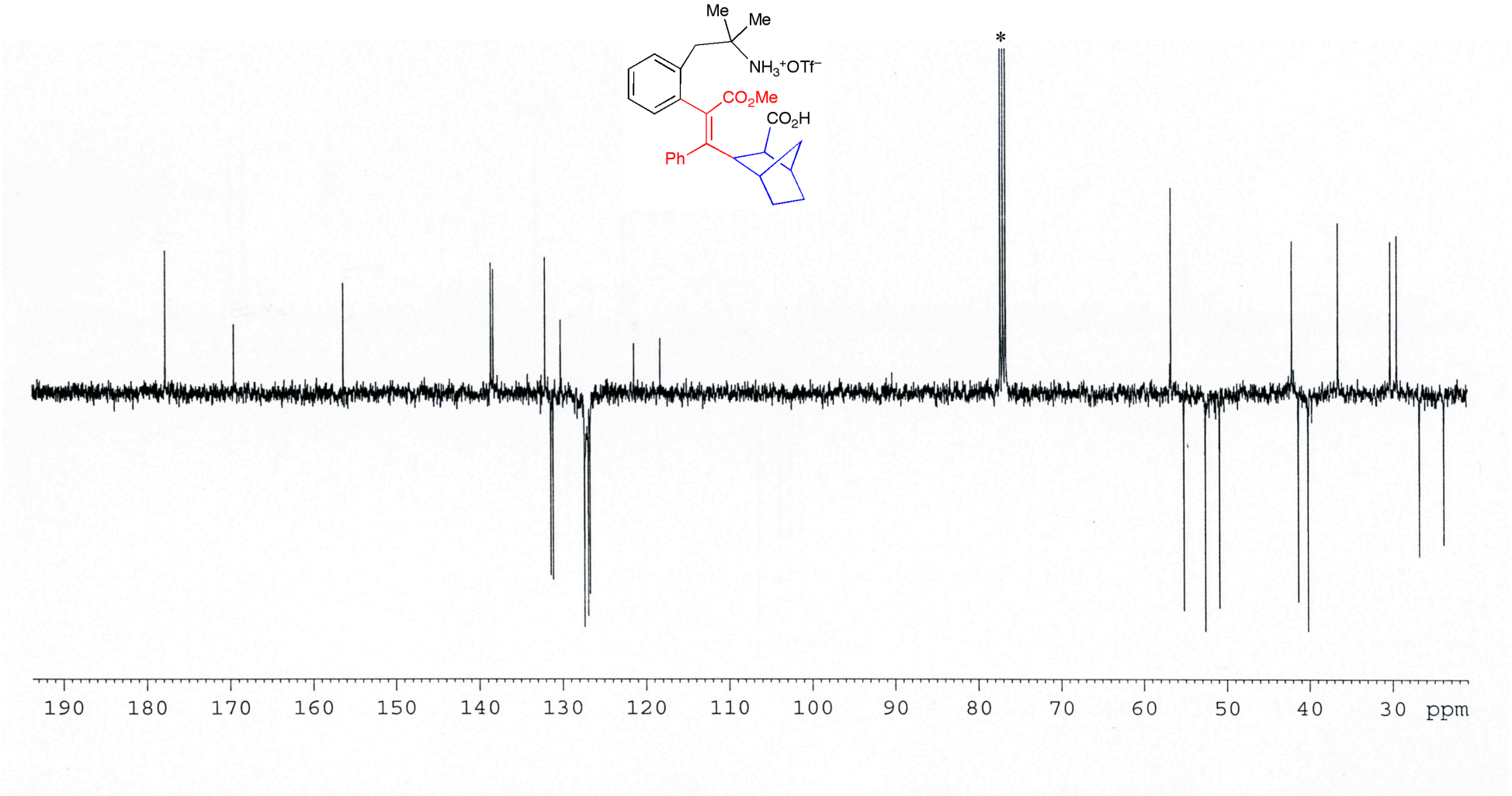

Figure S68. $^{13}C\{^{1}H\}$ APT NMR spectrum of **10d** (100.8 MHz, $CDCl_3$, 25 ºC)

(The asterik indicates the signal corresponding to $CDCl_3$)